University of Alberta

Proteolysis autoregulates expression of the cyanobacterial DEAD-box RNA helicase CrhR, in response to change in growth temperature

by

Oxana Sergeyevna Tarassova

A thesis submitted to the Faculty of Graduate Studies and Research
in partial fulfillment of the requirements for the degree of

Master of Science
in
Microbiology and Biotechnology

Department of Biological Sciences

Fall 2013
Edmonton, Alberta

Dedication

This work is dedicated to my precious family, who has been the ultimate source of inspiration throughout my whole life

Abstract

The DEAD box cyanobacterial RNA helicase redox, CrhR, in *Synechocystis* sp. PCC 6803 is induced in response to environmental stress conditions causing reduction of the redox status of the photosynthetic electron transport chain, with temperature being one of the major conditions commonly encountered in the environment. A basal level of CrhR protein abundance is observed at 30^{o}C, which is significantly increased at 20^{o}C. In this study CrhR protein abundance was found to be regulated by a temperature-controlled proteolytic mechanism that is most active in the first few hours of growth at 30^{o}C. CrhR proteolytic degradation was shown to be autoregulated as *crhR*$_{TR}$ mutant exhibits elevated levels of non-functional truncated CrhR$_{TR}$ protein regardless of growth temperature. Based on the results a model for CrhR post-translational regulation at 30^{o}C by autoregulated proteolytic degradation was proposed. CrhR represents the second example of proteolytically autoregulated protein, being the first known example among RNA helicases.

Acknowledgments

I would like to express my grateful appreciation and sincere gratitude to the following people, who made the completion of my thesis possible:

Dr. George Owttrim, for being a supportive and patient mentor throughout my degree; supervisor that is always ready to offer his guidance, help and encouragement when it mostly needed.

Dr. Julia Foght, for being in my supervisory committee and for the valuable suggestions, expertise and help with my project as well as personal advice and support during my program.

Richard Mah, for being a great support throughout my program, for being always ready to help and encourage me during the most difficult times.

Dr. Danuta Chamot, for assistance with techniques used in the Owttrim lab.

Jack Moore from Biochemistry department, for helping me with mass spectrometry analysis and being always ready to answer my questions.

Arlene Oatway, for teaching me microscopy skills, being extremely patient and providing lots of advice.

My amazing lab mates: Reem Skeik, Albert Rosana and Denise Whitford, who made every day that I spent at the university enjoyable and memorable.

I am thankful to God for an opportunity to meet a number of great people during my program and get valuable life experience that I will always remember.

Finally, I want to thank the most important people in my life: my parents and my husband, for their endless love, care and emotional support. Everything that I achieve in my life would not be possible without you.

Table of Contents

List of Tables

List of Figures

List of Abbreviation

A	Amps
Amp^R	Ampicillin resistant
APS	Ammonium persulfate
bp	Basepair(s)
CAN	Acetonitrile
Cm^R	Chloramphenicol resistant
CrhC	Cyanobacterial RNA helicase cold
CrhR	Cyanobacterial RNA helicase redox
Csp	Cold shock protein
Da	Daltons
DM	Degradation machinery
DNase	Deoxyribonuclease
DTT	Dithiothreitol
EDTA	Ethylene diamine tetra acetic acid
G	Gram(s)
H	Hour(s)
His	Histidine
His-R	His-tagged CrhR
IEM	Immunoelectorn microscopy
IPTG	Isopropyl-β-D-thiogalactoside
kb	Kilobasepair(s)

kDa	Kilodalton(s)
Km	Kanamycin
Km^R	Kanamycin resistant
LB	Luria Bertani medium
Mmol	Millimole(s)
mPa	Millipascal(s)
mRNA	Messenger RNA
^oC	Degrees centigrade
OD	Optical density
ORF	Open reading frame
PAGE	Polyarcrylamide gel electrophoresis
PBS	Phosphate buffered saline
PCR	Polymerase chain reaction
RNase	Ribonuclease
rpm	Rotations per minute
rRNA	Ribosomal RNA
SDS	Sodium dodecyl sulfate
sRNA	Small RNA
TCA	Trichloroacetic acid
TEMED	Tetramethyl ethylene diamine
TF	Trigger factor
tRNA	Transfer RNA

U	Units
UTR	Untranslated region
UV	Ultraviolet
WT	Wild type

I. INTRODUCTION

1.1 Physiological effects of cold shock

1.1.1 Bacterial response to cold shock

Constant changes in growth conditions represent one of the major challenges that bacteria face in the environment. Temperature shifts, either up or down, happen constantly in natural habitats and microorganisms have evolved sophisticated mechanisms, including alterations in membrane composition and changes in protein profile, to quickly respond and adapt to this type of stress. Research in recent years has primarily focused on the effect of heat shock and much less attention has been given to the phenomenon of cell response to cold temperatures. Decrease in normal growth temperature, usually referred to as cold shock or cold stress, forces cells to adapt their physiology to the new growth condition in order to survive and proliferate. For a long period of time, cold stress was thought to involve general changes in cell physiology such as slowing down growth and metabolism and alteration of membrane fluidity. However, more evidence has recently emerged about specific cellular responses at the level of transcription and translation (Thieringer *et al.*, 1998; Yamanaka *et al.*, 1998; Golovlev, 2003; Gualerzi *et al.*, 2003; Phadtare, 2004; El-Sharoud and Graumann, 2007; Phadtare and Severinov, 2010).

Apart from the changes in cellular physiology that gradually prepare the organism for the new condition, there are several other processes that immediately occur in the cell during cold stress. The two major immediate effects include a decrease in active transport and protein secretion across the membrane due to a

significant reduction in membrane fluidity and stabilization of secondary structures in mRNA leading to the reduction of ribosome function, which negatively affects translation. Improper folding or complete unfolding of proteins, which is considered a primary characteristic of the heat shock response and constitutes major damage to the cell, can also be caused by a temperature downshift (Bischof and He, 2005; Dias *et al.*, 2010).

There are also cold-induced changes in the structure of nucleic acids including stabilization of secondary structures of both RNA and DNA and increase in negative supercoiling of DNA. The increase in negative supercoiling of DNA causes impairment of DNA transcription, recombination and replication (Wang and Syvanen, 1992; Krispin and Allmansberger, 1995; Mizushima *et al.*, 1997). Stabilization of RNA secondary structure prevents normal movement and function of RNA polymerase and ribosomes, thus significantly reducing transcription and translation during the cold shock.

In order to reduce damage to cellular processes and still survive and proliferate, a set of cold-induced genes is transcribed during the cold shock, which leads to active production of proteins required for survival and proliferation of cells at low temperatures (Graumann and Marahiel, 1996; Graumann and Marahiel, 1998; El-Sharoud and Graumann, 2007; Jiang *et al.*, 2012).

1.1.2 Proteins involved in bacterial cold adaptation

Cells produce a specific set of proteins in response to cold stress in order to reduce damaging effects of low temperature on bacterial physiology.

As mentioned above, cold temperatures significantly decrease membrane fluidity leading to reduced active transport and protein secretion across the membrane. To overcome this problem, bacteria evolved a mechanism through which they are able to increase the proportion of unsaturated fatty acids in membrane lipids, thus increasing fluidity of the membranes. Desaturases, enzymes that are involved in this mechanism, are present in many cyanobacteria and *Bacillus subtilis*. In photosynthetic cyanobacteria, desaturases introduce double bonds into fatty acids bound to the thylakoid membranes (Murata and Wada, 1995). Desaturases are crucial for cell survival in the cold as they are associated with acclimatization of photosynthesis to low temperatures. Thylakoid membranes in cyanobacteria are vital cell compartments, where photosynthetic electron transport chains reside (Wilson *et al.*, 2006; Ducruet *et al.*, 2007). Thus, keeping these membranes fluid and functional during all growth conditions is necessary for the survival of cyanobacterial cells.

Desaturases genes, *desA* and *desB*, are among other genes in the cyanobacterium *Synechococcus* that are induced during temperature downshift from 38^{o}C to 22^{o}C (Blot *et al.*, 2011; Vijayan *et al.*, 2011; Gierga *et al.*, 2012). Cold-shock expression of these genes in *Synechococcus* is tightly regulated at the transcriptional and post-transcriptional level by a combination of mRNA synthesis and mRNA stabilization (Sakamoto and Bryant, 1997). Cold induction of desaturase genes in non-photosynthetic organisms was described in the most

detail in *Bacillus* (Aguilar *et al.*, 1999). *Bacillus* has a much more complex regulatory mechanism of cold-induction of desaturase genes, which involves a two-component signal transduction system with sensor kinase DesK and response regulator DesR (Aguilar *et al.*, 1999).

Desaturases are not the only enzymes involved in cold-adaptation of *Bacillus* membranes; there is also an isoleucine-dependent fatty acid branching adaptation mechanism (Klein *et al.*, 1999; Weber *et al.*, 2001). *B. subtilis* can use exogenous isoleucine as a precursor for anteiso-branched fatty acid synthesis to keep membrane fluidity in the cold. It was reported that *Bacillus* desaturase null mutants are capable of cold adaptation using the isoleucine-dependent mechanism (Klein *et al.*, 1999).

Besides the issues with fluidity of the membranes, cells also face other serious problems preventing normal growth at low temperatures. One of those problems is protein misfolding, which was previously only considered to be a major problem during heat shock (Phadtare, 2004). It was discovered that cold temperature also has negative effects on the proper folding of the protein. Therefore, refolding of already damaged proteins is as important process during cold stress as it is during the heat shock (Kandror and Goldberg, 1997). Certain proteins including caseinolytic proteases (Clps), trigger factor (TF) and molecular chaperones GroEL and GroES are among cold-induced proteins involved in proper folding and degradation of proteins damaged by cold shock. GroEL and GroES are molecular chaperonins that assist in proper folding of the proteins in various stress conditions including cold (Susin *et al.*, 2006; Sato *et al.*, 2008).

Trigger factor TF also has molecular chaperone activity as a peptidyl-prolyl isomerase (Kandror and Goldberg, 1997). TF associates with newly formed polypeptides on ribosomes and also binds to GroEL; the complex having enhanced affinity for unfolded proteins (Kandror and Goldberg, 1997). In cases when proteins are unfolded and cannot be refolded by chaperones during cold shock, proteases from the family of Clps assist the cell. Some Clp proteases are expressed constitutively and others are induced by stress such as temperature shifts, during which they help with degradation of misfolded proteins (Porankiewicz and Clarke, 1997; Phadtare and Inouye, 2008).

Apart from problems with membrane fluidity and protein misfolding, the cellular translation machinery experiences significant difficulties during cold shock. At low temperature, the translation initiation step becomes rate limiting for cell growth, resulting in accumulation of 70S ribosomes (Friedman *et al.*, 1971; Farewell and Neidhardt, 1998). There are a number of proteins involved in resolving this problem, including translation initiation factors such as IF-2 that assists tRNA binding to the 30S subunit (Jones *et al.*, 1987); ribosome binding factors such as RbfA, which is a free 30S ribosome binding factor required for optimal growth specifically at low temperatures (Jones *et al.*, 1996). Those proteins are just a few examples; there are many other proteins with various functions, whose participation in adaptation of the translation apparatus to the cold is crucial for cell survival.

Our focus will be on the other group of proteins, termed RNA chaperones, whose presence is crucial for the survival of cells during cold shock. As already

mentioned, stabilization of nucleic acid secondary structures in the cold impairs proper movement and function of RNA polymerase and ribosomes, which is one of the major factors contributing to reduced cell growth at low temperatures. To resolve RNA secondary structures in the cold cell induces production of cold shock proteins (Csp's) and stress-specific DEAD-box RNA helicases, which help to keep translation at normal levels even during stress conditions. Regulation of expression, structure and function of Csp's and DEAD RNA helicases will be discussed in more detail in the next sections.

1.2 RNA modulating cold shock proteins (Csp's)

1.2.1 CspA family

Cold shock protein A (CspA) was the first low temperature-induced protein discovered in *Escherichia coli* (Goldstein *et al.*, 1990). CspA is referred to as the major cold shock protein as it is the most abundant protein induced upon decrease in temperature (Brandi *et al.*, 1999). Production of CspA reaches an intracellular concentration of 100 μM within 1- 1.5 hours of temperature downshift (Goldstein *et al.*, 1990; Brandi *et al.*, 1999).

Since the time of CspA discovery eight additional cold-shock proteins closely related to CspA were identified in *E. coli* and named in alphabetical order from CspB to CspI (Yamanaka *et al.*, 1998). All of them are induced at different cell growth stages by various external stresses including increase and decrease of growth temperature, nutrition starvation and entering stationary phase (Yamanaka *et al.*, 1994; Yamanaka and Inouye, 1997). Three of them: CspB, CspG and CspI

are inducible specifically by cold stress similar to CspA, during temperature reduction from 37^{o}C to 15^{o}C or 10^{o}C (Lee *et al.*, 1994; Nakashima *et al.*, 1996; Wang *et al.*, 1999; Yamanaka, 1999). Proteins related to *E. coli* CspA are also found in *Bacillus subtilis*: CspB, CspC and CspD. These proteins are also shown to be induced by cold shock (Willimsky *et al.*, 1992; Graumann and Marahiel, 1996). This is a general phenomenon as proteins similar to *E. coli* and *B. subtilis* Csp's are found in more than 50 other Gram-positive and Gram-negative bacterial species (Graumann and Marahiel, 1996; Graumann and Marahiel, 1998) and even in the eukaryotic organism *Cladosporium herbarum* (Falsone *et al.*, 2002). However, not all organisms share Csp-protein homologues, for instance they are absent in archaea and cyanobacteria. Proteins that have no homology with Csp proteins, but possess some of their functions, are involved in cold adaptation of archaeal and cyanobacterial cells, which will be described in more detail in the next section.

Proteins belonging to the CspA family possess functional redundancy, since *E. coli* mutants harboring double or triple deletions of the *csp* genes are not cold sensitive (Xia *et al.*, 2001). For instance, in the triple deletion strain Δ*cspA*Δ*cspB*Δ*cspG*, CspE is overproduced and is proposed to functionally substitute for the lack of three other Csp proteins. However, a quadruple deletion Δ*cspA*Δ*cspB*Δ*cspG*Δ*cspE* is cold sensitive, but this defect is easily complemented by overproduction of any of the CspA-related proteins except for CspD (Xia *et al.*, 2001). In *B. subtilis*, the triple deletion mutant Δ*cspB*Δ*cspC*Δ*cspD* is lethal suggesting that the presence of at least one Csp protein is essential for its survival

(Graumann *et al.*, 1997). These observations suggest functional overlap of CspA-like proteins in different bacteria.

1.2.2 Structure and cellular function of CspA- like proteins

CspA and CspA-like proteins belong to a family of structurally related nucleic acid-binding proteins. It was shown that Csp's bind single stranded DNA and RNA (Jiang *et al.*, 1997; Lopez *et al.*, 1999; Lopez and Makhatadze, 2000). Even though there is no direct evidence that Csp's are able to melt secondary structures on nucleic acids, due to their structure and ability to bind single stranded RNA it was hypothesized that they are able to facilitate transcription and translation at cold temperatures by resolving unfavorable RNA structures and therefore they have been termed RNA chaperones (Jiang *et al.*, 1997; Bae *et al.*, 2000). As mentioned above, one of the detrimental effects of low growth temperature is stabilization of nucleic acid secondary structures. This phenomenon negatively affects essential cell processes such as transcription and translation.

At the transcriptional level, *E. coli* CspA can act as a transcriptional activator to enhance transcription of *hns* and *gyrA* genes encoding proteins involved in cold adaptation. H-NS is a cold-induced "histone-like" nucleoid and chromatin-associated protein that is involved in structuring chromosomal DNA and was shown to be involved in cold adaptation (Dersch *et al.*, 1994). It was demonstrated that CspA recognizes the 110-bp promoter region of the *hns* gene (Brandi *et al.*, 1994), harboring a CCAAT sequence. Recognition and binding of

this sequence is essential for CspA-mediated regulation of *hns* at the transcriptional level (Giangrossi *et al.*, 2001). Association of CspA with the *hns* promoter activates transcription of the cold-induced protein H-NS (Pon *et al.*, 1988; Friedrich *et al.*, 1988; Dersch *et al.*, 1994).

Transcription of the *gyrA* gene is also activated by CspA (Jones *et al.*, 1992). The *gyrA* gene encodes the α subunit of the DNA gyrase, whose elevated levels relieve the increase in negative supercoiling of DNA during the cold shock (Mizushima *et al.*, 1997). Negative supercoiling of DNA prevents normal movement of DNA and RNA polymerase, thus preventing such vital processes as DNA replication, recombination and transcription. CspA activation of *gyrA* transcription helps to increase the levels of DNA gyrase to assist bacterial survival and growth at cold temperatures. In addition to transcription activation, certain CspA homologues, specifically CspE and CspC in *E.coli*, were shown to act as transcription antiterminators by decreasing transcription pausing of *nusA*, *infB*, *rbfA*, and *pnp* genes during cold shock (Feng *et al.*, 2001).

Besides the involvement of Csp proteins in transcription itself, these proteins have diverse post-transcriptional and translational roles. As mentioned above, CspA and related proteins are thought to melt secondary structures of nucleic acids due to their specific protein structure and their affinity to preferentially bind single stranded DNA and RNA (Jiang *et al.*, 1997; Phadtare and Inouye, 1999; Bae *et al.*, 2000). This role of Csp's is also very important for their own mRNA at reduced temperatures, as extensively studied for the CspA in *E. coli*. Stability of *cspA* transcript is significantly reduced at higher temperatures

and significantly increases in the cold (Goldenberg *et al.*, 1996; Brandi *et al.*, 1996; Fang *et al.*, 1997). CspA binds to the long 5' UTR (159 bp) of its own mRNA at low temperatures, preventing the formation of secondary structures that may reduce mRNA stability and interfere with further translation (Mitta *et al.*, 1997; Bae *et al.*, 2000; Ermolenko and Makhatadze, 2002). CspA binds to the so-called "cold box" (UGACGUACAGA) in the 5' UTR, which is a highly conserved sequence present not only in CspA-family proteins, but also in the 5' UTR of the cold induced DEAD-box RNA helicase CsdA (Iost and Dreyfus, 1994; Jones *et al.*, 1996). It is proposed that during cold shock, CsdA cooperates with CspA to unwind secondary structure of *cspA* mRNA as well as other mRNAs to reduce their enzymatic degradation (Horn *et al.*, 2007).

Structure of CspA-related proteins plays an important role in their function as RNA chaperones. X-ray crystallography and NMR-analysis were used to resolve the three-dimensional structure of CspA from *E. coli* and CspB from *B. subtilis* (Schindelin *et al.*, 1993; Schnuchel *et al.*, 1993; Schindelin *et al.*, 1994; Newkirk *et al.*, 1994; Feng *et al.*, 1998). Analysis showed that the protein consists of five antiparallel β-strands that form a β-barrel structure with two β-sheets. There are two putative RNA-binding motifs, which include a surface patch of aromatic residues. These residues probably contribute to the ability of Csp's to bind nucleic acids by intercalating between DNA and RNA bases (Phadtare and Inouye, 2008). Three out of six surface aromatic rich residue patches were demonstrated to be essential for Csp function, since their mutation lead to loss of

RNA secondary structure melting, transcription anti-termination and cold acclimation ability (Phadtare *et al.*, 2002a; Phadtare *et al.*, 2002b).

Even though the primary role of CspA protein is cold acclimation of the cells, which is thought to be done by resolving secondary structures of nucleic acids, recent advances in the field of cold shock response have attributed several other cold-unrelated roles to Csp's. For instance, CspC and CspE from *E. coli* were shown to regulate the expression of a number of RpoS-regulated stress proteins such as Dps (osmotic, oxidative stress and stationary phase adaptation), OsmY (osmotic stress and stationary phase), ProP (osmotic stress) and KatG (oxidative stress) (Phadtare and Inouye, 2001). The exact mechanism of this regulation is still unknown, but proposed to be through the regulation of RpoS itself (Phadtare and Inouye, 2008). CspE and CspC are also involved in regulation of the expression of the universal protein A, UspA, which also responds to numerous stresses (Phadtare and Inouye, 2001). These are just a few examples; there are many other non-cold related functions that CspA-related proteins exhibit in different organisms and the list of their functions expands with research on almost every new Csp. These observations suggest that proteins from the family of CspA play a more complex role in a broad range of cellular processes than was previously thought.

1.2.3 Regulation of expression of Csp's

CspA and the related proteins CspC and CspE, are not only produced under stress conditions, they are also expressed at a basal level during *E. coli*

exponential phase at regular growth temperature of 37^{o}C (Brandi *et al.*, 1999). It was demonstrated that the intracellular concentration of these proteins in *E. coli* during early exponential phase is about 50μM, which is only half of the concentration that is measured after 1 h cold-induction (Brandi *et al.*, 1999). It is also known that at least one of CspB, CspC, CspD is required for the survival and normal growth of *B. subtilis* at 37^{o}C (Graumann *et al.*, 1997). These findings lead to the conclusion that cold-inducible proteins belonging to the CspA family play an important role at normal growth temperatures as well as under cold stress.

Temperature downshift is considered the main trigger of the induction of Csp expression, however there are several other factors that influence Csp production. Factors that increase expression of Csp proteins similar to cold-shock response include: culture dilution at 37^{o}C (Brandi *et al.*, 1999), addition of nutrients (Yamanaka *et al.*, 1998) and addition of various antibiotics that block different stages of ribosomal elongation (Vanbogelen and Neidhardt, 1990; Jiang *et al.*, 1993; Etchegaray and Inouye, 1999). It was also shown that production of Csp's is induced at low temperature even in the presence of kanamycin and chloramphenicol at concentrations that block protein synthesis (Etchegaray and Inouye, 1999). Etchegaray and Inouye (1999) proposed that *cspA* and *cspB* mRNA may be able to bypass inhibitory action of the antibiotics, due to the presence of a sequence in their mRNA called the "downstream box" (Mitta *et al.*, 1997) that is thought to enhance translation initiation (Sprengart *et al.*, 1996; Etchegaray and Inouye, 1999). Thus, even though these stress proteins are named after their cold-shock induction and most of their functions are proposed to be

involved in cold acclimation of the cells, there are other cell stresses that trigger expression of Csp's and require their, yet to be discovered, function.

Csp expression is regulated at various levels including transcription, mRNA stability, translation and post-translational events.

Several *csp* genes have an unusually long 5' untranslated regions (5'-UTR), which contains a highly conserved 11-base sequence UGACGUACAGA, called the "cold box". It was proposed that the "cold box" sequence functions as a binding site for a transcription repressor (Jiang *et al.*, 1996). However, it was shown *in vivo* that CspA protein regulates its own expression by binding to the "cold box" region and thus working as transcriptional derepressor (Jiang *et al.*, 1996; Fang *et al.*, 1998).

Another mechanism of Csp expression regulation is done through mRNA stabilization in the cold, which is likely the major factor affecting dramatic induction of *cspA* at low temperature (Phadtare and Severinov, 2005). It was shown that *cspA* mRNA is extremely unstable at 37^{o}C (half-life of 12 sec) and is stabilized upon cold shock (half-life of more than 20 min). Using chemical and enzymatic probing, it was recently demonstrated that *cspA* mRNA undergoes structural rearrangement with temperature reduction, which allows for more efficient translation of CspA protein and makes its mRNA less prone to degradation (Giuliodori *et al.*, 2010). In addition, overexpression of the CsdA cold-inducible DEAD-box RNA helicase makes *cspA* mRNA more stable (Awano *et al.*, 2007). It is proposed that CsdA RNA helicase helps to prevent formation of extended stem-loop structures, which are predicted for the 5'-UTR of the CspA,

CspE and CspC, leading to increased half-lifes of their mRNAs (Nakashima *et al.*, 1996).

It is predicted that there is also another level of Csp regulation, which is done post-translationally. It was shown *in vitro* that in the presence of nucleic acid ligands, Csp's become much less susceptible to proteolytic degradation (Feng *et al.*, 2001). This observation suggests that *in vivo* when Csp's are actively resolving secondary structures on the nucleic acids in the cold, their protein stability is mediated by target binding. However at normal growth temperature these secondary structures are unstable and chaperones like Csp's become unnecessary, thus they will be recognized and degraded by proteases.

Several questions regarding Csps' regulation still remain open and need to be clarified experimentally, but without a doubt it can be concluded that the regulation of the cold shock proteins is a complex process. Production of cold shock proteins, as the production of any other stress response proteins, is very expensive for the cell. Thus, in order to respond fast and efficiently to a constantly changing environment using fewer cell resources, living organisms evolved various stress proteins tightly regulated by sophisticated mechanisms, many of which are yet to be discovered and described.

1.3 DEAD-box RNA helicases

The DEAD-box RNA helicases constitute another family of proteins that can act as RNA chaperones in order to resolve secondary RNA structures during various environmental stress conditions. Similar to Csp's, DEAD-box RNA

helicases have several functions with the main one being RNA chaperones. Some RNA helicases were also shown to be induced by different stress conditions, including cold temperature (Iost and Dreyfus, 1994). For instance, DEAD-box RNA helicase CsdA was first isolated from *E. coli* as a cold shock protein (Jones *et al.*, 1996) and was shown to not only unwind RNA as other RNA helicases, but is also involved in ribosomal biogenesis of 50S subunits (Charollais *et al.*, 2004).

1.3.1 Structure and biochemical activities of the DEAD-box helicases

DEAD-box proteins form a large helicase family with members in humans, bacteria and yeast (Rocak and Linder, 2004; Cordin *et al.*, 2006; Fairman-Williams *et al.*, 2010; Linder and Jankowsky, 2011). These proteins belong to helicase superfamily 2 (SF2), which is characterized by the presence of a highly conserved helicase core of two domains that are similar in structure to the bacterial recombinase A (RecA) (Caruthers and McKay, 2002; Singleton *et al.*, 2007; Fairman-Williams *et al.*, 2010) (Figure 1.1). Within the conserved helicase core there are 12 characteristic amino acid sequence motifs at conserved positions, some of which are conserved among all SF2 helicases whereas others are DEAD-box family specific (Fairman-Williams *et al.*, 2010). Motif II contains Asp-Glu-Ala-Asp (D-E-A-D) a highly conserved sequence of amino acids, which is the origin of the name for this family of helicases (Linder *et al.*, 1989) (Figure 1.1). Even though the DEAD motif is very characteristic for the DEAD-box family, frequently it can be altered in individual proteins, which still belong

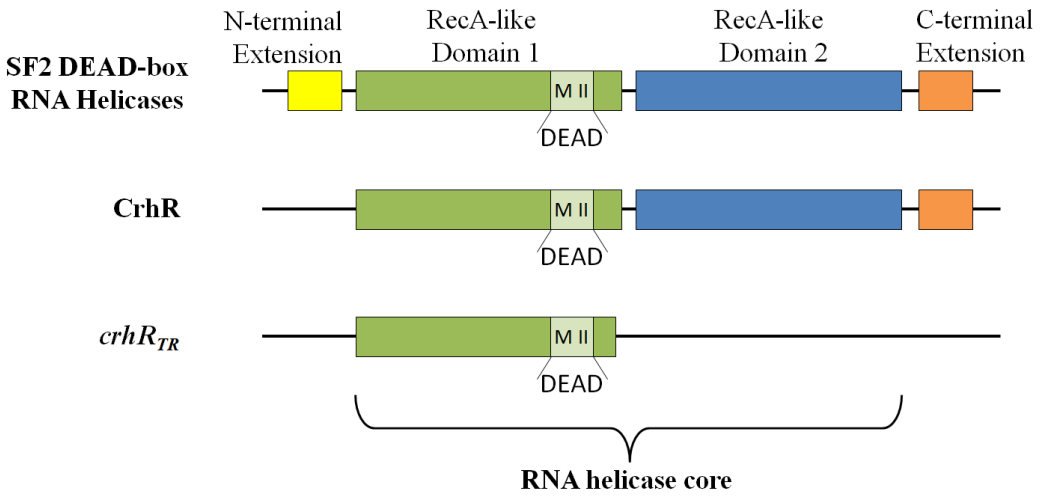

Figure 1.1: General structure of SF2 DEAD-box RNA helicases, CrhR and $crhR_{TR}$ mutant. General structure of DEAD-box RNA helicases from superfamily 2 (SF) is adapted from Fairman-Williams *et al.* (2010). Green and blue boxes represent RecA-like domains 1 and 2 respectively. Yellow and orange boxes represent N and C-terminal extensions respectively. Light green box inside of RecA-like Domain 1 represents motif 2 (MII) containing the highly conserved amino acid sequence Asp-Glu-Ala-Asp (DEAD). The CrhR DEAD-box RNA helicase, the object of studies in this thesis, does not contain N-terminal extension, but the RNA helicase core of its structure resembles the general structure of helicases from the SF2 family. $crhR_{TR}$ mutant (Rosana *et al.*, 2012) lacks the RecA-like domain 2 and the C-terminal extension.

to the family due to the presence of other conserved motifs (Linder, 2006; Fairman-Williams *et al.*, 2010).

Despite very high conservation of the helicase core structure, a wide array of biochemical activities has been reported for the proteins from the DEAD-box family. DEAD-box proteins are genuine helicases that use ATP to bind and unwind RNA duplexes (Kuhn *et al.*, 1979). However, there are several restrictions for this process, such as unwinding of the duplexes with less than two helical turns or inability of some helicases to unwind duplexes with more than 10 or 12 base pairs (Jarmoskaite and Russell, 2011). There are also other factors that affect unwinding efficiency like increasing duplex stability (Rogers *et al.*, 1999; Rogers *et al.*, 2001) or presence of single stranded extensions (Bizebard *et al.*, 2004; Yang and Jankowsky, 2006). DEAD-box helicases are distinct from other RNA or DNA helicases due to their specific unwinding mode termed local strand separation (Yang *et al.*, 2007). DEAD-box proteins do not unwind duplexes based on the translocation on the RNA (Rogers *et al.*, 1999; Bizebard *et al.*, 2004; Yang and Jankowsky, 2006; Tijerina *et al.*, 2006; Jankowsky, 2011; Jarmoskaite and Russell, 2011). Instead, they directly load on the duplex region and then pull the strands apart (Yang and Jankowsky, 2006; Yang *et al.*, 2007).

Several DEAD-box helicases show not only unwinding of duplexes, but also possess annealing activity, at least *in vitro* (Rossler *et al.*, 2001; Chamot *et al.*, 2005; Yang and Jankowsky, 2005; Uhlmann-Schiffler *et al.*, 2006; Jankowsky and Fairman, 2007; Halls *et al.*, 2007). Annealing activity can be ATP-independent as in the case of eukaryotic helicases p68, p72 and Mss116 (Rossler

et al., 2001; Yang and Jankowsky, 2005; Halls *et al.*, 2007). However, annealing activity of eukaryotic DEAD protein Ded1 (Yang and Jankowsky, 2005) and cyanobacterial RNA helicase CrhR (Chamot *et al.*, 2005) appears to be dependent on ATP-hydrolysis, as shown *in vitro.* As a part of their annealing activity some DEAD-box helicases can also promote active strand-exchange in the substrate RNA molecule, which also appears to be either ATP dependent (Chamot *et al.*, 2005) or not (Rossler *et al.*, 2001).

As a part of two main biochemical activities that DEAD-box proteins perform, such as unwinding and annealing of the RNA, they also possess ATPase activity and ability to displace proteins from RNA. Purified and biochemically characterized DEAD-box RNA helicases possess an ATPase activity, that is stimulated by or dependent on RNA substrate binding (Cordin *et al.*, 2006). As described above, one or both helicase main biochemical activities appear to be ATP-dependent. This differs from one helicase to another and so far has been shown only *in vitro*. ATP-hydrolysis also drives protein displacement from an RNA molecule. Proteins can be displaced from structured or unstructured RNA by DEAD RNA helicases, which suggests that duplex unwinding is not required for this activity (Fairman *et al.*, 2004).

Knowledge about a wide array of biochemical activities of DEAD-box helicases obtained from various mechanistic studies was used to devise physical models of their function (Iost and Dreyfus, 2006; Karow and Klostermeier, 2010; Linder and Jankowsky, 2011; Lehnik-Habrink *et al.*, 2013).

1.3.2 Cellular functions of DEAD-box helicases during abiotic stress

Most of the known eukaryotic and bacterial DEAD-box proteins have been assigned functions in one or more biological processes, however the molecular basis of those functions still remain a challenge for researchers. DEAD-box proteins as many other helicases usually function within complexes containing dozens or even hundreds of components. It is very important to know how biochemical functions of the DEAD-box helicases are modulated by other factors within those multicomponent complexes. It is mostly impossible to isolate or reconstitute the whole complex and thus most of the studies are restricted to DEAD-box helicases working in complete isolation or in the presence of only a few cofactors. Nevertheless, a number of models exist today to demonstrate how DEAD-box proteins participate in almost all aspects of RNA metabolism, from transcription to degradation.

For instance, eukaryotic helicases p68 and p72 were shown to act as co-repressors or co-activators of transcription and to interact with various transcription factors and nuclear receptors (Endoh *et al.*, 1999; Watanabe *et al.*, 2001; Wilson *et al.*, 2004). There is evidence available for p68 and p72 helicases working as transcriptional co-regulators for a number of transcription factors including estrogen receptor α, tumor suppressor p53, myogenic regulator MyoD and transcription factor essential for osteoblast development (Fuller-Pace and Ali, 2008). It was also shown that p68 and p72 can act as transcriptional repressors using different mechanisms, including repression through association with the well-established transcriptional repression protein histone deacetylase1 (HDAC1)

(Wilson *et al.*, 2004). It is very interesting to note that ATPase or helicase activity of p68 is not required for this transcriptional control. Therefore, DEAD helicases may or may not need their enzymatic activities in order to function during particular biological process (Cordin *et al.*, 2006). Another DEAD-box helicase, Dbp5, has a function in transcription and interacts with yeast transcription machinery (Estruch and Cole, 2003). However, in the case of Dbp5, it was suggested to play role as an RNA chaperone that exports mRNA through the nuclear pore (Zhao *et al.*, 2002; Weirich *et al.*, 2004).

DEAD-box helicases were also shown to play crucial roles at key steps of RNA splicing. Some eukaryotic DEAD-box proteins participate in the early events of pre-spliceosome assembly and its maturation into the active spliceosome (Luking *et al.*, 1998; Silverman *et al.*, 2003; Rocak and Linder, 2004). Ribosome biogenesis is another complex process that requires DEAD-box proteins. During ribosome biogenesis DEAD-box helicases play role in the rRNA maturation step in both eukaryotes and prokaryotes (Kressler *et al.*, 1999; de la Cruz *et al.*, 1999).

The ability to resolve RNA secondary structures enable DEAD-box helicases to take an active part in translation and RNA decay. It was observed that DEAD helicases elF4A and Ded1 from *S. cerevisiae* and their homologues in higher eukaryotes are essential during translation initiation (Linder, 2003). It is proposed that in order to aid in the scanning of mRNA by the 43S ribosomal subunit in eukaryotes, these helicases melt secondary structures and remove other proteins bound to the mRNA (Berthelot *et al.*, 2004). This biochemical activity of DEAD-box proteins is also important in the RNA decay process. The *E. coli*

degradasome consists of three proteins, one of which is DEAD-box protein RhlB; the other two are ssRNA endonuclease RNaseE and 3' exonuclease PNPase (Py *et al.*, 1996; Carpousis, 2002). PNPase movement and subsequent cleavage of RNA are easily inhibited by the presence of secondary structures on the target RNA molecule. The DEAD-box helicase RhlB resolves secondary structures on the RNA in ATP-dependent manner, which allows subsequent degradation of those RNAs by PNPase enzyme (Coburn *et al.*, 1999).

All of the examples above show that DEAD-box helicases perform essential cellular roles and possess several housekeeping functions in the life of eukaryotic and prokaryotic organisms. In addition, there is a lot of evidence about the roles of DEAD-box helicases during specific stress conditions.

1.3.3 Stress induced DEAD-box helicases

In the last decade, it became obvious that RNA helicases are involved not only in housekeeping roles in the cell, but also participate actively in adaptation to stress environments. It was observed that RNA helicase expression changed in response to external stresses, suggesting that these proteins are involved in the cellular adaptation to new environments. As already mentioned above, the DEAD-box family is the largest subgroup of RNA helicases, which contains a number of proteins involved in the adaptation process to temperature shift, change in light intensity, salinity, nutrient depletion, etc.

Temperature change is among the most common stresses that bacteria encounter in the environment. We already possess a significant amount of

information about increase in growth temperature and the heat-shock effect, which does not require an active participation of DEAD-box RNA helicases. However, the cold-shock effect, which is also detrimental to the cell, often requires DEAD-box proteins with cold-shock proteins (Csp's) or alone for cell adaptation in all domains of life. Examples of cold induced RNA helicases that are potentially involved in cold adaptation of cells include CsdA in Gram-negative *E. coli* (Jones *et al.*, 1996), CshB and CshA in Gram-positive *Bacillus subtilis* (Beckering *et al.*, 2002), DeaD homologue in Antarctic methanogenic archaeon *Methanococcoides burtonii* (Lim *et al.*, 2000), DED1 in yeast *Saccharomyces cerevisiae* (Schade *et al.*, 2004) and two helicases in Gram-negative cyanobacteria: CrhC in *Anabaena* sp. strain PCC 7120 (Chamot *et al.*, 1999; Chamot and Owttrim, 2000) and CrhR in *Synechocystis* sp. PCC 6803 (Rosana *et al.*, 2012a). It is important to note that cold induction of those helicases does not depend on one absolute temperature, but rather is affected by temperatures below their growth optimum (Owttrim, 2013).

It was noticed that prokaryotes in general encode fewer RNA helicases than eukaryotic organisms, meaning that bacterial helicases may have multi-tasking roles and be involved in several biological pathways as a part of their cellular function. For instance, *E. coli* DEAD-box helicase CsdA is structurally related to three helicases in yeast, implying that CsdA is important in several aspects of bacterial metabolism. It was also observed that some bacteria lack CspA-related stress response proteins, but DEAD helicases may substitute for their functions. This is the case with cyanobacteria that lack cold shock proteins

Csp's required for acclimation to the cold temperatures in *E. coli* and other bacteria. However, cyanobacteria have cold-inducible DEAD-box RNA helicases: CrhC in *Anabaena* sp. PCC 7120 or CrhR in *Synechocystis* sp. PCC 6803, which may potentially substitute for the function of Csp's during cold temperature adaptation.

Cold stress is not the only external factor that induces helicase expression. There are also examples of helicases in different organisms that are induced by other environmental stresses in addition to low temperature, but this list is very limited, especially in the prokaryotic domain. For example CrhR DEAD-box RNA helicase expression is induced by various stresses that influence redox status of the photosynthetic electron transport chain: cold temperature, dark/light cycles and salinity change in cyanobacterium *Synechocystis* sp. PCC 6803 (Kujat and Owttrim, 2000; Chamot *et al.*, 2005). There are also some other factors that impact helicase expression, such as presence of lithium in the case of *S. cerevisiae* helicase Tif2 (Montero-Lomeli *et al.*, 2002) or dehydration and wounding for unique DEAD-box helicase PDH45 in higher plants (Sanan-Mishra *et al.*, 2005). However, three last helicases mentioned above also respond to a decrease in growth temperature (Kujat and Owttrim, 2000; Montero-Lomeli *et al.*, 2002; Sanan-Mishra *et al.*, 2005). It was observed that some of these external stresses are very similar to low temperature stress based on what cellular response they cause. For instance, salt stress stabilizes secondary structures on RNA, which raises the need for RNA unwinding similar to cold (Vinnemeier and Hagemann, 1999; Mukhopadhyay *et al.*, 2006) and lithium toxicity causes inhibition of

protein synthesis at the level of translation initiation (Vinnemeier and Hagemann, 1999) similar to cold stress. Even though some helicases are proposed to be induced by different stress conditions, it may not be entirely true. These stress conditions may activate the same cellular response pathway, which then affects helicase expression and therefore helicase appears to be induced by each condition activating that cellular response.

There is a lot of information about the induction of DEAD-box helicases in various organisms; however the exact cellular function of those proteins during cold shock and other external stress conditions is not entirely understood. Based on the biochemical analysis of these helicases it can be proposed that DEAD-box proteins, similar to Csp's, use their RNA chaperone activity to resolve secondary RNA structures, which are concominantly stabilized by the lower temperatures.

In order to further examine the function and regulation of this family of helicases, various model organisms were used, including several cyanobacterial species.

1.4 DEAD-box helicases in cyanobacteria

1.4.1 *Synechocystis* sp. PCC 6803

The cyanobacterium *Synechocystis* sp. PCC 6803 (hereafter *Synechocystis*) is a powerful model for studying stress responses in photosynthetic organisms and bacteria in general. Cyanobacteria are Gram negative photosynthetic bacteria, whose ancient ancestor is thought to be a progenitor of chloroplasts in higher plants (Giovannoni *et al.*, 1988). Unicellular, fresh water

bacteria from *Synechocystis* genus belongs to the Chroococcacean subgroup of cyanobacteria that was extensively studied in the last decades.

Synechocystis was the first autotrophic organism to have its genome completely sequenced. Its 3,573,470 bp genome contains 3264 open reading frames (ORFs), approximately 60% of which have been annotated (Kaneko *et al.*, 1996; Okajima *et al.*, 2006; Das *et al.*, 2012). *Synechocystis* is a naturally transformable organism that can take up and incorporate exogenous DNA into its genome by homologous recombination (Grigorieva and Shestakov, 1982). Availability of full information about its genome, and natural transformability made *Synechocytsis* a popular model system for genetic and biochemical studies of various metabolic pathways and photosynthesis (Pakrasi, 1995).

There are three DEAD-box helicases that have been studied in cyanobacteria: CrhB and CrhC in *Anabaena* sp. PCC 7120 (Chamot *et al.*, 1999) and helicase CrhR in *Synechocystis* (Kujat and Owttrim, 2000). CrhB expression resembles expression of CrhR as they are both expressed under broad range of conditions (Chamot *et al.*, 1999). CrhC is different from the other two, since it exhibits elevated levels only in the cold and doesn't have any basal expression at normal growth temperature (Chamot *et al.*, 1999). CrhR is the only DEAD-box RNA helicase present in *Synechocystis* cells, which will be discussed in more detail in the next section.

1.4.2 Cyanobacterial DEAD-box RNA helicase CrhR

The *Synechocystis* genome encodes a single DEAD-box helicase named **C**yanobacterial **R**NA **H**elicase **R**edox or CrhR (Figure 1.1). Expression of this helicase is regulated by the redox status of the photosynthetic electron transport chain (Kujat and Owttrim, 2000) and is induced by the environmental stresses that cause enhanced reduction of the chain, such as light intensity, salt (Vinnemeier and Hagemann, 1999) and cold temperature (Suzuki *et al.*, 2000; Rosana *et al.*, 2012a). It was shown that CrhR transcript and protein levels increase in response to the presence of light (Kujat and Owttrim, 2000) (Figure 1.2). In the case of salinity, CrhR transcript increases 5 fold in response to increased salt concentration after 3 h of induction (Vinnemeier and Hagemann, 1999). However, an even more profound effect on CrhR expression is observed during cold-shock, as CrhR transcript increases about 8-fold only after 1 h (Rosana *et al.*, 2012a; Rosana *et al.*, 2012b) (Figure 1.2). Redox-regulated helicase CrhR does not have known true homologues among other cyanobacteria. Its core is similar to *E. coli* helicase CsdA, however it possesses unique C-terminal extension that may be responsible for the ability of CrhR to catalyze not only unwinding of secondary RNA structures, as most of other DEAD-box helicases, but also annealing and strand exchange (Chamot *et al.*, 2005) (Figure 1.1).

The exact cellular function and targets of CrhR still remain unknown. In order to unravel this complex biological question various mutants in the *crhR* gene were constructed and their effect on the *Synechocystis* morphology and physiology was observed. Since a decrease in temperature has the most profound effect among all the external stresses on the induction of this helicase, cold-shock

Figure 1.2: *crhR* expression in response to abiotic stress. Abiotic stresses used for the purposes of this thesis, including light intensity and temperature, affect the redox status of the photosynthetic electron transport chain, which in turn affects expression of the CrhR DEAD-box RNA helicase in *Synechocystis* cells (Kujat and Owttrim, 2000). Levels of *crhR* expression in the wild type and $crhR_{TR}$ mutant are indicated using solid and dotted lines respectively. Levels of *crhR* and $crhR_{TR}$ transcript and proteins levels from *Synechosytis* strains initially grown at 30^{o}C and after cold shock at 20^{o}C are adapted from Rosana *et al.* (2012). The accumulation of CrhR and $CrhR_{TR}$ protein observed when cells are transferred back to 30^{o}C after cold shock, represent preliminary data for this thesis. These data were extended in this thesis to analyze the process that controls the rapid decrease of protein levels at 30^{o}C in wild type cells.

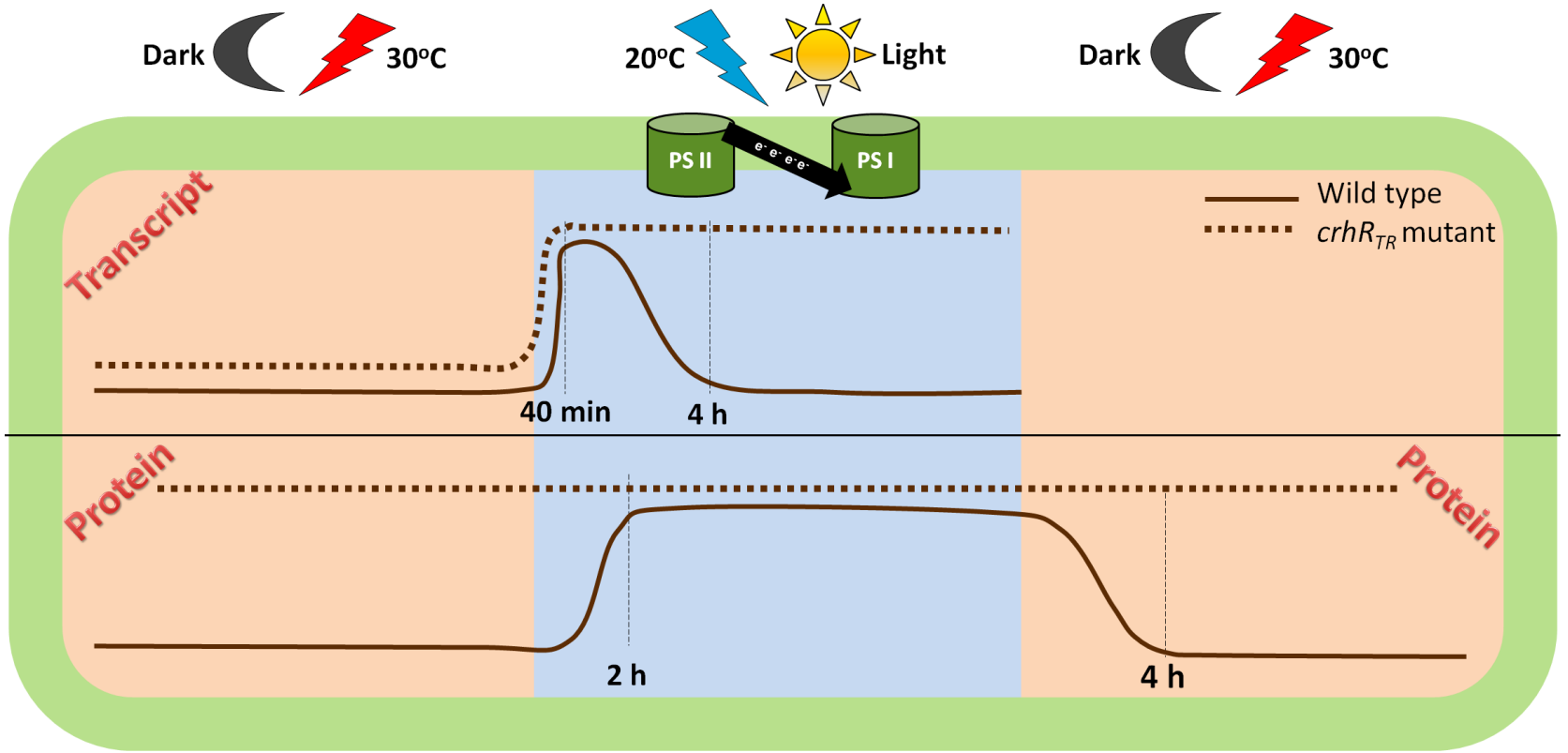
Dark
30°C
20°C
Light
Dark
30°C
PS II
e- e- e- e-
PS I
Transcript
Wild type
crhR_TR mutant
40 min
4 h
Protein
Protein
2 h
4 h

was used to observe the effects it causes in wild type *Synechocystis* and a partial *crhR* mutant (Rosana *et al.*, 2012a) (Figure 1.1 and 1.2). It was observed that *crhR* mutation has drastic effects on the cellular physiology and morphology that are visible at normal temperature (30^{o}C) as well as at cold shock (20^{o}C) temperatures, indicating that CrhR may have roles at both temperatures. The major physiological effect of *crhR* mutation was rapid termination of photosynthesis at low temperature, resulting in impaired cell growth, decreased cell size, DNA content and viability of the mutant. This phenomenon was demonstrated by inability of the mutant to actively fix carbon at the required rate (Rosana *et al.*, 2012a). This study suggested that CrhR helicase activity may be involved in photosynthesis at all temperatures, but is crucial specifically in the cold.

Since CrhR was shown to have an effect during cold adaptation of the *Synechocystis* cells, other studies were done to explore this topic in more detail. The latest CrhR-related published research was studying the effect of low temperatures on the expression of this DEAD-box helicase (Rosana *et al.*, 2012b). This study suggests that CrhR expression is regulated at several levels in response to decreased temperature. It was shown that a major aspect of *crhR* transcript abundance in the cold is its mRNA stabilization, similar to other cold shock proteins such as CspA and CsdA in *E. coli* (Goldenberg *et al.*, 1996; Prud'homme-Genereux *et al.*, 2004). Induction of *crhR* expression was also shown to be related to its transient transcript accumulation at 20^{o}C, which is a common observation for cold induced genes in bacterial systems (Sato, 1995; Goldenberg *et al.*, 1996; Aguilar *et al.*, 1999). It was proposed by Rosana *et al.* (2012b) that there is also a

mechanism that regulates CrhR protein abundance in response to temperature changes, involving either altered translational efficiency or proteolysis. This thesis provides data to support the hypothesis that CrhR protein levels are autoregulated by proteolysis in response to temperature upshift.

1.4.3 Proteolysis as a method of protein regulation

Increased expression of stress-induced proteins essential for environmental adaptation has the same importance as the subsequent limitation of this response when external conditions return to a more "normal" state. For instance, cold-induced proteins required for regulation of bacterial cold acclimation need to be eliminated when growth temperature increases. In other cases, proteins required for the heat shock response in bacteria need to be degraded, once the cell is adapted to new elevated growth temperatures.

Change in transcription of stress proteins is a rapid process, however it does not translate into rapid reduction of protein levels. This happens simply because most of bacterial proteins are stable and their concentration can remain high even after a reduction in transcription. In this case, an additional level of regulation is required: proteolytic degradation of the key stress-induced proteins upon return to favorable growth conditions.

There are many examples of proteolytic regulation of stress proteins, some of which are related to temperature stress. A prime example is the major regulator of the heat shock response in *E.coli*, transcription factor σ^{32}. Proteolytic degradation of σ^{32} coupled with slow translation maintains a basal low level at

normal growth temperature (Tomoyasu *et al.*, 1995). However, the level of σ^{32} is dramatically increased after heat shock, to allow rapid production of the heat-shock proteins (Straus *et al.*, 1990). This increase in σ^{32} protein level is transient and returns to basal after 10-15 min (Straus *et al.*, 1990). Return to the normal state is also regulated by proteolysis.

Another example of proteolytic regulation of the temperature induced protein involves cold shock protein CspC, which performs RNA chaperone activity during *E.coli* cold acclimation (Gur *et al.*, 2011). CspC is produced at a basal level at normal growth temperatures and is induced during cold shock of bacterial cells. One of the functions of CspC is thought to be stabilization of mRNAs encoding the protein chaperones GroE and DnaK. The levels of GroE and DnaK are induced by two factors: increase in temperature and increase in activity of σ^{32}, which is also temperature regulated. CspC is needed to stabilize mRNAs of GroE and DnaK, once they are transcribed upon the temperature shift. As mentioned above, the heat shock response is transient in nature and involves rapid return to the steady-state levels after temperature induction (Straus *et al.*, 1989; Straus *et al.*, 1990; Tomoyasu *et al.*, 1998; Meyer and Baker, 2011). CspC is rapidly degraded by proteolysis during heat stress, which leads to lowered stability of GroE and DnaK mRNAs and subsequent cessation of the production of these heat-shock proteins (Phadtare and Inouye, 2001; Shenhar *et al.*, 2009). Similar proteolytic regulation was recently observed in *E. coli* exoribonuclease RNase R, which is induced and stabilized in the cold, but at normal growth

temperature it becomes sensitive to proteolytic degradation (Cairrao *et al.*, 2003; Chen and Deutscher, 2010).

As mentioned in the previous section, CrhR is a novel example of a protein regulated by proteolysis, which is discussed in this thesis. To my knowledge, CrhR represent the first DEAD-box helicase that is autoregulated by this mechanism in response to abiotic stress.

1.5 Thesis objective

In this thesis, I identify proteolysis as a major contributor involved in regulation of differential CrhR protein expression at two temperatures, 30^{o}C and 20^{o}C (Figure 1.2). Recent analysis by Rosana *et al.* (2012b) showed that *crhR* expression and CrhR protein levels increase when *Synechocystis* cells are transferred from warm (30^{o}C) to cold temperatures (20^{o}C) (Figure 1.2). It was shown that *crhR* transcript as well as CrhR protein remains at a basal low level at 30^{o}C, however upon transfer to 20^{o}C, which is considered to be a cold shock temperature for *Synechocystis*, the level of transcript significantly increases. The initial rapid increase in *crhR* transcript is transient and returns to its basal level after 4 h at 20^{o}C. The situation is different with CrhR protein in the cold: its levels rapidly increase until they reach their maximum around at around 3 h of incubation at 20^{o}C (Rosana *et al.*, 2012b) (Figure 1.2). For the remaining time at 20^{o}C, CrhR protein levels remain high for as long as 72 hours with very low transcript level and even without any *de novo* protein synthesis due to the addition of translation inhibitors (Rosana, personal communication, Rosana *et al.*, 2012b),

indicating very high stability of CrhR protein. Preliminary data for my project indicated that CrhR protein levels rapidly decrease if a *Synechocystis* culture is transferred from 20^{o}C back to 30^{o}C (Figure 1.2). In just a few hours, levels of highly stable protein CrhR rapidly reduce to basal level observed after prolonged incubation at 30^{o}C, suggesting that there is active degradation mechanism involved. I used several *in vivo* and *in vitro* approaches to determine that there is proteolytic degradation machinery that is only present and active at 30^{o}C that degrades CrhR protein at warm temperatures in wild type cells.

The *crhR$_{TR}$* mutant, that produces a truncated version of CrhR (CrhR$_{TR}$), was previously used to observe morphological changes in the cells due to the mutation (Rosana *et al.*, 2012a). This mutant has elevated levels of non-functional CrhR$_{TR}$ protein at all temperatures, even though the transcript level appears to be increased only in the cold (Figure 1.2). I used this mutant in my degradation experiments to determine that full length functional CrhR protein is required for its proteolytic degradation and therefore proteolysis of CrhR at 30^{o}C in the wild type is autoregulated.

In attempt to identify the proteases involved in this proteolytic degradation mechanism, I measured levels of FtsH and Clp proteases in *Synechocystis* at two temperatures and also pulled down interacting protein partners of CrhR.

I also constructed a complete deletion mutant and CrhR overexpression mutants to observe the effects of complete absence or presence of abnormal levels of CrhR helicase on *Synechocystis* growth and CrhR degradation process.

As an additional side project, I determined that CrhR protein localizes to the region of the thylakoid membranes.

The findings presented in this thesis identify that a proteolytic mechanism controls differential expression of CrhR in response to temperature change. To my knowledge, CrhR represents the first DEAD-box helicase that is autoregulated by a proteolytic mechanism. In addition, the data obtained through localization and pull-down studies combined with the current knowledge of CrhR brings more insights into the possible cellular function of the DEAD-box RNA helicase CrhR in *Synechocystis* sp. PCC 6803.

II. MATERIALS AND METHODS

2.1 Strains, plasmids and growth conditions

2.1.1 Cyanobacterial strains and plasmids

The *Synechocystis* sp. PCC 6803 strains used in this study include the wild type (WT) and two strains, in which *crhR* gene (slr0083) was inactivated, $crhR_{TR}$ mutant that produces a truncated, inactive version of the CrhR protein ($CrhR_{TR,}$ 27 kDa) (Rosana *et al*., 2012) and a complete deletion mutant (Δ*crhR*). WT, Δ*crhR* and $crhR_{TR}$ expressing His-tagged CrhR protein (His-R) were also used in this study. These strains contained pMon36556 (Monsanto, St. Louis, USA) plasmid with 6xHis tagged *crhR* sequence under the regulation of the pNir promoter, called pMon-HisR (described in 2.2.2.).

2.1.2 Growth and maintenance of cyanobacterial strains

All *Synechocystis* strains were maintained on BG-11 medium (1.5 g/L $NaNO_3$, 0.04 g/L K_2HPO_4, 0.075 g/L $MgSO_4 \cdot 7H_2O$, 0.036 g/L $CaCl_2 \cdot 2H_2O$, 0.006 g/L citric acid H_2O, 0.006 g/L ferric ammonium citrate, 0.001 g/L EDTA, 0.002 g/L $NaCO_3$ and 1 mL of A5 microelements (2.86 g/L H_3BO_3, 1.81 g/L $MnCl_2 \cdot 4H_2O$, 0.222 g/L $ZnSO_4 \cdot 7H_2O$, 0.079 g/L $CuSO_4 \cdot 5H_2O$ and 0.040 g/L $CoCl_2 \cdot 6H_2O$)) plates containing 1% [w/v] Bacto agar and corresponding antibiotics if necessary (Allen and Stanier, 1968; Allen, 1968; Castenholz, 1988). Cyanobacteria on solid media were grown at 30^oC under constant illumination (30 mmol photons/m^2). To prepare liquid cultures, cells from a solid BG-11 medium

plate were used to inoculate 50 ml of liquid BG-11 medium with addition of the corresponding antibiotics, if required. Liquid culture (50 mL) at OD_{750}~1 were used to inoculate 300 ml of liquid BG-11 media. *Synechocystis* strains in liquid media were cultured photoautotrophically at 30^{o}C with continuous shaking at 200 rpm, under constant illumination (30 mmol photons/m^{2}) and bubbling with humidified sterile air (Chamot and Owttrim, 2000).

Media for both mutants and His-R expressing strains was supplemented with appropriate antibiotics, kanamycin (50 µg/ml) for Δ*crhR*, a mixture of spectinomycin and streptomycin (50 µg/ml each) for the $crhR_{TR}$ mutant. All His-R expressing strains (containing plasmid pMon-HisR) were also supplemented with gentamycin (10 µg/ml). For induction of CrhR expression, *Synechocystis* cells were cold stressed by incubating cells for 1.5-3 hours at 20^{o}C with shaking, aeration and constant light as described above.

2.1.3. *E. coli* strains and plasmids

pBluescript II SK(+) (Amp^{R}) (Stratagene, Santa Clara, USA) was used in the construction of Δ*crhR* mutant (described in 2.2.1.). pRSET-R (Amp^{R}) plasmid containing His-R (Chamot, personal communication) was used in the construction of pMon-HisR for constitutive His-R expression in *Synechocystis* strains (described in 2.2.2.).

The *E. coli* strain BL21 containing pLysS (Cm^R) and pRSET-R (Amp^R) was used for overexpression of exogenous His-R for *in vitro* degradation experiments (described in 2.3.1).

E. coli DH5α was used for the propagation of plasmid constructs. Constructed plasmids to be transformed into *Synechocystis* were cloned into *E.coli* DH5α with pRL626 (Cm^R, Km^R) (Elhai and Wolk, 1988; Elhai *et al*., 1997) helper plasmid before transformation into *Synechocystis. Synechocystis* possesses several restriction-modification systems that reduce transformation efficiency. pRL626 plasmid encodes methyltransferases necessary to methylate endonuclease cites on the transferred DNA. Therefore, transformation of prepared DNA constructs into *E. coli* with pRL626 plasmid ensures necessary plasmid methylation before transformation into *Synechocystis* cells.

E. coli J53/RP4 (Amp^R, Km^R) was used as a helper strain during cyanobacterial transformation by tri-parental mating (Ng *et al*., 2000), described in 2.2.3iii.

2.1.4 Growth and maintenance of *E. coli* strains

E. coli strains were maintained in 20% glycerol at -80^{o}C. *E. coli* cultures were streaked for single colonies from glycerol stocks and grown overnight at 37^{o}C on the LB plates (Luria Bertani broth media containing 5 g/L Bacto tryptone, 5 g/L yeast extract, 5 g/L NaCl, buffered with 1 mL of 1N NaOH, and 1.2% [w/v] Bacto agar). Media were supplemented with corresponding antibiotics

for antibiotic-resistant strains: ampicillin at 100 µg/ml ($LBAmp_{100}$), chloramphenicol at 30 µg/ml ($LBCm_{30}$) and kanamycin at 50 µg/ml ($LBKm_{50}$). Liquid LB (5 ml) with corresponding antibiotic(s) was inoculated with a single colony from an overnight plate and incubated at 37^{o}C for 12-24 h. For His-R overexpression 1 ml of the overnight culture was used to inoculate 100 ml of liquid LB media containing corresponding antibiotic. *E. coli* strains were maintained as frozen stocks in 20% glycerol at -86^{o}C.

2.2 Construction of the Δ*crhR* mutant and His-R expressing strains

2.2.1. Construction of the Δ*crhR* mutant

A diagram of the Δ*crhR* mutant construction is presented in Figure 3.4A. Two 1.5 kb fragments corresponding to sequences upstream of *crhR* open reading frame (ORF) ATG start codon and downstream of *crhR* TAA stop codon were amplified with PCR using OT1F (*Xba* I), OT1R (*Hind* III) and OT2F (*Hind* III), OT2R (*Xho* I) primers respectively (primer sequences are listed in Table 2.1). An annealing temperature of 52^{o}C was used for OT1F and OT1R primers and 62^{o}C for OT2F and OT2R primer pair. PCR products were purified with a QIAquick PCR purification kit (QIAGEN, Maryland, USA) and digested with *Xba* I, *Hind* III and *Xho* I (Fermentas, Burlington, Canada) respectively. Resulting fragments were ligated into pBluescript II SK (+) (Fermentas, Burlington, Canada) using *Xba* I and *Xho* I (Fermentas, Burlington, Canada) cut sites.

A 2.3 kb *Hind* III fragment encoding the Kanamycin (Km) resistant cassette was isolated from pBSL128 (Alexeyev *et al*., 1995). The fragment was ligated into *Hind* III digested pBluescript containing 1.5 kb *crhR* upstream and downstream fragments. This final construct, termed pBS-Δ*crhR*, was confirmed by sequencing and transferred into *E.coli* DH5α containing the pRL626 helper plasmid (Elhai and Wolk, 1988, Elhai *et al*., 1997). Transformation of cyanobacteria was carried out using the method adopted from Zang *et al*., (2007) (described in 2.2.3ii). To ensure every genome copy was inactivated, potential transformants were replated every week on the BG-11 solid media supplemented with gradually increasing concentrations of kanamycin (up to 150 µg/ml) over a period of four months. Complete deletion mutants were selected by screening for resistance to kanamycin (150 µg/ml) and sensitivity to cold temperature (20^{o}C). Complete segregation was verified by PCR using two primer sets: GWO74 and LPF45 at annealing temperature of 55^{o}C, dcsr11F and DC29 at annealing temperature of 60^{o}C (Table 1) and western blot analysis to show that CrhR protein was undetectable.

2.2.2. Construction of His-R expressing *Synechocystis* strains

The His-R expression plasmid was constructed by cloning the *crhR* ORF into pRSET A (Invitrogen) in frame with polyhistidine (6 x His) region using *BamH* I and *EcoR* I restriction sites, resulting in pRSET-R (Chamot, personal communication). The His-R sequence was isolated from pRSET-R with *Xba* I and *EcoR* I and ligated into pMon 36456 (Monsanto, St. Louis, USA) using the same

restriction enzyme sites. The final construct was verified by sequencing. The resulting plasmid, pMon-HisR, was transformed into *Synechocystis* wild type, Δ*crhR* and $crhR_{TR}$ mutant cells by triparental mating (Wolfgang Hess, personal communication) (described in 2.2.3iii). Expression of His-R protein was confirmed with western blot analysis using anti-CrhR and anti-His antibodies (described in 2.6.2).

2.2.3 Bacterial transformation

2.2.3i Chemical transformation of *E. coli*

Transformation of plasmids into competent *E. coli* was done chemically. Total volume of the ligation product was combined with 200 µl of chemically competent *E. coli* DH5α. The mixture was incubated on ice for 30 min. *E. coli* cells were heat shocked at 42^{o}C for exactly 2 min, followed by the addition of 800 µl of room temperature LB broth. Cell mixtures were then incubated at 37^{o}C for 1 h and aliquots were plated on selective LB plates containing antibiotic that corresponds to the antibiotic resistance cassette present on the transformed plasmid. Plates were incubated overnight at 37^{o}C. Surviving colonies were picked and inoculated into liquid LB medium with corresponding antibiotic. Liquid culture was incubated overnight at 37^{o}C, Qiagen plasmid miniprep kit (Qiagen, Maryland, USA) was used to isolate resulting plasmid. Presence of the correct construct was confirmed by restriction enzyme digestion and sequencing. Confirmed constructs were transformed into *Synechocystis* cells either by natural transformation or tri-parental mating (described in 2.2.3ii and 2.2.3iii).

2.2.3ii Natural transformation of *Synechocystis*

Transformation of cyanobacteria was carried out using the modified method described by Zang *et al*. (2007). *Synechocystis* cells were grown at 30^{o}C to mid-log phase, harvested by centrifugation at 6,000 rpm in a Janetzki T5 table top centrifuge (Jena Instruments Ltd., Surrey, Canada) for 15 min at 30^{o}C. Cells were washed with liquid BG-11 medium and resuspended in 400 µl of pre-warmed to 30^{o}C BG-11. Plasmid DNA was added to the cells to final concentration of 20 ng/µl. This mixture was incubated under the constant light at 30^{o}C for 5 hours and then plated on the BG-11 plates. BG-11 plates were incubated at 30^{o}C for 24 h. After this incubation, the BG-11 agar was lifted with a sterile spatula and underlayed with diluted antibiotic depending on the plasmid being transformed (5 µg/ml of kanamycin for pBS-Δ*crhR* construct for Δ*crhR* mutant construction). Every week surviving colonies were picked with a sterile toothpick and transferred to BG-11 plates with gradually increasing concentration of corresponding antibiotic (5-150 µg/ml of kanamycin for pBluescript construct for Δ*crhR* construction).

2.2.3iii Transformation of *Synechocystis* by tri-parental mating

Transformation of cyanobacteria was conducted using the method adopted from the Hess lab (personal communication with Wolfgang R. Hess, Freiburg, Germany). *Synechocystis* cells were grown at 30^{o}C to OD_{750}~0.9. *E. coli* strains used in the transformation: *E. coli* J53/RP4 (helper strain) and *E. coli* DH5α

(donor strain) containing plasmid of interest were grown in liquid LB supplemented with the corresponding antibiotic overnight at 37^{o}C. *E. coli* overnight cultures were diluted 1:40 with LB media without antibiotics to a final volume of 10 ml and incubated 2.5 h at 37^{o}C with shaking at 180 rpm. *E. coli* cultures were centrifuged at 2500 rpm for 8 min at room temperature and the resulting pellet was resuspended in 1 ml of LB without antibiotics. The total volume of helper and donor bacterial strains were combined and centrifuged at 2500 rpm for 5 min at room temperature. The pellet was resuspended in 100µl LB and incubated without shaking for 1 h at 30^{o}C. Eight hundred microliters of *Synechocystis* cells at OD_{750}~0.9 washed twice with warm LB were added to the tube with *E. coli*, resulting mixture of cells was harvested by centrifugation at 2500 rpm for 5 min at room temperature. The resulting pellet was resuspended in 30 µl of BG-11 medium. A sterile mixed cellulose ester 0.45 µm filter (Millipore, Billerica, USA) was placed on top of the BG-11 plate containing 5% LB without antibiotics. The cell mixture was plated on the filter and the plate was incubated overnight at 30^{o}C in the light. The filter was removed next day and placed on the BG-11 solid agar supplemented with a low amount of the corresponding antibiotics (3 µg/ml of gentamycin for pMon-HisR constructs). Every week surviving colonies were picked with a sterile toothpick and transferred to BG-11 plates with gradually increasing concentration of corresponding antibiotic (3-10 µg/ml of gentamycin for pMon-HisR constructs).

2.2.4 PCR amplification and sequencing and DNA isolation

2.2.4i PCR amplification

PCR amplification was performed using the primer pairs listed in section 2.2.1. Approximately 200 ng of genomic DNA from *Synechocystis* wild type cells was combined with 0.2 mM dNTPs, 1X HF Buffer (New England BioLabs, NEB, Ipswich, USA), 0.5 µM of forward and reverse primers and 1U of Phusion DNA polymerase (NEB, Ipswich, USA) and water to a total volume of 50 µl. The DNA was amplified in a Techgene Thermal Cycler (Life Sciences, Penzberg, Germany) for 30 cycles. Each cycle consisted of 10 sec denaturation at 98^{o}C, 30 sec annealing at 60-68^{o}C (the exact temperature was determined for each primer pair depending on their melting temperatures) and 30 sec of elongation at 72^{o}C. In addition initial denaturation was done at 98^{o}C for 30 sec and a final elongation at 72^{o}C for 10 min.

2.2.4ii DNA sequencing

DNA sequencing was performed using the BigDye Terminator v3.1 Cycle Sequencing Kit (Applied Biosystems, Carlsbad, USA). Plasmid DNA isolated using Qiagen plasmid mini prep kit (Qiagen, Maryland, USA), 500 ng was combined with 2 µl of BigDye premix (Thermo sequenase II DNA polymerase, ddNTPs, dNTPs, 200 mM Tris pH 9.0, 5 mM $MgCl_2$), 0.75X dilution buffer (200 mM Tris pH 9.0, 5 mM $MgCl_2$) and 5 pmol of the appropriate sequencing primer. DNA was amplified in the Techgene Thermal Cycler (Life Sciences, Penzberg, Germany) for a total of 25 cycles (each cycle consisted of 30 sec denaturation at 95^{o}C, 15 sec annealing at 50^{o}C and 1 min elongation at 60^{o}C).

The reaction was precipitated by the addition of 2 µl of NaOAc/EDTA (150 mM NaOAc, pH 8.0 and 225 mM EDTA) and 80 µl of ice cold 95% [v/v] ethanol for 15 min on ice. Precipitated samples were centrifuged at 14,000 rpm for 5 min at 4^{o}C. The resulting pellet was washed with 1 ml of ice cold 70% [v/v] ethanol and centrifuged again for 5 min at 14,000 rpm. The pellet was air dried and provided to the Molecular Biology Services Unit (University of Alberta, Edmonton, Canada) for automated sequencing on an Applied Bioscience 377 analyzer.

2.2.4iii Plasmid and genomic DNA extractions

To check the final constructs by PCR and sequencing plasmid DNA was extracted from *E. coli* cells using Qiagen plasmid mini prep kit per manufacturer's instructions (Qiagen, Maryland, USA).

Synechocystis Δ*crhR* mutant was confirmed with PCR using genomic DNA isolated from cyanobacterial cells. About 20 ml of mid-log cyanobacterial cells were pelleted at 3,000 rpm for 10 min at room temperature. Cell pellet was washed with STE buffer (0.1 M NaCl, 1 mM EDTA, 10mM Tris pH 8) and resuspended in 0.5 ml STE. Equal volume of glass beads, phenol and 0.2 % SDS was added to resuspended cell pellet. The resulting mixture was vortexed for 1 min with subsequent rest on ice for 1 min. Four cycles of vortexing and resting on ice were repeated. The mixture was centrifuged at 8,000 rpm for 5 min. Supernatant was treated with RNase (0.1 mg/ml) at 37^{o}C for 15 min. Phenol-chloroform extraction was done, followed by ethanol precipitation.

DNA was precipitated by adding 1/10 volume of sodium acetate pH 5.2 and 2.5 volumes of ice-cold 100 % ethanol. Mixture was well mixed and incubated at -20^{o}C for 30 min. Tubes with the mixture were centrifuged at 11,000 rpm at 4^{o}C for 15 min. Resulting pellet was washed with ice-cold 70 % ethanol and centrifuged briefly. DNA pellet was air-dried and resuspended in appropriate volume of sterile water.

2.3 CrhR degradation experiments

2.3.1 *In vitro* degradation experiments

Wild type or $crhR_{TR}$ mutant cells were grown at 30^{o}C (warm) in liquid BG11 media to mid-log phase, one-half of the culture was transferred to 20^{o}C (cold) for 3 h. Cells were harvested by centrifugation at the growth temperature and the pellets resuspended in cyanobacterial protein extraction buffer B (CPEB B) (20 mM Tris-HCl pH 8.0, 100 mM KCl and 1 mM $MgCl_2$). An equal volume of Dyno-Mill Lead-free 0.2-0.3 mm glass beads (Impandex Inc., Clifton, USA) and DTT to a final concentration of 3 mM were also added to the resuspended cells. Cells were mechanically lysed by ten cycles of vortexing at top speed for 30 sec followed by 30 sec in an ice water bath. Lysates were clarified by centrifuging for 15 min at the corresponding growth temperature. The Bradford assay was used to determine protein concentrations in the lysates. Cold and warm lysates with equal protein amounts were mixed and incubated in water bath at 30^{o}C for up to 4 h, alternatively cold lysate was incubated alone at 30^{o}C as a control. Aliquots of the mixtures were removed at 0, 0.5, 1, 2, 3, 4 h and immediately quenched by

addition of one-third volume of 3x SDS-PAGE loading dye (125 mM Tris, pH 6.8, 4% [w/v] SDS, 20% [v/v] glycerol, 10% [v/v] β-mercaptoethanol and 0.02% bromophenol blue). The samples were separated by 10% SDS-PAGE and CrhR detected by western blot analysis.

In *in vitro* degradation experiments involving His-R purified from *E. coli*, *E. coli* BL21 containing pLysS and pRSET-R plasmid (Chamot, personal communication) was used as a source of exogenous His-R protein. His-R was affinity-purified using a Ni-column (Qiagen, Maryland, USA) (described in 2.3.2).

2.3.2 Overexpression and affinity purification of His-R from *E. coli*

An overnight *E. coli* culture expressing His-R from pRSET-R was diluted 100-fold in liquid LB medium, grown at 37^{o}C to an OD_{600} of 0.4-0.6 and induced with IPTG at final concentration of 1 mM. Induced cultures were grown for an additional 4 h and harvested by centrifugation at 6,000 rpm in a Janetzki T5 table top centrifuge (Jena Instruments Ltd., Surrey, Canada) for 15 min. Cell pellet were stored at -86^{o}C until needed.

Cell pellets were thawed on ice and resuspended in the Ni-column specific lysis buffer (50 mM NaH_2PO_4, 300 mM NaCl and 50 mM Imidazole) and the ells were lysed by sonication with a Sonic 2000 sonicator (B. Braun, Melsungen, Germany) at 4^{o}C. Lysis was done by sonication for 15 sec followed by 30 sec in an ice water bath for 4 consecutive cycles. Lysates were clarified by

centrifugation at 14,000 rpm for 15 min at 4^{o}C and the supernatant was used for affinity purification of His-R protein.

His-R was purified on a Ni-NTA column (Qiagen, Maryland, USA). Ni-beads were first equilibrated with the lysis buffer (50 mM NaH_2PO_4, 300 mM NaCl and 50 mM Imidazole). Cell lysates were incubated with equilibrated Ni-beads for 1 h at 4^{o}C with gentle shaking. After binding, beads were washed 5 times with the wash buffer (50 mM NaH_2PO_4, 300 mM NaCl and 75 mM Imidazole). Each time beads were pulse centrifuged using Eppendorf 5415D centrifuge (Eppendorf, Hamburg, Germany) and the wash was discarded without disturbing the beads. Washed beads were incubated with elution buffer (50 mM NaH_2PO_4, 300 mM NaCl and 250 mM Imidazole) on ice for 30 min to elute bound proteins.

2.3.3 *In vivo* degradation experiments

Synechocystis wild type or the *crhR*$_{TR}$ mutant was grown at 30^{o}C to mid-log phase in liquid BG-11 medium. The culture was transferred to 20^{o}C incubator and 15 ml aliquots of culture were taken at indicated time points (0, 0.5, 1, 3, 6, 12, 24 h). Aliquots were centrifuged at 20^{o}C and pellets were frozen at -86^{o}C. After 24 h of incubation at 20^{o}C, cultures were transferred back to 30^{o}C and 15 ml aliquots were taken at 0.5, 1, 2, 3, 6, 12, 24 h, centrifuged at 30^{o}C and cell pellets were stored at -86^{o}C for further mechanical protein extraction (described in 2.3.1) and western blot analysis (2.6.2).

2.3.3i *In vivo* degradation experiment with addition of translation inhibitors

Synechocystis wild type cells were grown at 30^{o}C to mid-log phase in liquid BG-11 medium. The culture was divided in three parts and all of them were transferred to 20^{o}C. Fifteen millilitres aliquots of cultures were taken after 0, 1, 2 and 3 h. Aliquots were centrifuged at 20^{o}C and pellets were frozen at -86^{o}C. At the 2 h time point at 20^{o}C chloramphenicol (250 µg/ml) or kanamycin (200 µg/ml) were added to one third of the culture. After 3 h of incubation at 20^{o}C all three cultures were transferred back to 30^{o}C and aliquots were taken after 0.5, 1, 2, 3 and 4 h, centrifuged at 30^{o}C. Cell pellets were stored at -86^{o}C.

2.3.3ii *In vivo* degradation experiment with incubation in the dark

Synechocystis wild type cells were grown at 30^{o}C to mid-log phase in liquid BG-11 medium. The culture was divided in half and both halves were transferred to 20^{o}C. Fifteen millilitres aliquots of cultures were taken after 0, 1, 2 and 3 h. Aliquots were centrifuged at 20^{o}C and pellets were frozen at -86^{o}C. After 3 h of incubation at 20^{o}C both halves of the culture were transferred to 30^{o}C and one of the flasks was wrapped with aluminum foil (0.024 mm thick, Reynolds Wrap, Lake Forest, USA) to imitate complete darkness. Aliquots were taken from both flasks at 0.5, 1, 2, 3 and 4 h of incubation at 30^{o}C with or without light. Aliquots were centrifuged at 30^{o}C and cell pellets were stored at -86^{o}C.

2.4 Pull-down of CrhR-interacting proteins

2.4.1 Cyanobacterial protein extraction using French press lysis

Synechocystis cells, specifically Δ*crhR* and Δ*crhR* His-R mutants (300 ml of each culture), were grown at 30^{o}C in liquid BG-11 medium (supplemented with kanamycin 50 µg/ml and gentamycin at 10 µg/ml respectively) to mid- log phase, transferred to 20^{o}C for 1.5 h. After cold shock for 3 h at 20^{o}C, cells were harvested at 6,000 rpm and cell pellets resuspended in 15 ml of cold Buffer R (20 mM Tris-HCL pH 8.0, 150 mM KCl, 5 mM EDTA, 1 mM DTT) containing complete mini-protease inhibitor cocktail (Roche, Penzberg, USA). Cells were lysed three times by passage through a French pressure cell (SLM Aminco, Rochester, USA) at 6.9 mPa. Lysates were clarified by centrifugation at 14,000 rpm for 20 min at 4^{o}C. Supernatant (soluble fraction) and pellet (membrane fraction) resuspended in Buffer R with protease inhibitor cocktail were immediately used for affinity purification of proteins interacting with CrhR (described in 2.4.2ii).

2.4.2 Affinity purification of CrhR- interacting proteins

2.4.2.i Coupling anti-CrhR antibody to protein A immobilized on sepharose beads

Coupling of anti-His antibody (Sigma-Aldrich, St. Louis, USA) to protein A immobilized on sepharose beads was done as described in Harlow and Lane (1988). Briefly, 400 mg of lyophilized protein A immobilized on Sepharose CL-

4B (Sigma-Aldrich, St. Louis, USA) were swollen for 30 min at room temperature in 10 ml of immunoprecipitation coupling buffer (100 mM $NaHCO_3$, 50 mM NaCl, pH 8.3). Anti-Histidine (anti-His) antibody (Sigma-Aldrich, St. Louis, USA) was added to the swollen beads at a final dilution of 1:50 and the mixture of beads and antibody was incubated at room temperature for 60 min with continuous gentle rotation. The beads were washed twice with 10 volumes of borate buffer (0.2 M Sodium borate, pH 9) followed by centrifugation at 1,000 rpm for 5 min at room temperature. The pellet was resuspended in 10 volumes of borate buffer, dimethyl pimelimidate dihydrochloride (Sigma-Aldrich, St. Louis, USA) was added to a final concentration of 20 mM. The mixture was incubated for 30 min at room temperature to allow for crosslinking. Crosslinking was halted by washing the beads twice in 0.2 M ethanolamine pH 8.0 (Sigma-Aldrich, St. Louis, USA) and then incubating in ethanolamine for 2 h at room temperature with continuous gentle rotation. Following the incubation, beads were pelleted at 11,000 rpm for 1 min at room temperature, washed with 10 volumes of Buffer R and centrifuged at 1,000 rpm for 1 min. The beads were used for the co-immunoprecipitation procedure.

2.4.2.ii Co-immunoprecipitation of CrhR and interacting proteins

Protein A-anti His conjugated beads coupled (2.4.2i) were combined with soluble and membrane lysis fractions (2.4.1) and the mixture was incubated for 60 min at 4^{o}C with gentle agitation. Beads were pelleted at 6,000 rpm for 5 min at 4^{o}C; supernatant was collected as a column “flow through” sample. Beads were

washed 5 times with 10 ml of cold Buffer R. His-R and proteins that potentially interact with it were eluted from the column by incubating beads in 1 ml of Elution Buffer B (0.2 M Na_2HPO_4, 0.1 M Citric acid, pH 4.5) for 10 min on ice. Beads were pelleted by centrifugation at 6,000 rpm for 5 min at 4^{o}C and the supernatant was collected. A second elution was performed in the same conditions for 15 min. After the second elution beads were boiled with 1X SDS loading dye for 5 min to generate "Boiled beads" fraction. SDS loading dye was collected from the beads and stored at room temperature.

2.4.3 TCA protein precipitation

Proteins from "column flow through" sample and both eluates were concentrated by TCA precipitation before separating on the SDS-PAGE. The whole volume of "flow through" fraction was used, while the two elutions were combined together prior to precipitation. One volume of each sample was mixed with one-tenth volume of TCA and one-tenth volume of deoxycolate at 10 mg/ml. Mixtures were incubated on ice for 30 min. Samples were pelleted at 14,000 rpm for 15 min at room temperature and washed two times with ice cold acetone. Samples were centrifuged at 14,000 rpm for 5 min at room temperature and pellets were air-dried for 5 min. Resulting pellets from "flow through" fraction and combined elutions, were each resuspended in 50 µl of 0.1M DTT/CO_3 and mixed with one-third of 3xSDS loading buffer. Proteins were separated by SDS-PAGE, followed by overnight Commassie staining as described in 2.6.3.

2.4.4 Mass spectrometry identification of proteins interacting with CrhR

Commassie stained gels were submitted to the Institute for Biomolecular Design in the Biochemistry Deptartment of the University of Alberta (Edmonton, Canada). Trypsin digestion and mass spectrometry analysis was performed as follows (details of the procedure are provided by Jack Moore, Biochemistry Department, University of Alberta, Edmonton, Canada).

The excised gel bands were destained twice in 100 mM ammonium bicarbonate/acetonitrile (50:50). The samples were then reduced (10 mM BME in 100 mM bicarbonate) and alkylated (55 mM iodoacetamide in 100 mm bicarbonate). After dehydration, trypsin (6 ng/µl) was added to cover the gel pieces and the digestion was allowed to proceed overnight at room temperature. Tryptic peptides were first extracted from the gel using 97% water/2% acetonitrile/1% formic acid followed by a second extraction using 50% of the first extraction buffer and 50% acetonitrile.

Fractions containing tryptic peptides dissolved in aqueous 25% v/v ACN and 1% v/v formic acid were resolved and ionized by using nanoflow HPLC (Easy-nLC II, Thermo Scientific, Waltham, USA) coupled to the LTQ XL-Orbitrap hybrid mass spectrometer (Thermo Scientific, Waltham, USA). Nanoflow chromatography and electrospray ionization were accomplished by using a PicoFrit fused silica capillary column (ProteoPepII, C18) with 100µm inner diameter (300 Å, 5 µm). Peptide mixtures were injected onto the column at a flow rate of 3000 nl/min and resolved at 500 nl/min using 60 min linear ACN

gradients from 5 to 50% v/v aqueous ACN in 0.2% v/v formic acid. Mass spectrometer was operated in data-dependent acquisition mode, recording high-accuracy and high-resolution survey Orbitrap spectra using external mass calibration, with a resolution of 60 000 and *m*/*z* range of 400–2000. Ten most intense multiply charged ions were sequentially fragmented by using collision induced dissociation, and spectra of their fragments were recorded in the linear ion trap; after two fragmentations all precursors selected for dissociation were dynamically excluded for 60 s. Data were processed using Proteome Discoverer 1.3 (Thermo Scientific, Waltham, USA) and the Uniprot protein database was searched using SEQUEST (Thermo Scientific, Waltham, USA). Search parameters included a precursor mass tolerance of 10 ppm and a fragment mass tolerance of 0.8 Da. Peptides were searched with carbamidomethyl cysteine as a static modification and oxidized methionine as a dynamic modification.

The following criteria were applied to the mass spectrometry analysis data (Jack Moore, personal communication). All of the proteins that were identified in both experimental and control group were removed from the final data set. Within each identified protein two or more peptides should have high confidence. There should be not more than two missed cleavages for each high confidence peptide. Majority of identified peptides should be unique. The identified proteins had to meet all criteria above to remain in the final data set.

2.4.5 *In silico* prediction of CrhR-interacting proteins

Search Tool for the Retrieval of Interacting Genes/Proteins (STRING, www.string-db.org, accessed on November 15th, 2012) was used for the *in silico*

prediction of interacting partners for CrhR. High (0.700) confidence scores were used during the online search.

2.5 Localization of CrhR

2.5.1 Preliminary analysis of membrane association of CrhR protein

Wild type *Synechocystis* cells were grown in the liquid BG-11 media at 30^{o}C to mid-log phase. One-half of the culture was transferred to 20^{o}C for 2 h. Cells were harvested at 6,000 rpm at the growth temperatures and resuspended in a small volume of CPEB B. Mechanical lysis of cells was performed by vortexing in an equal volume of Dyno-Mill Lead-free 0.2-0.3 mm glass beads (Impandex Inc., Clifton, USA) for 30 sec followed by 30 sec rest period on ice for 15 cycles. To remove unbroken cells mixtures were centrifuged at 1,000 rpm for 1 min, supernatant was centrifuged at 14,000 rpm for 20 min to produce a crude membrane-containing pellet (membrane fraction). Equal volumes of this membrane fraction were treated with the indicated denaturants: STS extraction buffer (SDS, 0.4%; Triton X100, 0.5%; Sarkosyl, 0.5%), Na_2CO_3, 0.1 M (pH 11), NaCl, 1 M; CHAPS, 1%; Brij 35, 1%; Triton X100, 1%; and Triton X114, 2%. The treatment was done by resuspending membrane fraction in the buffers containing above detergents and incubating these mixtures on ice for 30 min except for STS extraction buffer which was performed at room temperature. Following incubation the samples were centrifuged at 14,000 rpm for 20 min at 4^{o}C and the resulting supernatant and pellet fractions were analyzed for the presence of CrhR by western blot analysis.

2.5.2 Immunoelectron microscopy (IEM)

IEM analysis to determine intracellular localization of CrhR was performed as decribed by Mustardy *et al.* (1996) with slight alterations. Wild type *Synechocystis* cells were grown in the liquid BG-11 media at 30^{o}C to mid-log phase. One-half of the culture was transferred to 20^{o}C for 2 h. Cells were harvested at 6,000 rpm for 10 min at the growth temperatures and fixed in a mixture of freshly prepared formaldehyde (4%, v/v) and glutaraldehyde (0.8%, v/v) in 0.1M sodium phosphate buffer (pH 7.2) for 60 min at the growth temperatures with gentle mixing. Cells were washed three times with 0.1M sodium phosphate buffer (pH 7.2) and dehydrated by incubation in ascending ethanol concentrations (30- 100%). Infiltration and embedding in LR white resin (London Resin Company Ltd., Reading Berkshire, England) was performed by incubation in LR White-ethanol mixture (1:1) for 2 h at room temperature, followed by overnight incubation in pure LR White at 4^{o}C. The next day incubation in pure LR White was performed at room temperature with two changes of pure LR White every 2 h followed by an overnight incubation in pure LR White at 50^{o}C. Serial ultrathin sections (76 nm) of the embedded cells in LR White were made using Ultramicrotome (Reichert-Jung Ultracut E, Wien, Austria). Sections were mounted on 200 mesh nickel grids with support (Formvar, Ted Pella Inc., London, England). Grids with mounted sections were incubated in PBG blocking solution (10 mM Sodium phosphate buffer pH 7.2, 600nM NaCl, 0.5% BSA) for 20 min at room temperature. Primary anti-CrhR antibody was

added to the PBG blocking solution (1:100 dilution) and incubated overnight at 4^{o}C. Grids were extensively washed with 0.1 M Sodium phosphate buffer (pH 7.2) and incubated overnight at 4^{o}C with goat anti-rabbit IgG coupled to 10 nm colloidal gold particles (Sigma-Aldrich, St. Louis, USA) diluted 1:20 in phosphate buffer as a secondary antibody. The next day sections were extensively washed with Tween 20 (0.1%) in phosphate buffer and stained with uranyl acetate (4%). Sections were examined at 70 kV with Philips/FEI Transmission electron microscope equipped with Gatan digital camera (Morgagni, FEI, Hillsboro, USA).

2.6 Protein Electrophoresis

2.6.1 SDS-polyacrylamide gel electrophoresis (SDS-PAGE)

Mixtures of extracted protein and 1xSDS loading buffer were denatured by boiling in a heat block for 4 min and separated by 10% SDS- PAGE. 10% SDS- PAG consisted of 3.75 ml of resolving gel (40% [w/v] acrylamide: bis (37.5:1) (Bio-Rad, Hercules, USA); 468.75 µl of 3M Tris, pH 8.8; 37.5 µl of 10% [w/v] SDS; 2.12 ml of mQH_2O; 187.5 µl of 1.5% [w/v] APS; 1.875 µl of TEMED) and 1.25 ml of stacking gel (125 µl of 40% [w/v] acrylamide: bis (37.5:1) (Bio-Rad); 315 µl of 0.5 M Tris-HCl, pH 6.8; 12.5 µl of 10% [w/v] SDS; 741.25 µl of mQH_2O; 62.5 µl of 1.5% APS; 1.25 µl of TEMED). The wells of the solidified gel were flushed extensively with SDS reservoir running buffer (25 mM Tris, 0.192 M glycine, 0.1% [w/v] SDS) before loading. Prestained protein ladder (2 µl) (Page-ruler^{TM}, Fermentas, Burlington, Canada) and 10-25 µg of protein,

depending on the experiment, were loaded and electrophoresed at 200 V for 0.5-1.5 h in SDS reservoir running buffer.

2.6.2 Western blot analysis

Proteins separated on SDS-PAGE gels that required immune-detection were immobilized to a solid matrix by electroblotting using a semi-dry transfer method. Once electrophoresis was finished, the SDS- PAGE gel was removed from the glass plates and soaked for 5 min in Tyler transfer buffer (25 mM Tris; 150 mM glycine, pH 8.3; 20% [v/v] methanol) along with four pieces of 3MM Whatman paper (Whatman, GE Healthcare, Wauwatosa, USA) and one 0.45 micron Hybond ECL nitrocellulose membrane (Amersham Pharmacia Biotech, Uppsala, Sweden), each of the same size as a gel. An electrophoretic transfer system ET-10 apparatus (Tyler Research Instruments, Edmonton, Canada) was used to transfer proteins from the gel to the membrane. Two pieces of soaked 3MM Whatman paper were placed into the apparatus, they were overlaid with the PAGE gel, the nitrocellulose membrane and two pieces of Whatman paper. Transfer was performed at 52 mA for 1 h. If more than one gel was transferred at the same time in the apparatus, the current was increased to 80 mA for 2 gels, 100 mA for 3 gels and 120 mA for 4 gels.

After transfer, the membranes were incubated at room temperature in BLOTTO blocking solution (1X TBS, 5% [w/v] skim milk powder, 0.02% [v/v] sodium azide) for about 30 min with gentle shaking. Membranes were incubated overnight at room temperature in 10 ml of fresh BLOTTO solution containing the

indicated primary antibody. For detection of wild type CrhR, His-R or mutant truncated $CrhR_{TR}$ proteins anti-CrhR antibody (1:5000) was used, frequently simultaneously the membranes were also probed with anti- Rps1 antibody (1:5000) used to detect control for protein loading; anti-ClpC (1:1000) and anti-FtsH (1:5000) antibodies were used to detect proteases ClpC and FtsH respectively.

Membranes were washed with 20 ml of 1X TBS (150 mM NaCl, 10 mM Tris-HCl, pH 8.0) for 15 min, followed by 1X TBST (0.05% [v/v] Tween-20 in 1X TBS) for 15 min and 1X TBS for 15 min with gentle shaking at room temperature. Membranes were incubated for 30 min at room temperature in 20 ml 1X TBS containing anti- rabbit IgG conjugated to horse-radish peroxidase (1:10,000) (Sigma-Aldrich, St. Louis, USA) as secondary antibody. The washes were repeated with final 1X TBS wash for 30 min. Proteins were visualized using ECL Western Blotting Detection Kit (Amersham, Bioscineces, GE Healthcare, Wanwatosa, USA), chemilluminescence was detected using autoradiography.

2.6.3 Coomassie staining of SDS-PAG

Gels that were analyzed by western blot analysis were stained after the transfer; however gels that were analyzed by mass spectrometry were stained without electroblotting transfer. Gels were incubated in Colloidal Coomassie stain (0.08% [v/v] coomassie brilliant blue G250, 1.6% ortho-phosphoric acid, 8% [w/v] ammonium sulfate, 20% [v/v] methanol) at room temperature with gentle shaking until the proteins could be visualized, in most cases 12-36 h. If needed,

excess stain was removed by incubating in distilled H_2O with gentle shaking until the desired intensity was reached.

Table 2.1: Primers used for the construction and verification of *ΔcrhR* mutant

Primer	Sequence (5' - 3')	Origin of Sequence
OT1F	ACTCAGTCTAGAGTCAGTTAATCC	Forward primer for 1.5kb sequence upstream of *crhR*
OT1R	ATGGAAAAGCTTAATAATTTCGG	Reverse primer for 1.5kb sequence upstream of *crhR*
OT2F	AAGGTAAAGCTTGCAAACCCCGTC	Forward primer for 1.5kb sequence downstream of *crhR*
OT2R	GACGGACTCGAGATTGCCCATATC	Reverse primer for 1.5kb sequence downstream of *crhR*
dcsr11F	TAATACGACTCACTATAGGAACCGC CGCAGACCTCAAAC	Forward primer 818 bp into the *crhR* open reading frame
DC29	CGCGGTCTAGATAATACGACTCACT ATAGGGTTACTGTTGGCGATCAC	Reverse primer for the 3' end of *crhR* open reading frame
LPF45	TGTTATTGACGGTTGGTTCC	Forward primer for a region 51 bp upstream of *crhR* open reading frame
GWO74	TTGGGAAGAATCCTTAGG	Reverse primer for a region 198 bp downstream of *crhR* open reading frame stop codon

III. RESULTS

3.1 Growth of wild type *Synechocystis* cells in comparison to *crhR* mutants and His-CrhR expressing strains

3.1.1 Growth and survival of wild type and $crhR_{TR}$ mutant at 30°C and 20°C

In order to study the importance of CrhR helicase in *Synechocystis* cells, growth of wild type at 30°C (warm) and 20°C (cold) was compared to $crhR_{TR}$ mutant growing under the same conditions. The $crhR_{TR}$ mutant has a spectinomycin resistance cassette inserted into the open reading frame of CrhR. This insertion also affects the neighbour gene *argC*, which is responsible for arginine biosynthesis (Figure 3.1) (Rosana *et al.*, 2012). To monitor the growth of wild type and $crhR_{TR}$ mutant, OD_{750} was taken daily from the cultures growing at warm and cold temperatures (Figure 3.2). It was observed that wild type and mutant cells grow exponentially at approximately same rate at 30°C. However, the wild type exhibits slower growth in the cold after the first 4 days of incubation. As judged by OD_{750} the $crhR_{TR}$ mutant does not grow at 20°C (Figure 3.2).

Observing this interesting situation with the lack of growth of the mutant at 20°C, we were curious whether $crhR_{TR}$ remained alive at 20°C. For this reason viability tests were performed on cell cultures growing at 30°C and 20°C. Plates were incubated at 30°C, growing colonies were counted and resulting numbers were used for the construction of Figure 3.2. Viability tests revealed that mutant cells from the culture grown at 20°C were not surviving, as the number of

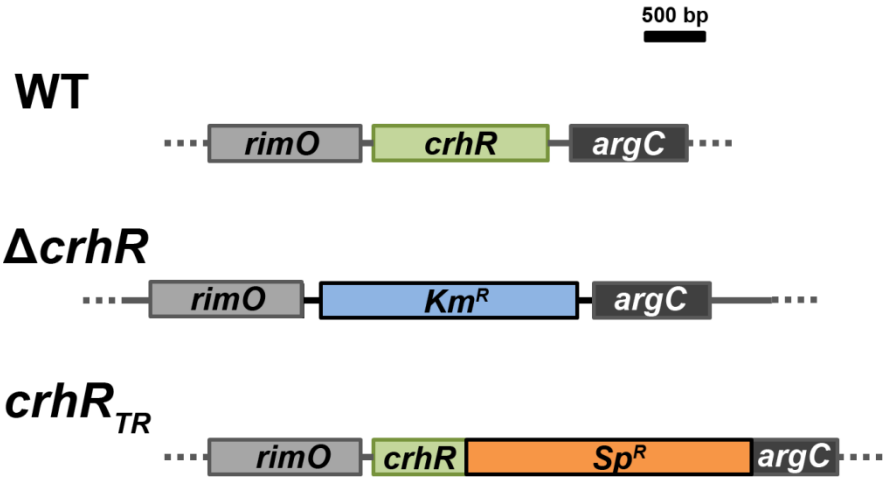

Figure 3.1: Schematic of the genomic region containing the *crhR* gene (slr0083) from three strains used in this study: wild type, Δ*crhR* and $crhR_{TR}$. Wild type produces the wild type version of CrhR protein (55 kDa), Δ*crhR* mutant does not produce CrhR protein and the $crhR_{TR}$ strain produces a truncated version of CrhR, $CrhR_{TR}$ (27 kDa) (Rosana *et al.*, 2012).

Figure 3.2: Growth and cell viability of wild type and $crhR_{TR}$ mutant at 30^{o}C and 20^{o}C. Cultures were grown at 30^{o}C and 20^{o}C, OD_{750} was taken at the same time daily in triplicate to estimate the growth. Viability was measured using the colony plate count method after the indicated growth period. Diluted cells were plated in triplicate and incubated at 30^{o}C, resulting colonies were counted after one week of incubation.

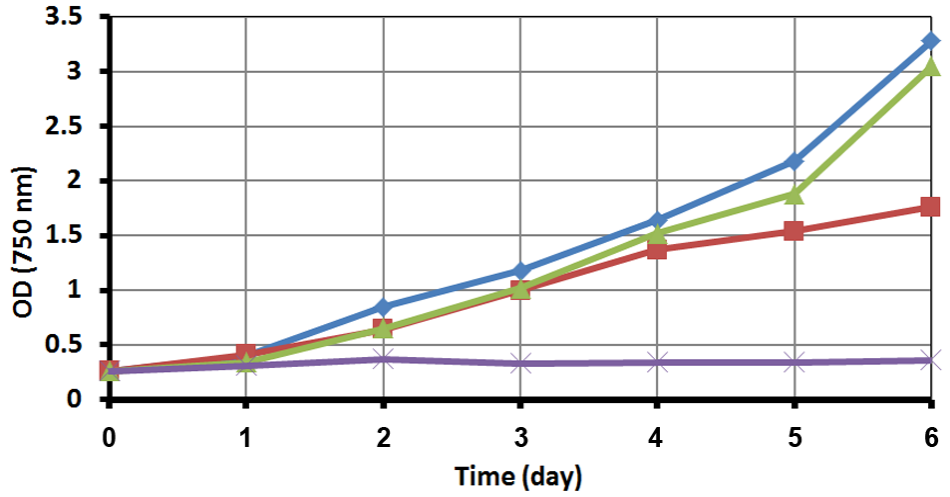

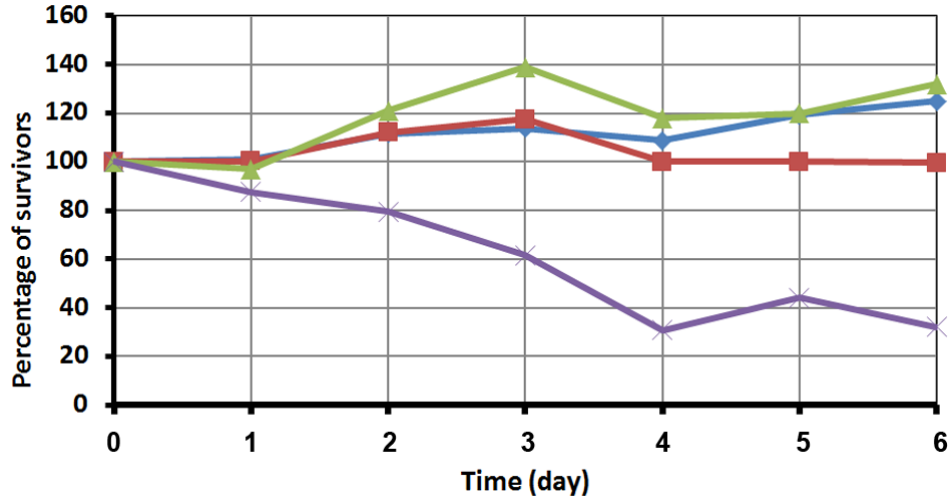

WT 30°C
WT 20°C
crhR$_{TR}$ 30°C
crhR$_{TR}$ 20°C

survivors decreased by 70% in 4 days. After the fourth day of growth the percentage of survivors remained the same until the end of the experiment (Figure 3.2), demonstrating that some of *crhR*$_{TR}$ mutant cells may start to adapt their metabolism to the cold and try to remain in the dormant state until external conditions, mainly temperature becomes favourable.

These growth and viability experiments indicate that the *crhR*$_{TR}$ mutant is very sensitive to temperature downshift either due to the absence of functional CrhR helicase and/or due to the overproduction of the truncated non-functional CrhR$_{TR}$ protein at both temperatures, which will be further discussed in more detail.

3.1.2 Growth of wild type, Δ*crhR* mutant and His-CrhR expressing strains

3.1.2i Δ*crhR* mutant construction

Since some of the growth patterns observed in *crhR*$_{TR}$ mutant (Figure 3.2) could have been attributed to excessive production of CrhR$_{TR}$ protein or mutation of the neighbour gene *argC* (Figure 3.1), it was decided to construct another *crhR* mutant with a complete deletion of the *crhR* ORF. The inactivation plasmid used to create this mutant was constructed by cloning a kanamycin resistance cassette between 1.5 kb upstream and downstream regions of the *crhR* ORF in pBluescript (Figure 3.3). This construct, termed pBS-Δ*crhR*, was transformed into wild type *Synechocystis* cells. Resulting mutants were grown on

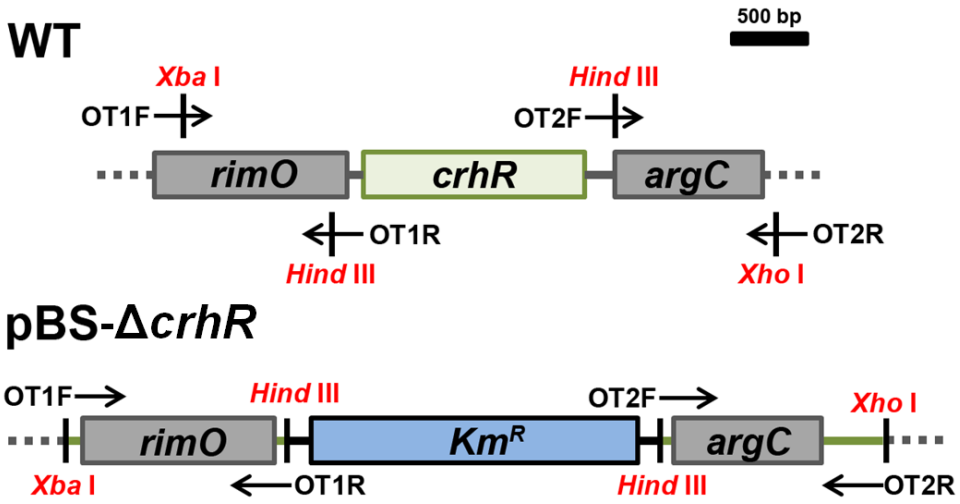

Figure 3.3: Δ*crhR* mutant construction. 1.5 kb regions downstream and upstream of the *crhR* gene were amplified using the indicated primer pairs, OT1F + OT1R and OT2F + OT2R, containing the indicated restriction enzyme cut sites. The 1.5 kb fragments were ligated with a 2.3 kb *Hind* III fragment carrying the kanamycin cassette into *Xba* I/*Xho* I cleaved pBluescript. The resulting plasmid, pBS-CrhR, was transformed into *Synechocystis* and inserted into the genome by a double cross-over event during homologous recombination.

Figure 3.4: PCR confirmation of the absence of the *crhR* ORF in the genome of Δ*crhR* mutant.

(A) An illustration of wild type and Δ*crhR* mutant genomic region with location of the primers and sizes of the expected PCR products.

(B) DNA agarose gel with PCR products produced using the primers indicated in (A). Blue arrow pair underneath the gel picture indicates the use of LPF45 and GWO74 primers for PCR, green pair indicates dcsr11F and DC29 primers.

Genomic DNA was isolated from a potential Δ*crhR* mutant and wild type as a control. Primers GWO 74 and LPF 45 (lanes 1 and 3) produce a 1.7 kb fragment from the wild type *crhR* gene and should amplify a 2.5 kb fragment containing the kanamycin cassette and surrounding genomic sequence. A PCR reaction performed with primers dcsr11F and DC 29 (lanes 2 and 4) should only amplify from the intact *crhR* gene, producing a 0.7 kb product in the wild type and no product in the Δ*crhR* mutant.

A

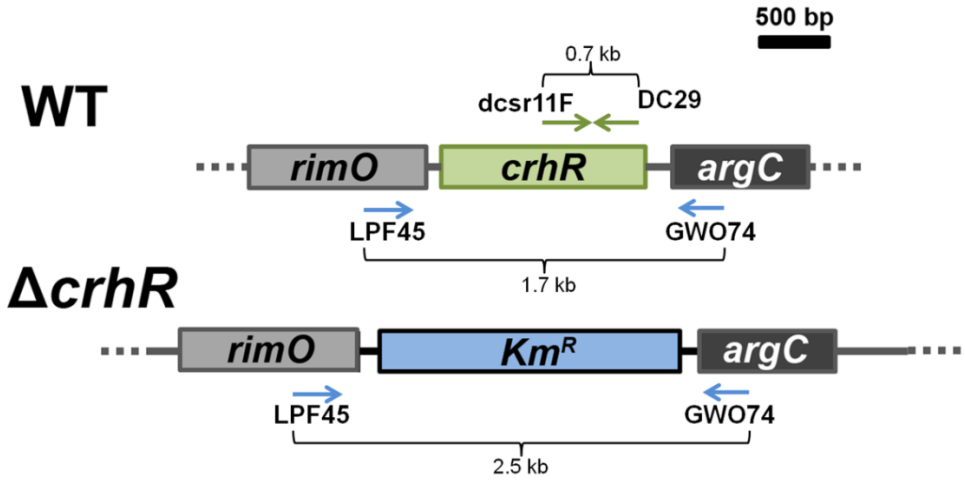
500 bp
0.7 kb
WT
dcsr11F
DC29
rimO
crhR
argC
LPF45
GWO74
1.7 kb
ΔcrhR
rimO
Km^R
argC
LPF45
GWO74
2.5 kb

B

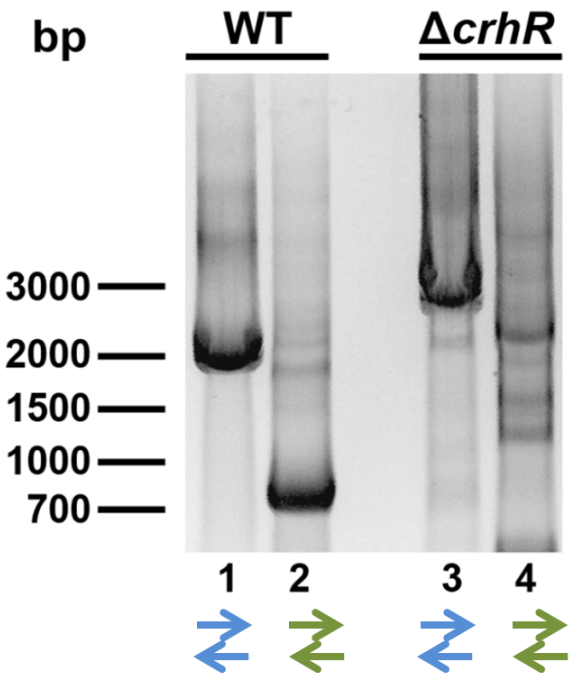
bp
WT
ΔcrhR
3000
2000
1500
1000
700
1
2
3
4

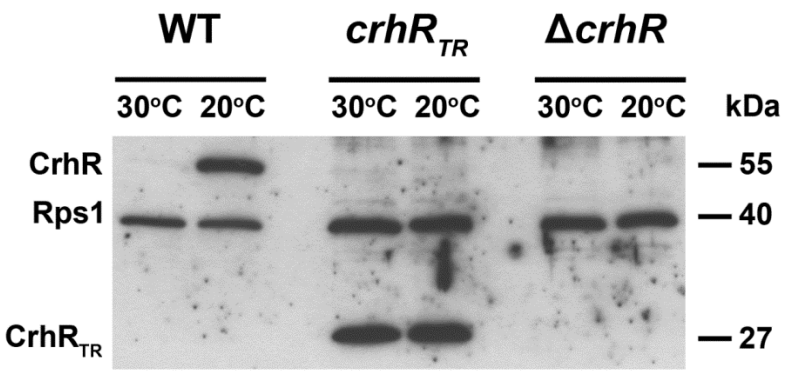

Figure 3.5: Western confirmation of the Δ*crhR* mutant. Total soluble protein (30 µg) from cells grown at 30°C and cold shocked at 20°C for 3 h was probed with anti-CrhR (1:5000) and anti- *E. coli* Rps1 (1:5000) antibodies, ECL was used for detection. Polypeptides detected included the 55 kDa CrhR protein in wild type, the truncated 27 kDa protein in the $crhR_{TR}$ mutant and no CrhR was identified in the Δ*crhR* mutant. Rps1 protein served as a loading control and was detected at equal levels, at 40 kDa in all of the strains at both temperatures. The X-ray film was exposed for 1 h to increase visibility of any low quantities of CrhR protein.

the BG11 medium with kanamycin and the absence of the crhR gene was confirmed with PCR (Figure 3.4) and western blot analysis (Figure 3.5). PCR was performed on the genomic DNA from both wild type and the ΔcrhR mutant using primer pairs designed to amplify an internal section of the *crhR* ORF (primers dcsr11F and DC29) and the region outside of *crhR* (primers LPF45 and GWO74) (Figure 3.4 A). Both primer pairs confirmed the absence of the *crhR* ORF, which was replaced by the kanamycin cassette in the Δ*crhR* mutant (Figure 3.4 B). Western blot analysis was also used to confirm the absence of the *crhR* gene by observing the lack of its product, CrhR protein, at 30^{o}C and 20^{o}C. Even though CrhR (55 kDa) protein is present at high levels in the wild type cells at 20^{o}C and $CrhR_{TR}$ (27 kDa) protein is present in the $crhR_{TR}$ mutant at both temperatures, CrhR protein is not detectable in the Δ*crhR* mutant at any growth temperature, confirming the absence of the *crhR* gene (Figure 3.5).

3.1.2ii Efect of complete *crhR* deletion and CrhR protein overexpression on the growth of *Synechocystis* cells at 30^{o}C and 20^{o}C

The confirmed Δ*crhR* mutant was used for the study of *Synechocystis* cell growth in the complete absence of CrhR protein. In an attempt to assess the effect of CrhR overexpression in *Synechocytsis,* 6 xHis-CrhR (His-R) expressing strains were produced by cloning the His-R ORF into pMon 36456 (Monsanto, St. Louis, USA). His-R expression in this plasmid is under control of the pNir promoter. pNir is a nitrate reductase promoter that is constitutive when used in *Synechocystis* cells grown with a source of nitrate. The resulting pMon-HisR

plasmid was transformed into wild type, *crhR*$_{TR}$ and Δ*crhR* strains to observe whether overexpression of the functional His-R has an impact on wild type cells and if pMon-HisR can rescue mutant phenotypes exhibited by *crhR*$_{TR}$ and Δ*crhR*. To test this, the Δ*crhR* mutant and three His-R expressing strains (wild type, *crhR*$_{TR}$ and Δ*crhR* containing pMon-HisR plasmid) were grown at 30^{o}C and 20^{o}C (Figure 3.6).

As shown in Figure 3.6, the Δ*crhR* mutant has the most rapid growth at 30^{o}C compared to all of the strains expressing His-R. The Δ*crhR* strain with pMon-HisR (Figure 3.6) grows very similar to the wild type (Figure 3.2) at 30^{o}C and 20^{o}C, which shows that the presence of His-R in the complete deletion mutant rescues the mutant phenotype. It was very interesting to observe that wild type and the *crhR*$_{TR}$ mutant with pMon-HisR grow slower at 30^{o}C and 20^{o}C than the wild type. This suggests that the presence of additional CrhR protein in the wild type interferes with growth as CrhR levels above basal has a detrimental effect on *Synechocystis* cells. In addition His-R presence does not revert the mutant phenotype of *crhR*$_{TR.}$ The Δ*crhR* mutant shows no growth at 20^{o}C (Figure 3.6), which is very similar to *crhR*$_{TR}$ growth at the same temperature (Figure 3.1.2). These results suggest that the reason temperature has a profound effect on the growth of the *crhR*$_{TR}$ mutant is the absence of functional CrhR helicase.

There are number of factors to be considered in this experiment and the accumulation of CrhR protein in the cell is of major importance. Even though His-R was expressed under the control of a promoter that is constitutive in

Figure 3.6: Growth of the Δ*crhR* mutant and His-CrhR expressing strains at 30^{o}C and 20^{o}C. Cultures were grown at 30^{o}C to the mid-log phase, splitted in half and diluted with fresh media to OD_{750} of 0.5. Half of the cultures were left at 30^{o}C, the other half was transferred to 20^{o}C. OD_{750} was taken daily in triplicate to monitor the growth of cultures at 30^{o}C and 20^{o}C. (Sampling and OD_{750} measurements were done at Owttrim lab at the University of Alberta by Dr. Guo Huiqin from Inner Mongolia Agricultural University, China).

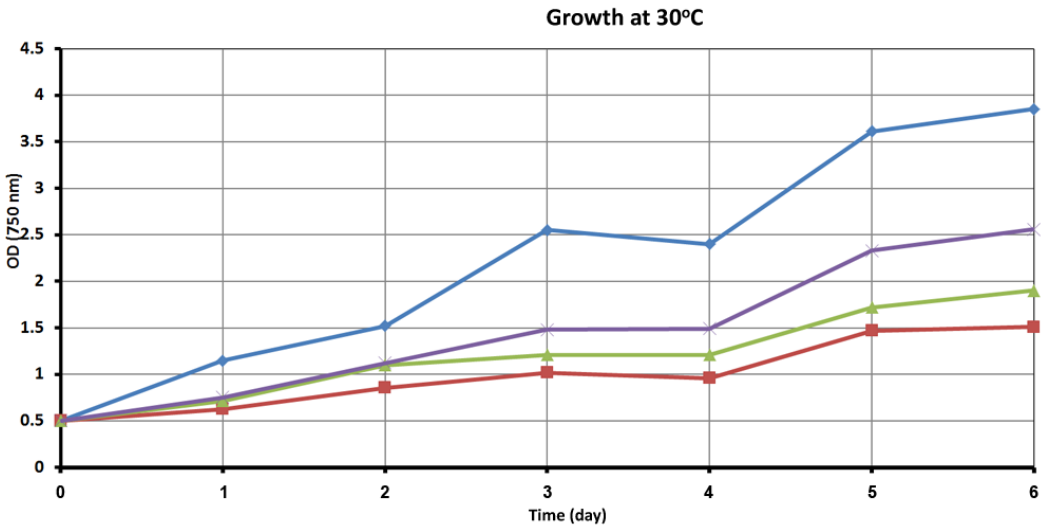
Growth at 30°C
OD (750 nm)
Time (day)
0
0.5
1
1.5
2
2.5
3
3.5
4
4.5
0
1
2
3
4
5
6

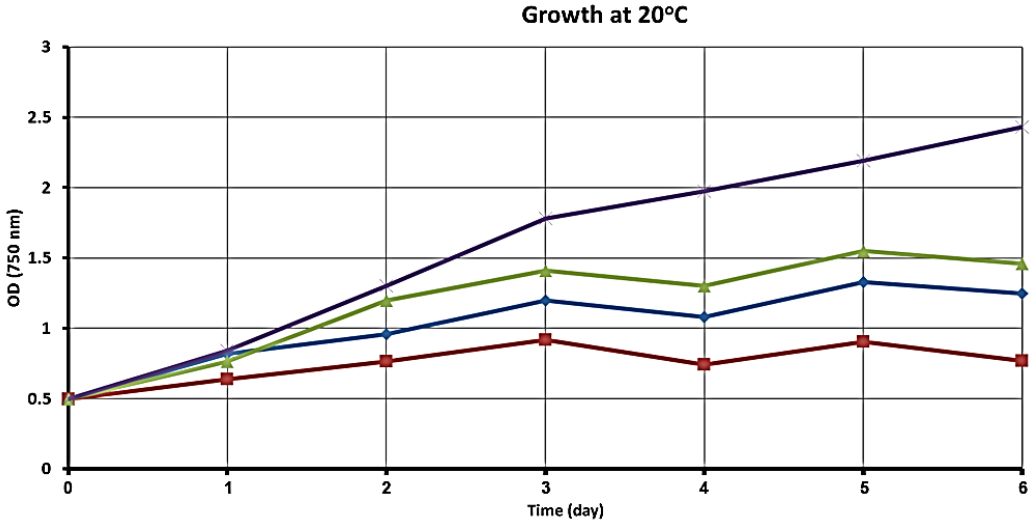
Growth at 20°C
OD (750 nm)
Time (day)
0
0.5
1
1.5
2
2.5
3
0
1
2
3
4
5
6

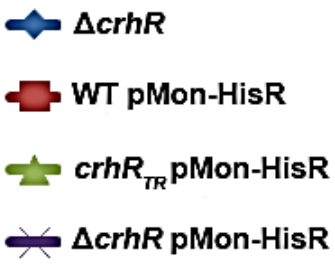
ΔcrhR
WT pMon-HisR
crhR_tR pMon-HisR
ΔcrhR pMon-HisR

Synechocystis under the growth conditions used, the level of CrhR protein in all of the strains was examined (Figure 3.7). As expected, wild type showed increased levels of CrhR protein at 20^{o}C, *crhR$_{TR}$* mutant had high levels of the truncated protein CrhR$_{TR}$ at both temperatures and CrhR was not detected in the Δ*crhR* mutant. However, differential expression of His-R was observed in pMon-HisR containing strains (Figure 3.7) at 30^{o}C and 20^{o}C, even though His-R expression is controlled by a constitutive promoter. Especially, in the wild type expressing His-R, levels of this protein decrease significantly at 30^{o}C and slightly at 20^{o}C. It was also observed from Figure 3.7 that expression of His-R altered accumulation of CrhR$_{TR}$ in *crhR$_{TR}$* mutant expressing pMon-HisR plasmid. The presence of His-R in the *crhR$_{TR}$* mutant leads to the overall decrease in levels of non-functional protein CrhR$_{TR}$ at both temperatures. This strain also shows less CrhR$_{TR}$ protein at 30^{o}C compared to 20^{o}C, which is a pattern typical of CrhR levels in the wild type cells. Therefore, expression of His-R is capable of rescuing regulation of CrhR$_{TR}$ mutant protein. In summary, there appears to be a post-translational mechanism that controls the level of CrhR in the cell, which is altered depending upon the presence or absence of functional CrhR. This mechanism will be investigated in more detail in the following sections.

3.2 Proteolytic degradation of CrhR in response to temperature shift

The idea of proteolytic degradation of CrhR protein was tested using two different approaches: *in vivo* and *in vitro* assays. *Synechocystis* wild type, *crhR$_{TR}$* and Δ*crhR* mutants were used in those assays.

Figure 3.7: Western blot analysis of CrhR protein levels in all of the *Synechocystis* strains used for cell growth analysis. Total soluble protein (20 µg) from cells grown at 30^{o}C and cold shocked at 20^{o}C for 2 h was probed with anti-CrhR (1:5000) and anti-*E. coli* Rps1 (loading control) (1:5000) antibodies, ECL was used for detection. Polypeptides detected: the 55 kDa protein in wild type, the truncated 27 kDa protein in the $crhR_{TR}$ mutant and no CrhR was detected in the Δ*crhR* mutant. His-CrhR at 58 kDa was identified in addition to other forms of CrhR originating from the pMon-HisR construct. Rps1 protein served as a loading control and was detected at 40 kDa in all of the strains at both temperatures.

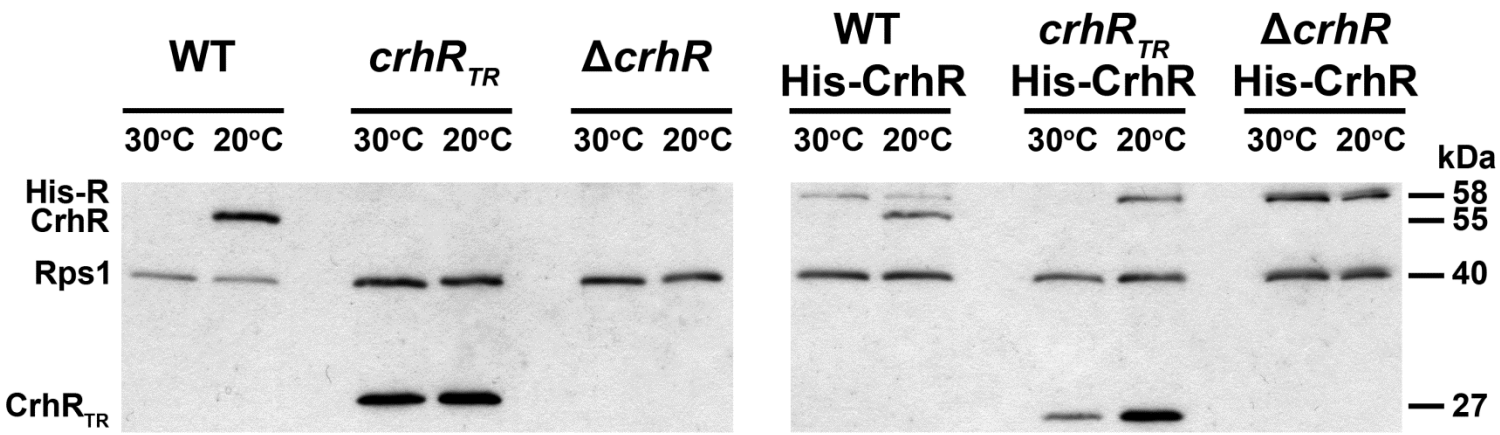
WT
crhR_TR
ΔcrhR
WT His-CrhR
crhR_TR His-CrhR
ΔcrhR His-CrhR
30°C 20°C
30°C 20°C
30°C 20°C
30°C 20°C
30°C 20°C
30°C 20°C
kDa
His-R CrhR
Rps1
CrhR_TR
58
55
40
27

3.2.1 *In vivo* abundance of CrhR in wild type and mutant cells

In order to observe how CrhR levels change in response to temperature shift from unfavourable 20^{o}C to more preferred for growth and development at 30^{o}C, an *in vivo* time course of CrhR abundance was performed. *In vivo* levels of CrhR protein were monitored in wild type and *crhR$_{TR}$ Synechocystis* cells growing at 30^{o}C after 20^{o}C cold stress. Cells were shifted to 20^{o}C to induce production of CrhR protein and then shifted back to 30^{o}C to observe how the increase in temperature affects CrhR accumulation. Immunoblot analysis showed that in the wild type cells, levels of CrhR protein (55 kDa) increase in the first 3h of incubation at 20^{o}C and remain at this maximum for the entire period of cold stress (24 h) (Figure 3.8). However, transfer of the culture back to 30^{o}C causes CrhR protein levels to rapidly decrease from the maximal to the basal level within the first 3 h of warm incubation. This basal level of CrhR is usually observed in the wild type cells at 30^{o}C. These changes are not a result of protein loading as levels of the loading control, Rps1 (40 kDa), remain fairly constant throughout the experiment regardless of the temperature.

The time course of CrhR degradation was investigated in more detail by shifting wild type cells grown at 20^{o}C for 3 h to 30^{o}C and sampling every 10 min for a period of almost 2 h (Figure 3.9). CrhR protein degradation initiates in the first 30 min at 30^{o}C and continues to be degraded in a linear fashion for the duration of experiment. In the same experiment cellular levels of Rps1 protein, used as a loading control, remain constant regardless of incubation temperature (Figure 3.9).

Figure 3.8: Temperature-dependent accumulation of CrhR *in vivo.* Wild Type (WT) and *crhR*$_{TR}$ mutant (*crhR*$_{TR}$) cells were grown at 30^{o}C to mid-log phase, cultures were transferred to 20^{o}C for 24 h and then transferred back to 30^{o}C for 24 h. Aliquots were harvested for protein extraction at the indicated times. Wild type CrhR protein (55 kDa) or CrhR$_{TR}$ (27 kDa) and loading control Rps1 were identified by western analysis using anti-CrhR antibody (1:5000) and anti- *E. coli* Rps1 antibody (1:5000) respectively. ECL was used for the detection.

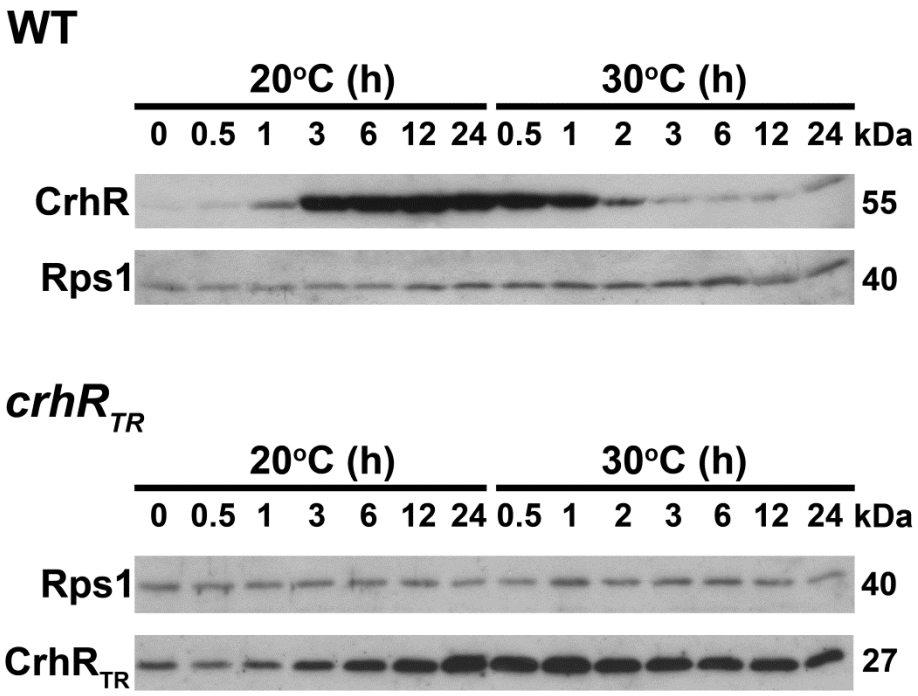
WT
20°C (h)
30°C (h)
0 0.5 1 3 6 12 24 0.5 1 2 3 6 12 24 kDa
CrhR
55
Rps1
40
crhR_TR
20°C (h)
30°C (h)
0 0.5 1 3 6 12 24 0.5 1 2 3 6 12 24 kDa
Rps1
40
CrhR_TR
27

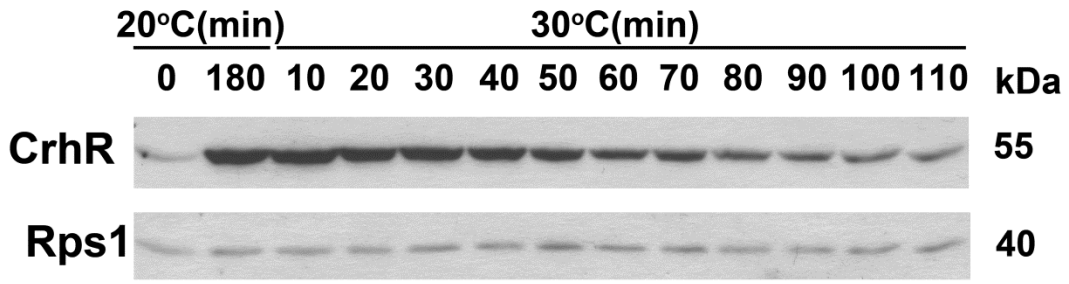

Figure 3.9: Rapid *in vivo* degradation of CrhR protein wild type cells. Wild type (WT) cells were grown at 30°C to mid-log phase, cultures were transferred to 20°C and then transferred back to 30°C. Aliquots were harvested for protein extraction at the indicated times. CrhR protein (55 kDa) and the loading control, Rps1, were identified by western analysis using anti-CrhR antibody (1:5000) and anti-*E. coli* Rps1 antibody (1:5000) respectively. ECL was used for the detection.

The *in vivo* temperature shift assay was also performed with the *crhR*$_{TR}$ mutant (Figure 3.8 *crhR*$_{TR}$). The truncated version of CrhR (CrhR$_{TR}$) is present at elevated levels at 30^{o}C compared to wild type cells as previously shown in Figure 3.7. The level of CrhR$_{TR}$ gradually increases in response to a downshift in temperature, however once the cells are shifted back to 30^{o}C, the amount of CrhR$_{TR}$ does not decrease in the manner observed in wild type cells and remains elevated for the duration of experiment. Levels of loading control Rps1 protein in *crhR*$_{TR}$ mutant remain constant throughout the experiment. This result suggest that CrhR$_{TR}$ levels are not proteolytically regulated in *crhR*$_{TR}$ mutant.

3.2.2 *In vitro* proteolytic degradation of CrhR and exogenous *E. coli* His-CrhR

The potential proteolytic degradation of CrhR protein, observed *in vivo*, was further examined using several *in vitro* experiments. Initially, mixing experiments were performed, in which total soluble lysates from wild type and/or *crhR*$_{TR}$ cells grown at 30^{o}C or 20^{o}C were mixed and a time course of CrhR abundance was determined as outlined in Figure 3.10 A. Subsequently, a similar strategy was utilized to investigate if affinity-purified His-R from *E. coli* was also degraded *in vitro*.

3.2.2i *In vitro* CrhR degradation with wild type lysate

Cell lysates from *Synechocystis* cells grown at 20^{o}C (cold) and 30^{o}C (warm) were mixed and incubated at 30^{o}C for 4 h, and aliquots of the mixture were taken at the indicated time points to observe the effect of the source of cell lysate on the abundance of CrhR protein *in vitro*. It was observed that there is a linear reduction of CrhR protein (55kDa) in the mixture of cell lysates incubated at 30^{o}C (Figure 3.10 B). However, 20^{o}C lysate from wild type cells incubated alone at 30^{o}C for a period of 4 hours does not show reduction in the amount of CrhR protein (55kDa) (Figure 3.10 C). The only source of CrhR protein that we can visualize in this immunoblot analysis originates from the 20^{o}C lysate where it is present at elevated levels, whereas the basal level of CrhR helicase at 30^{o}C is not detected with the protein amount loaded on these gels (Figure 3.10 A). This *in vitro* experiment suggests that proteolytic degradation of CrhR protein occurs only in the presence of 30^{o}C lysate in the mixture, which suggests that the proteolytic machinery is present and/or active in cells grown at 30^{o}C.

3.2.2ii *In vitro* CrhR$_{TR}$ degradation with cell lysate from *crhR$_{TR}$* mutant

The same *in vitro* experiment was performed with the cell lysates from *crhR$_{TR}$* mutant cells growing at 30^{o}C and 20^{o}C. There is no a linear visible reduction in the amount of truncated CrhR$_{TR}$ (27 kDa) in the mixture of cell lysates from *crhR$_{TR}$* mutant cells (Figure 3.11 A). Cell lysate from *crhR$_{TR}$* mutant cells grown at 20^{o}C was also incubated alone and served as a control in the experiment (Figure 3.11 B). Cold lysate incubated for a period of 4 h showed

Figure 3.10: *In vitro* degradation of CrhR with wild type lysate. (A) An illustration of the *in vitro* mixing experiment, in which cell lysate from *Synechocystis* cells grown at 30^{o}C serves as a source of active degradation machinery (DM) and cell lysate from 20^{o}C serves as a source of detectable amounts of CrhR protein. (B) A 1:1 mixture of total soluble protein, extracted from wild type (WT) cells grown at 30^{o}C and 20^{o}C, was incubated at 30^{o}C and aliquots were taken at the indicated times. Wild type CrhR protein (55 kDa) was identified by western analysis using anti-CrhR antibody (1:5000) and detected by ECL. (C) The *in vitro* degradation experiment described in A was repeated using only soluble protein isolated from wild type cells grown at 20^{o}C.

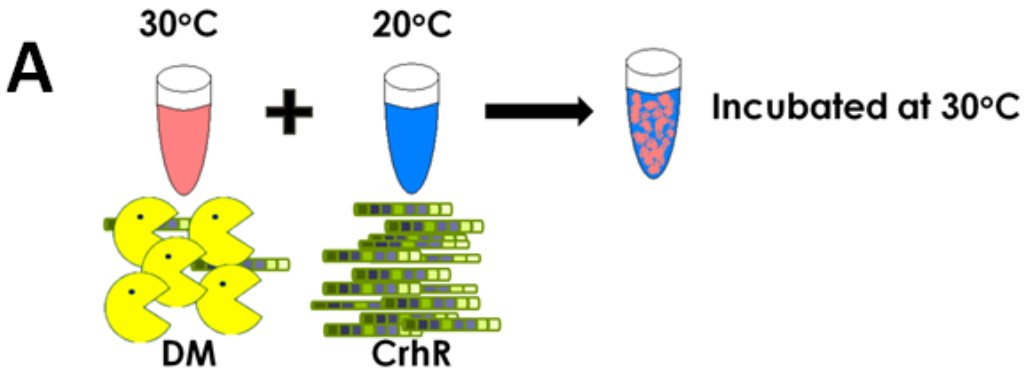
A
30°C
20°C
Incubated at 30°C
DM
CrhR

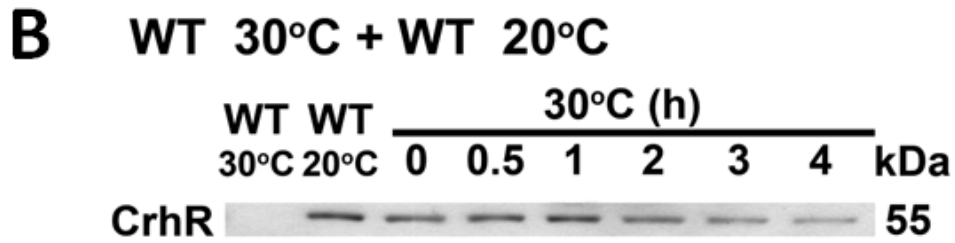
B
WT 30°C + WT 20°C
WT WT
30°C 20°C
30°C (h)
0 0.5 1 2 3 4
kDa
CrhR
55

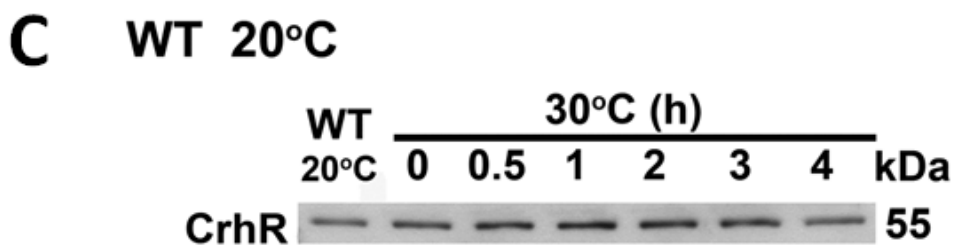
C
WT 20°C
WT
20°C
30°C (h)
0 0.5 1 2 3 4
kDa
CrhR
55

Figure 3.11: *In vitro* degradation of $CrhR_{TR}$ protein with cell lysate from the *$crhR_{TR}$* mutant. (A) A mixture of soluble protein, extracted from *$crhR_{TR}$* mutant cells (*$crhR_{TR}$*) grown at 30^{o}C and 20^{o}C, was incubated at 30^{o}C and aliquots were taken at the indicated times. Truncated $CrhR_{TR}$ protein (27 kDa) was identified by western analysis using anti-CrhR antibody (1:5000) and detected by ECL. (B) The *in vitro* degradation experiment described in A was repeated using only soluble protein isolated from *$crhR_{TR}$* mutant cells grown at 20^{o}C.

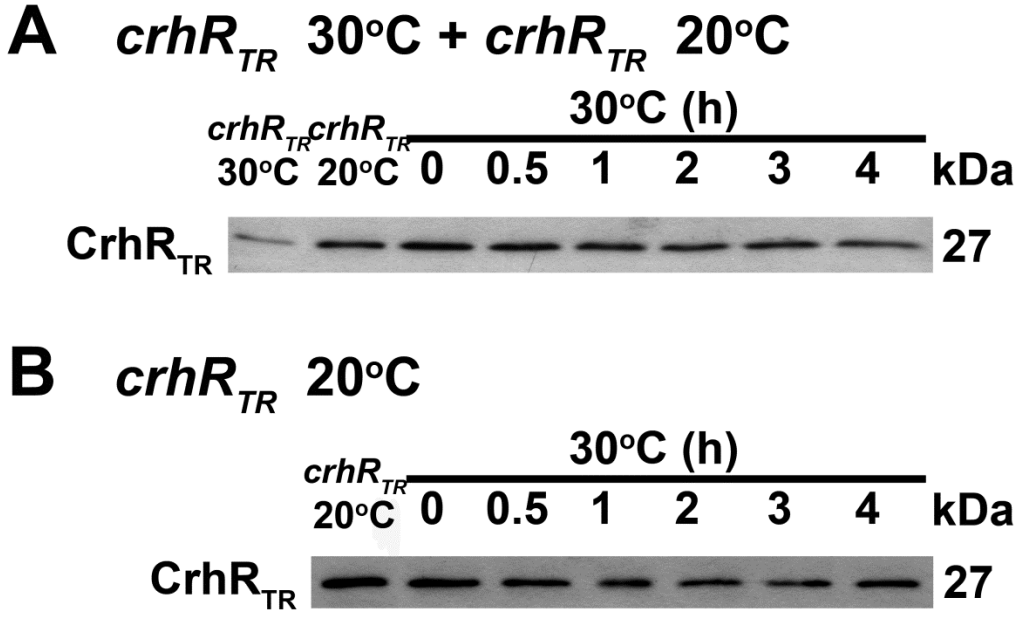
A
crhR_TR 30°C + crhR_TR 20°C
30°C (h)
crhR_TRcrhR_TR
30°C 20°C 0 0.5 1 2 3 4 kDa
CrhR_TR
27
B
crhR_TR 20°C
30°C (h)
crhR_TR
20°C 0 0.5 1 2 3 4 kDa
CrhR_TR
27

no visible reduction in the amount of $CrhR_{TR,}$ similar to the mixture of cold and warm lysates shown in Figure 3.11 A. This experiment indicates that proteolytic degradation of mutant $CrhR_{TR}$ protein does not occur in the presence of 20^oC lysate alone and after mixing it with 30^oC lysate, suggesting that functional CrhR protein is required for its own proteolytic autoregulation.

3.2.2iii *In vitro* His-R degradation with cell lysates from wild type and mutant cells grown at 30^oC and 20^oC

His-R affinity-purified from *E. coli* harboring the pRSET-R plasmid was used as a source of exogenous CrhR protein in an *in vitro* degradation experiment. *E. coli* His-R was mixed with wild type and mutant cell lysates from *Synechocystis* cells grown at 30^oC and 20^oC. Taking into account the loading control, Rps1, a visible reduction in the amount of exogenous *E. coli* His-R protein (58 kDa) is visible only when protein lysate from wild type cells grown at 30^oC is used as a source of degradation machinery (Figure 3.12 A). Wild type cells cold shocked at 20^oC do not produce detectable degradation of either the exogenous His-R (58 kDa) or the native CrhR protein (55 kDa) (Figure 3.12 B). Lysates obtained from $crhR_{TR}$ mutant cells grown at either temperature also do not have functional CrhR degradation machinery, suggesting that the degradation machinery is either not produced or activated in $crhR_{TR}$ mutant cells, supporting the hypothesis that CrhR degradation is autoregulated (Figure 3.12 C and D). The results observed in this experiment support earlier findings of other *in vitro* experiments (described in 3.2.2i and 3.2.2ii).

Figure 3.12: *In vitro E. coli* His-R degradation with cell lysates from wild type and mutant cells grown at 30^{o}C and 20^{o}C. Affinity purified His-R protein (58 kDa) from *E. coli* was mixed with soluble protein from (A) wild type (WT) *Synechocystis* cells grown at 30^{o}C, (B) wild type cells grown at 20^{o}C, (C) $crhR_{TR}$ mutant ($crhR_{TR}$) grown at 30^{o}C and (D) $crhR_{TR}$ mutant ($crhR_{TR}$) grown at 20^{o}C. Mixtures were incubated at 30^{o}C and CrhR was detected in aliquots taken at the indicated times. CrhR (55 kDa) or $CrhR_{TR}$ (27 kDa) and Rps1 loading control were identified by western analysis using anti-CrhR antibody (1:5000) and anti-*E. coli* Rps1 antibody (1:5000) respectively. ECL was used for the detection.

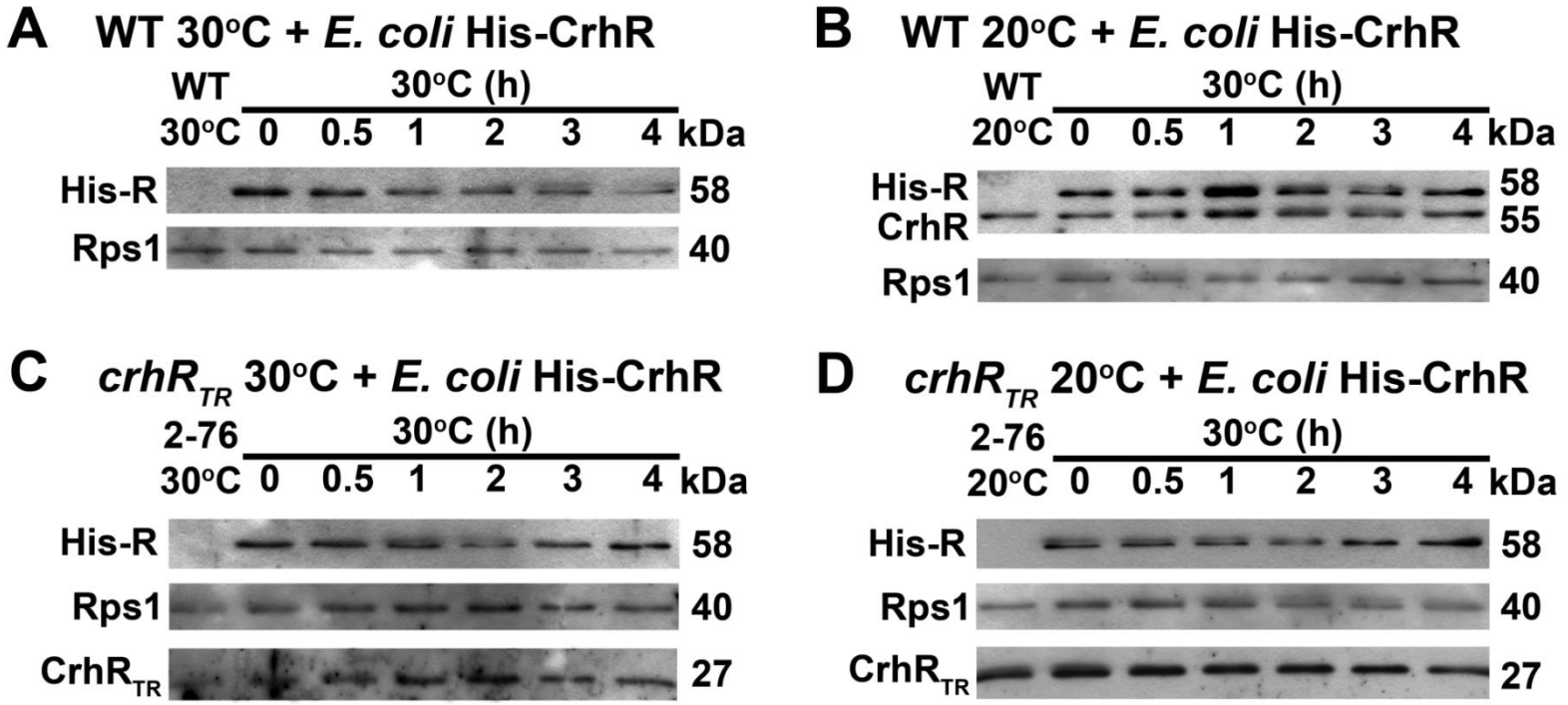
A
WT 30°C + E. coli His-CrhR
WT
30°C (h)
30°C 0 0.5 1 2 3 4 kDa
His-R
58
Rps1
40
B
WT 20°C + E. coli His-CrhR
WT
30°C (h)
20°C 0 0.5 1 2 3 4 kDa
His-R
CrhR
58
55
Rps1
40
C
crhR_TR 30°C + E. coli His-CrhR
2-76
30°C (h)
30°C 0 0.5 1 2 3 4 kDa
His-R
58
Rps1
40
CrhR_TR
27
D
crhR_TR 20°C + E. coli His-CrhR
2-76
30°C (h)
20°C 0 0.5 1 2 3 4 kDa
His-R
58
Rps1
40
CrhR_TR
27

3.2.2iv *In vitro* CrhR and $CrhR_{TR}$ degradation in mixtures of wild type and $crhR_{TR}$ mutant cell lysates

The lack of $CrhR_{TR}$ degradation observed in Figures 3.11 and 3.12 could result from the lack of functional degradation machinery in the *$crhR_{TR}$* mutant. However it may also be attributed to the absence of a required degradation signal in the truncated $CrhR_{TR}$ protein. In order to investigate these possibilities, cell lysates from wild type and *$crhR_{TR}$* mutant cells grown at 30°C and 20°C were mixed in two different combinations (Figure 3.13).

A time course of wild type warm combined with *$crhR_{TR}$* cold lysates produces a reduction in the amount of $CrhR_{TR}$ protein (27 kDa) (Figure 3.13 A). In this case, wild type lysate serves as a source of active degradation machinery and mutant lysate provides $CrhR_{TR}$ protein as a substrate for degradation. The experiment indicates that the truncated version of $CrhR_{TR}$ protein can be degraded by the functional degradation machinery provided by the wild type warm lysate. This suggests that any potential degradation signal is not present in the C-terminus of CrhR.

In the mixture of mutant lysate from 30°C and wild type lysate from 20°C, there is no visible reduction in the amount of wild type CrhR protein (55 kDa) (Figure 3.13 B). In this experiment, mutant 30°C lysate is the potential source of proteolytic machinery and wild type cold lysate provides the detected 55 kDa wild type CrhR protein. The results again confirm that there is no functional degradation machinery in the *$crhR_{TR}$* mutant, which would be capable of degrading full length CrhR protein from wild type cells.

Figure 3.13: *In vitro* CrhR and $CrhR_{TR}$ degradation in mixtures of wild type and $crhR_{TR}$ mutant cell lysates. (A) A mixture of soluble protein, extracted from wild type (WT) and $crhR_{TR}$ mutant ($crhR_{TR}$) cells grown at 30^{o}C and 20^{o}C, respectively, was incubated at 30^{o}C and aliquots were taken at the indicated times. (B) The *in vitro* degradation experiment described in A was repeated using cell lysates from $crhR_{TR}$ and WT cells grown at 30^{o}C and 20^{o}C, respectively. CrhR (55 kDa) or $CrhR_{TR}$ (27 kDa) and loading control Rps1 were identified by western analysis using anti-CrhR antibody (1:5000) and anti-*E. coli* Rps1 antibody (1:5000) respectively. ECL was used for the detection.

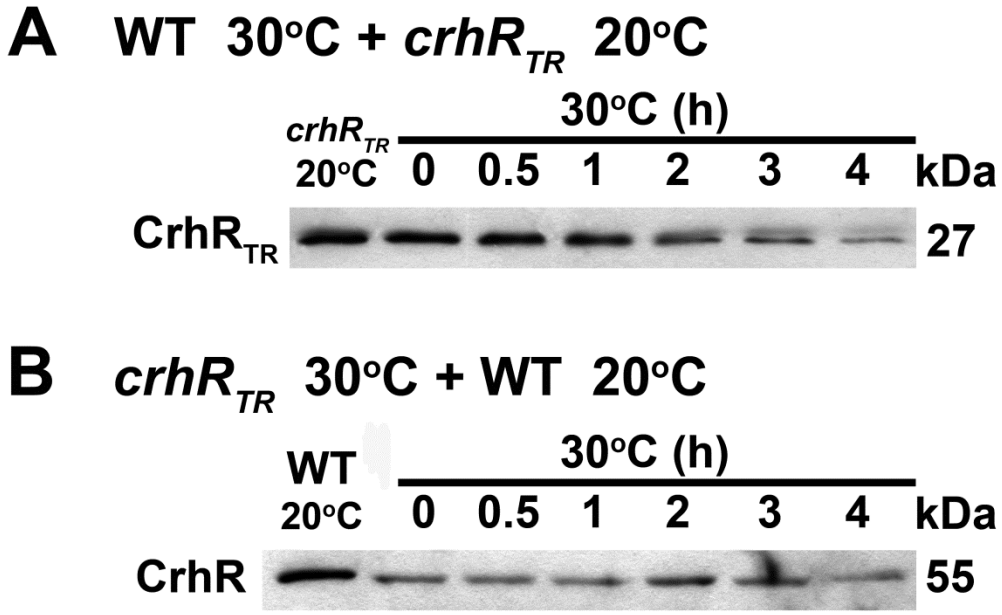
A
WT 30°C + crhR_TR 20°C
30°C (h)
crhR_TR
20°C 0 0.5 1 2 3 4 kDa
CrhR_TR
27
B
crhR_TR 30°C + WT 20°C
30°C (h)
WT
20°C 0 0.5 1 2 3 4 kDa
CrhR
55

3.2.3 Proteolytic degradation of CrhR in *Synechocystis* strains expressing His-R

Synechocystis wild type and two mutants, *crhR*$_{TR}$ and Δ*crhR*, transformed with pMon-HisR were used to determine whether the level of constitutively expressed His-R will be altered in response to temperature *in vivo*. This experiment was performed to also investigate if degradation of CrhR$_{TR}$ protein can be restored by the presence of functional His-R helicase in the *crhR*$_{TR}$ mutant. Immunoblot analysis was used to monitor CrhR, His-R and CrhR$_{TR}$ protein levels in all three strains (Figure 3.14).

Expression of His-CrhR in the wild type cells does not change the pattern of the accumulation of 55 kDa CrhR protein, which increases at 20^{o}C and rapidly decreases in the first hours of warm incubation (Figure 3.14 WT). It would be expected that the level of His-R would remain constant under all growth conditions as it is being expressed from the pNir constitutive promoter. However, it is interesting to note that expression of the 58 kDa His-R changes in response to temperature in wild type cells. It is observed that His-R is present at elevated levels when cells are grown continuously at 30^{o}C and also at the same level in response to growth at 20^{o}C. However, unexpectedly the level of His-R protein decreases during the first 3 hours after upshift of the culture from 20^{o}C to 30^{o}C. During this period, native CrhR is also decreasing in a linear fashion, with levels returning to the basal level observed at 30^{o}C within 24 h. In contrast, His-R abundance rapidly increases between 3 and 6 h of growth at 30^{o}C, remaining constant for the rest of the experiment.

Figure 3.14: *In vivo* abundance of CrhR in *Synechocystis* strains expressing His-R. Wild Type (WT), complete *crhR* deletion mutant (Δ*crhR*) and $crhR_{TR}$ mutant ($crhR_{TR}$) cells were grown at 30^{o}C to mid-log phase, cultures were transferred to 20^{o}C for 3 h and then transferred back to 30^{o}C for 24 h. Aliquots of the cultures were taken at the indicated time points for isolation of soluble protein. His-tagged CrhR (58 kDa), wild type CrhR protein (55 kDa) and truncated $CrhR_{TR}$ protein (27 kDa) were identified by western analysis using anti-CrhR antibody (1:5000) and detected by ECL. Rps1 protein, used as a loading control, was identified using anti-*E. coli* Rps1 antibody (1:5000).

WT

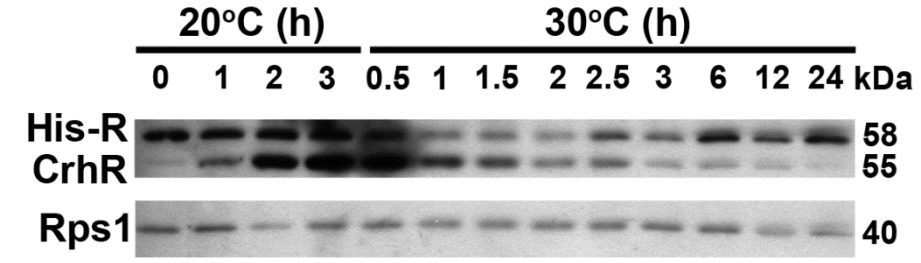

Δ*crhR*

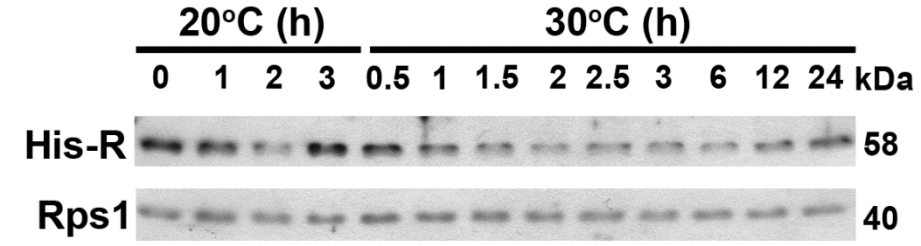

***crhR*$_{TR}$**

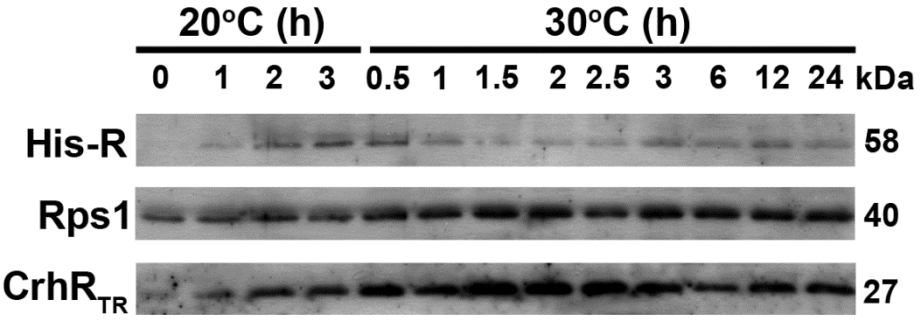

A similar pattern of His-R accumulation is observed in the Δ*crhR* and *crhR*$_{TR}$ mutant (Figure 3.14 Δ*crhR* and *crhR*$_{TR}$). In addition and unexpectedly, expression of His-R does not restore degradation of CrhR$_{TR}$ protein at 30^{o}C in the *crhR*$_{TR}$ mutant, similar to the response observed in wild type cells (Figure 3.14 *crhR*$_{TR}$).

Levels of loading control Rps1 remain constant regardless of the temperature in all of the strains, confirming that the observed changes in protein levels in response to temperature shifts are CrhR-specific.

In order to assure that His-R protein is produced constitutively and temperature does not play any direct role in the regulation of the pNir promoter, levels of His-R were monitored in *E. coli* cells at various temperatures (Figure 3.15). This experiment shows that His-R protein levels remain constant in *E. coli* cells even in response to temperature shifts between 37^{o}C and 15^{o}C, confirming that pNir promoter activity is not responsive to temperature shifts.

3.2.4 Requirement of *de novo* protein synthesis for activity of degradation machinery

Two translation inhibitors were used in the *in vivo* degradation assay to determine if *de novo* protein synthesis is required for degradation activity. After a 2 h cold induction to generate maximum CrhR levels, chloramphenicol (Cm) or kanamycin (Km), were added to the *Synechocystis* wild type 1 hour prior to transfer of cells back to 30^{o}C. Wild type cells treated identically but without addition of antibiotic served as a control (Figure 3.16).

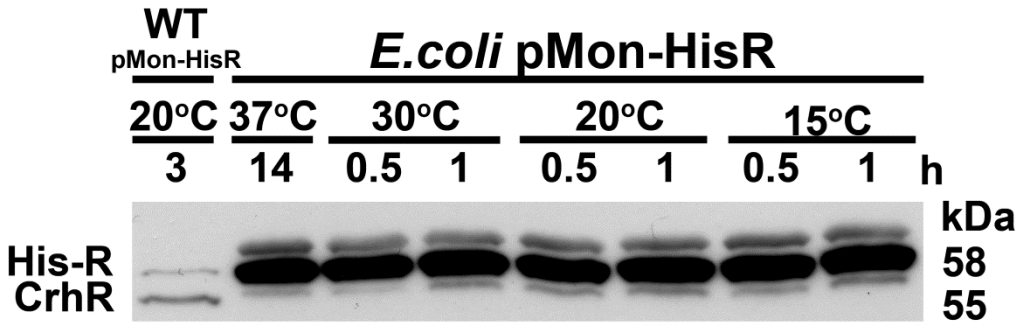

Figure 3.15: His-R abundance in *E. coli* cells containing pMon-HisR at various temperatures. Overnight culture of *E. coli* BL 21with pMon-HisR was incubated at the indicated temperatures for 1 hour. Aliquots of the cultures were taken at the indicated time points for isolation of soluble protein. His-tagged CrhR (His-R) (58 kDa) was identified by western analysis using anti-CrhR antibody (1:5000) and detected by ECL. Cold shocked *Synechocystis* wild type cells containing pMon-HisR served as a positive control.

As expected from previous findings (Figure 3.8), in the control cells induction of CrhR is observed after transfer from 30^{o}C to 20^{o}C and then a rapid decrease back to basal levels in response to transfer back to 30^{o}C. However, with addition of chloramphenicol no degradation of CrhR is observed at 30^{o}C (Figure 3.16 +Cm). In contrast, the pattern of CrhR accumulation is not altered in the presence of kanamycin (Figure 3.16 +Km). Chloramphenicol and kanamycin inhibit different stages of translation, elongation and initiation, respectively. These results indicate that *de novo* protein synthesis of degradation machinery is required after the transfer of cells from 20^{o}C to 30^{o}C. In addition results suggest that initiation of elongation of degradation machinery mRNAs starts at 20^{o}C, but elongation proceeds only at 30^{o}C.

3.2.5 Effect of light/dark transition on the CrhR degradation

Light/dark transitions were introduced into the *in vivo* experiments as one of the conditions that may influence CrhR protein degradation at 30^{o}C, since CrhR expression is also regulated by the light driven reduction of the components of the photosynthetic electron transport chain (Kujat and Owttrim, 2000). While transferring wild type cells after cold shock back to 30^{o}C, the culture was split into two, one of which was wrapped in aluminum foil to imitate darkness. Immunoblot analysis of the samples collected during this *in vivo* assay showed that CrhR degradation is delayed at 30^{o}C when cells are incubated in the dark (Figure 3.17). It is already observed in the previous experiments that it takes about 1.5-2.5 hours at 30^{o}C for CrhR levels to return to basal levels (Figure 3.8 A).

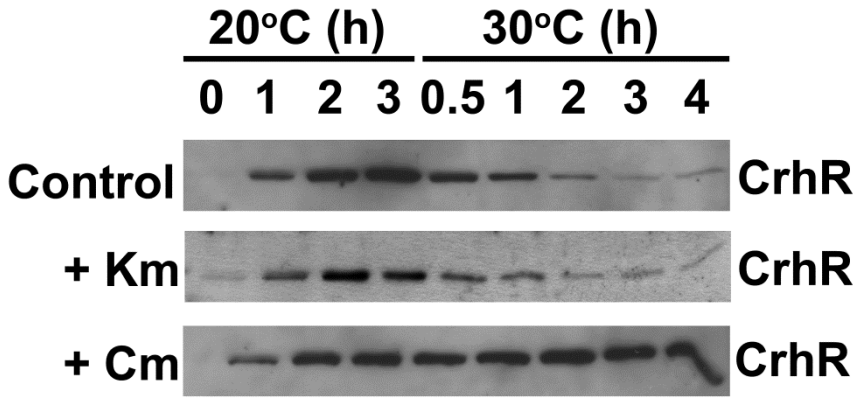

Figure 3.16: Effect of translation inhibitors on *in vivo* degradation of CrhR protein in wild type cells. Wild type *Synechocystis* cells were grown at 30^{o}C to mid-log phase and then divided into three aliquots. Aliquotes were transferred to 20^{o}C for 3 hours. At the 2 h time point at 20^{o}C, chloramphenicol (Cm) at 250µg/ml or kanamycin (Km) at 200µg/ml, were added to one of the flasks as indicated; nothing was added to the control flask. After 3 h cold shock at 20^{o}C all three cultures were transferred to 30^{o}C for 4 h. Soluble proteins were extracted from aliquots taken at the indicated time points. Wild type CrhR protein (55 kDa) was identified by western analysis using anti-CrhR antibody (1:5000) and detected by ECL.

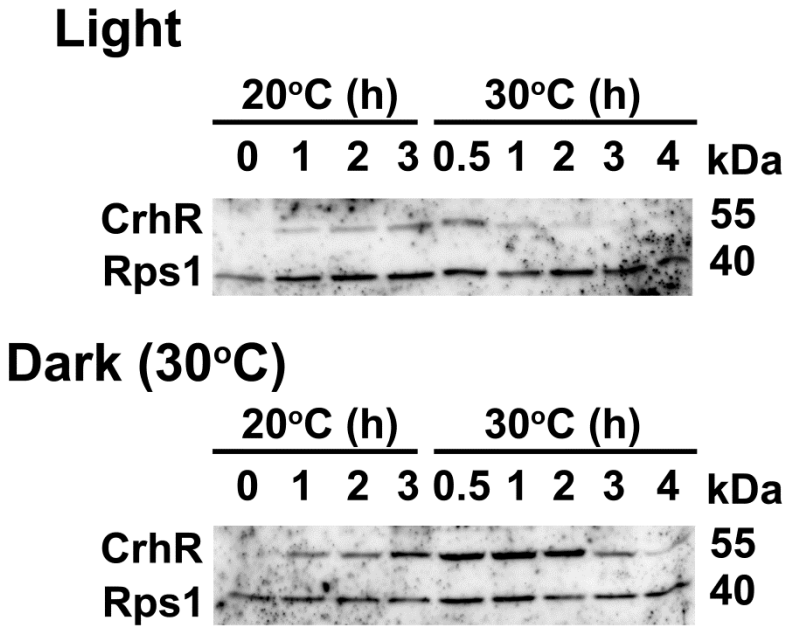

Figure 3.17: Effect of a light-dark transition on CrhR degradation. Wild type cells were grown at 30^{o}C to mid-log phase, then divided into 2 aliquots and both were transferred to 20^{o}C for 3 h. One of the flasks was wrapped with aluminum foil to imitate dark conditions. Soluble proteins were extracted from aliquots taken at the indicated time points. Wild type CrhR (55 kDa) and Rps1 (40 kDa) proteins were identified by western analysis using anti-CrhR antibody (1:5000) and anti-*E. coli* Rps1 antibody (1:5000) respectively and detected by ECL.

It can also be seen from the control that CrhR levels responded normally to temperature shift in cells that did not experience the dark treatment (Figure 3.17 Light). Unlike the control, cells kept in the dark at 30^{o}C show delayed CrhR degradation (Figure 3.17 Dark). It takes about 4 h, which is about twice as long as the control, for CrhR levels to return to basal in the dark. Therefore, dark may interrupt or reduce the formation and/or activation of the proteins involved in CrhR proteolytic degradation.

3.3 Proteases potentially involved in CrhR degradation

3.3.1 Temperature regulation of FtsH and ClpC proteases in wild type cells

It was previously observed that transcript abundance of the proteases FtsH and ClpC is reduced in response to *crhR* mutation (Jens Georg, unpublished data). In an attempt to determine the protease(s) involved in CrhR degradation, levels of those proteases were monitored in wild type and the *crhR* mutants using antibodies against *Arabidopsis thaliana* FtsH and ClpC proteins (a generous gift from Zach Adam, University of Jerusalem, Israel) (Figures 3.18 and 3.19).

The pattern of FtsH protein accumulation in wild type cells (Figure 3.18) resembles CrhR levels (Figure 3.8 WT). FtsH protein levels increase in the cold and return to basal levels after the shift to 30^{o}C. The Δ*crhR* mutant shows a very similar pattern. However the opposite is observed in the $crhR_{TR}$ mutant, in which

Figure 3.18: FtsH protein abundance. Wild Type (WT), complete *crhR* deletion mutant (Δ*crhR*) and $crhR_{TR}$ mutant ($crhR_{TR}$) cells were grown at 30^{o}C to mid-log phase, cultures were transferred to 20^{o}C for 24 h and then transferred back to 30^{o}C for 24 h. Aliquots of the cultures were taken for soluble protein isolation at the indicated time points. FtsH (74 kDa) was identified by western analysis using an antibody against *Arabidopsis thaliana* FtsH (1:5000) and detected by ECL reagent.

WT

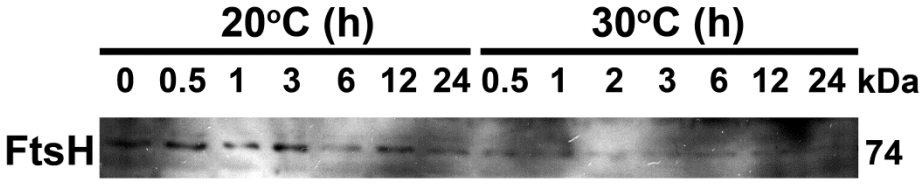

Δ*crhR*

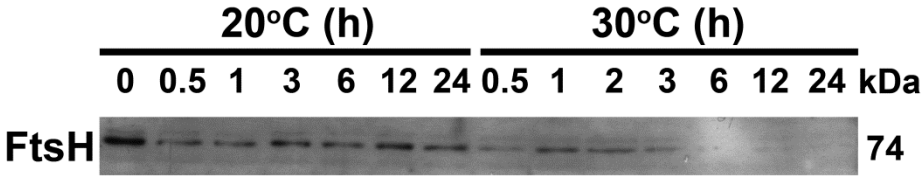

***crhR*$_{TR}$**

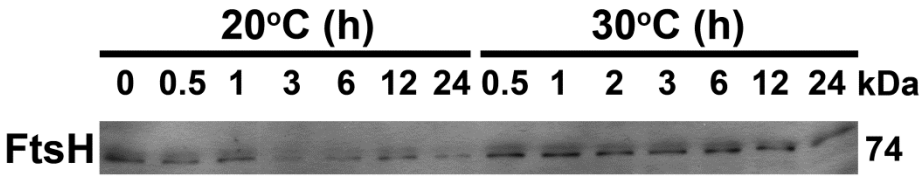

FtsH levels decrease in the cold and then rapidly increase in response to shift to 30^{o}C. FtsH amounts induce in the first half an hour at 30^{o}C and then remain at the same elevated level for 24 h during incubation of *crhR*$_{TR}$ mutant cells in the warm. However, since the same effect is not observed in both mutants, it can be concluded that elevated levels of FtsH protein observed at 30^{o}C in *crhR*$_{TR}$ cells are not directly related to the absence of functional CrhR helicase. Levels of FtsH protease may be induced due to the presence of high levels of non-functional CrhR$_{TR}$ at 30^{o}C.

ClpC protein shows different patterns of accumulation between wild type and *crhR* mutant strains (Figure 3.19). Wild type cells have basal levels of ClpC when growing continuously at 30^{o}C, which increases slowly at 20^{o}C. Observed levels remain high when cells are transferred back to 30^{o}C. In contrast, Δ*crhR* and *crhR*$_{TR}$ mutants have relatively constant levels of ClpC regardless of the temperature. This observation implies that CrhR may be involved in regulation of *clpC* expression.

3.3.2 Effect of FtsH mutation on CrhR abundance

There are four *ftsH* genes in the *Synechocystis* genome. Mutants for two of these genes, *ftsH2* and *ftsH4* (a generous gift from Yu Jianfeng, Imperial College London, United Kingdom), were used to test FtsH participation in CrhR degradation. An i*n vivo* degradation experiment was performed using these two *ftsH* mutants. Mutants were grown continuously at 30^{o}C, then cold shocked at 20^{o}C and returned back to 30^{o}C, to observe whether CrhR degradation will be

Figure 3.19: ClpC protein abundance. Wild Type (WT), complete *crhR* deletion mutant (Δ*crhR*) and $crhR_{TR}$ mutant ($crhR_{TR}$) cells were grown at 30^{o}C to mid-log phase; cultures were transferred to 20^{o}C for 24 h and then transferred back to 30^{o}C for 24 h. Aliquots were taken for soluble protein isolation at the indicated time points. ClpC (90 kDa) was identified by western analysis using antibody against *Arabidopsis thaliana* ClpC (1:1000) and detected by ECL reagent.

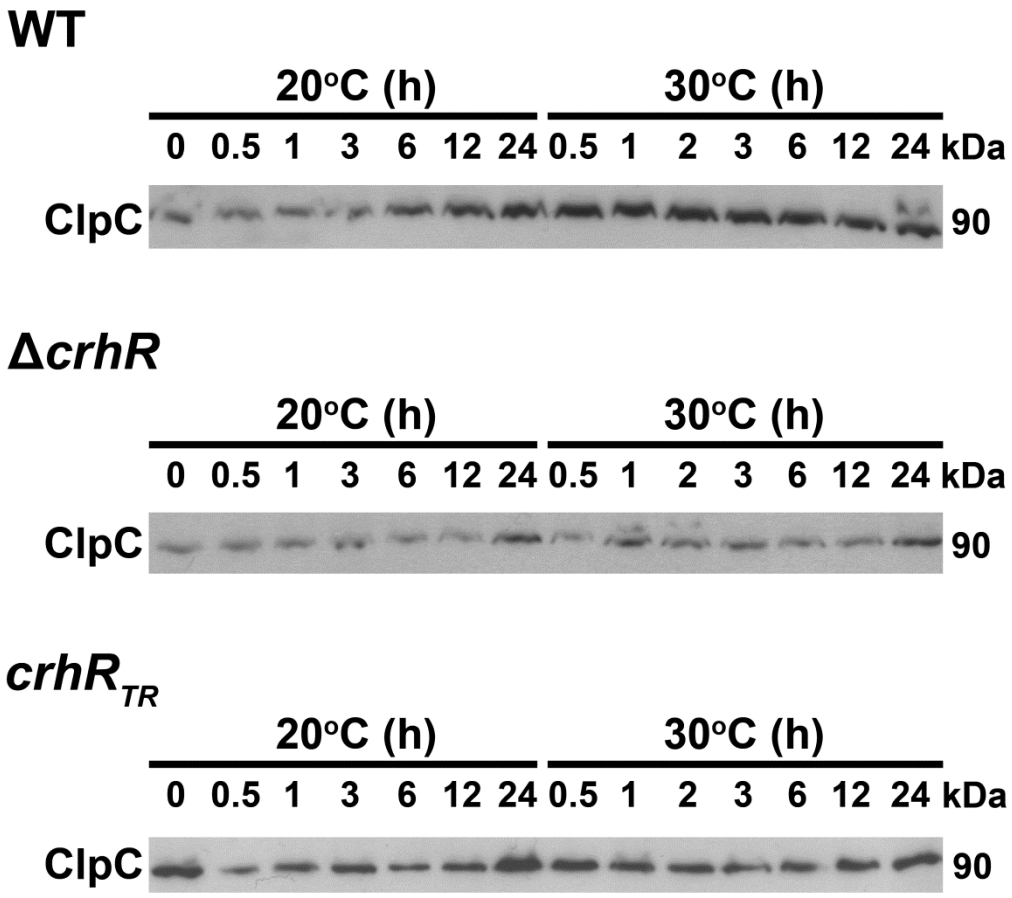
WT
20°C (h)
30°C (h)
0 0.5 1 3 6 12 24 0.5 1 2 3 6 12 24 kDa
ClpC
90
ΔcrhR
20°C (h)
30°C (h)
0 0.5 1 3 6 12 24 0.5 1 2 3 6 12 24 kDa
ClpC
90
crhR_TR
20°C (h)
30°C (h)
0 0.5 1 3 6 12 24 0.5 1 2 3 6 12 24 kDa
ClpC
90

observed in the warm. Immunoblot analysis of CrhR protein levels over the time course indicates that the pattern of CrhR accumulation at 20^{o}C and degradation at 30^{o}C previously observed in the wild type (Figure 3.8) is similar to the pattern in *ftsH* mutants (Figure 3.20). This suggests that these two FtsH proteases are not involved in the proteolytic regulation of CrhR levels in the warm. There is another possibility, that there are several proteases involved in this process, one of which is FtsH. It is also observed that CrhR levels are decreased with respect to Rps1 levels at all temperatures in *ftsH* mutants (Figure 3.20). This may be due to increasing proteolysis by another protease(s) due to knockout of FtsH activity, that occurs uncontrollably at all temperatures. Unexpectedly, during western analysis a peptide of unknown origin approximately 48 kDa was detected on the blot.

3.4 Post-translational modification of CrhR protein

During several *in vitro* experiments, in which experimental mixtures of two lysates were detected on the same blot, it was noticed that there was a slight difference in the migration of CrhR protein that happens with addition of warm protein lysate to the cold lysate (Figure 3.21). Specifically, CrhR protein appears to be 1-2 kDa smaller immediately after mixing cold cell lysate with warm lysate than CrhR in the cold lysate alone. Several methods were tried in order to further resolve those CrhR proteins appearing to have slightly different size, including resolving with lower (6%) and higher (15%) percent acrylamide gels, gradient gel (4-16%) and long 10% polyacrylamide gel (PAG). None of those methods

Figure 3.20: Effect of *ftsH* mutation on CrhR abundance. *ftsH* mutant cells were grown at 30^{o}C to mid-log phase, cultures were transferred to 20^{o}C for 24 h and then transferred back to 30^{o}C for 24 h. Aliquots were harvested for soluble protein extraction at indicated times. Wild type CrhR (55 kDa) and Rps1 (40 kDa) proteins were identified by western analysis using anti-CrhR antibody (1:5000) and anti-*E. coli* Rps1 antibody (1:5000) respectively and detected by ECL.

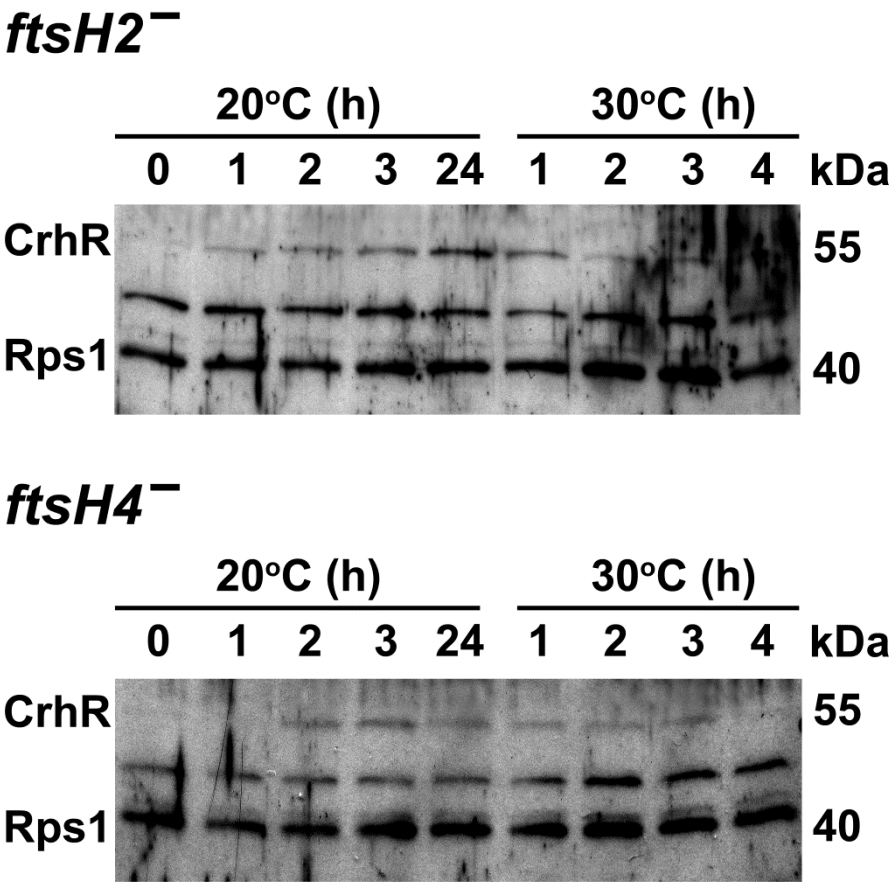
ftsH2⁻
20°C (h)
30°C (h)
0 1 2 3 24 1 2 3 4 kDa
CrhR
Rps1
55
40
ftsH4⁻
20°C (h)
30°C (h)
0 1 2 3 24 1 2 3 4 kDa
CrhR
Rps1
55
40

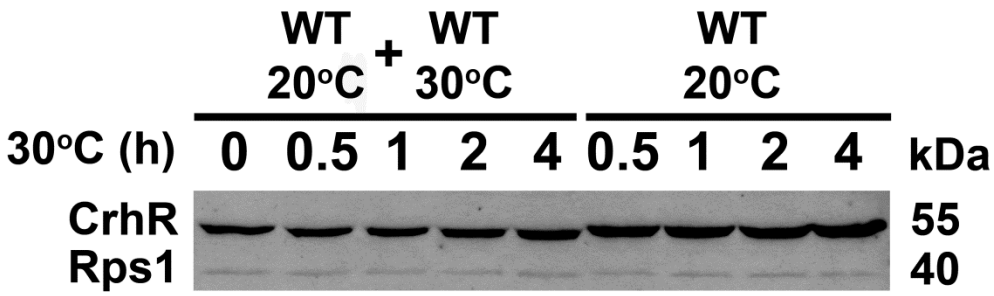

Figure 3.21: Post-translational modification of CrhR protein. A mixture of soluble protein, extracted from wild type (WT) cells grown at 30^{o}C and 20^{o}C, was incubated at 30^{o}C and aliquots were taken at the indicated times. As a control, WT lysate from cells grown at 20^{o}C was incubated alone at 30^{o}C. Wild type CrhR (55 kDa) and Rps1 (40 kDa) proteins were identified by western analysis using anti-CrhR antibody (1:5000) and anti-*E. coli* Rps1 antibody (1:5000), respectively and detected by ECL. Experiment was performed in conjunction with Albert Rosana.

resolved those CrhR bands better than the regular 10% PAG that was used in all of the other experiments. It was concluded that this slight decrease in size immediately after mixing with warm lysate is due to removal of some post-translational modification or cleavage of CrhR protein by proteases present in the warm lysate. Since one of the most common post-translational modifications is phosphorylation, wild type cold lysate was treated with two phosphatases: shrimp alkaline phosphatase and calf intestine alkaline phosphatase. For the treatment we used the amount suggested by the manufacturer instructions as well as tripled the concentration of the enzyme. Neither shrimp phosphatase (SP), nor calf intestine phosphatase (CIP) at either concentration visibly changed the size of CrhR (Figure 3.22). It is possible that CrhR is post-translationally modified by some other mechanism rather than phosphorylation. This modification occurs rapidly and only in the presence of cell lysate from cells grown at 30^{o}C, thus proteins present in the cells grown at warm temperature are involved in the potential post-translational modification of CrhR.

3.5 Cellular localization of CrhR

In attempt to confirm that rapid reduction of CrhR levels in the warm is due to degradation and is not related to sequestration of CrhR in cellular compartments, the cellular location of CrhR protein at 30^{o}C and 20^{o}C was investigated.

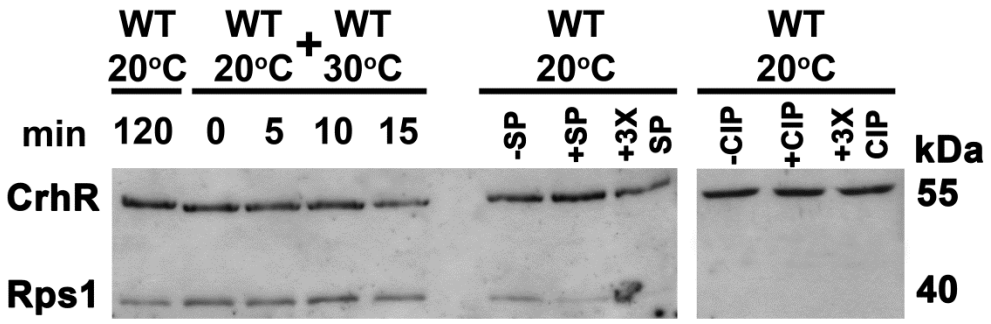

Figure 3.22: Phosphatase addition to identify post-translational modification of CrhR. A mixture of soluble protein, extracted from wild type (WT) cells grown at 30^{o}C and 20^{o}C, was incubated at 30^{o}C and aliquots were taken at the indicated times. Shrimp alkaline phosphatase (SP) and calf intestine phosphatase (CIP) in the amounts recommended by the manufacturer (3 U per 10µg of total protein) or triple the amount (9 U) was added to the lysate from cold grown cells. Lysates with phosphatase were incubated at 37^{o}C for 30 min to allow for phosphatase activity. Wild type CrhR (55 kDa) and Rps1 (40 kDa) proteins were identified by western analysis using anti-CrhR antibody (1:5000) and anti-*E. coli* Rps1 antibody (1:5000), respectively, and detected by ECL.

3.5.1 Determination of CrhR cellular localization of CrhR by using different extraction techniques

In order to determine the cellular localization of CrhR, several experiments using different extraction buffers were performed. During preliminary analysis two protein extraction methods were used: STS buffer, which contains a mixture of three detergents, and CPEBB buffer, which is utilized in the lab during mechanical lysis of cyanobacterial cells. CPEBB buffer does not contain any detergents and is used to isolate soluble proteins from cyanobacteria. In contrast, STS buffer is capable of solubilizing cell membranes due to the presence of detergents and therefore is expected to extract membrane proteins. In this experiment, CPEBB was used for mechanical lysis of cells to extract soluble proteins and STS buffer was utilized to extract total proteins the cells.

Analysis comparing two protein extraction methods indicated that STS buffer extracts more CrhR protein than the mechanical lysis (Figure 3.23). It is also important to note that the same immunoblot analysis (Figure 3.23) shows that the amount of soluble Rps1 is lower in the STS extraction. This is exactly what should be expected, because Rps1 is known to be a cytoplasmic protein and thus should be easily extracted only by mechanical lysis. However, the amount of CrhR is much higher when extracted from the membrane pellet with STS detergent buffer (Figure 3.23). Especially, it is interesting to note that CrhR is present at high levels even at 30^{o}C when detergents were used for extraction (Figure 3.23). This result suggests that a significant portion of CrhR is membrane associated in *Synechocystis* wild type cells.

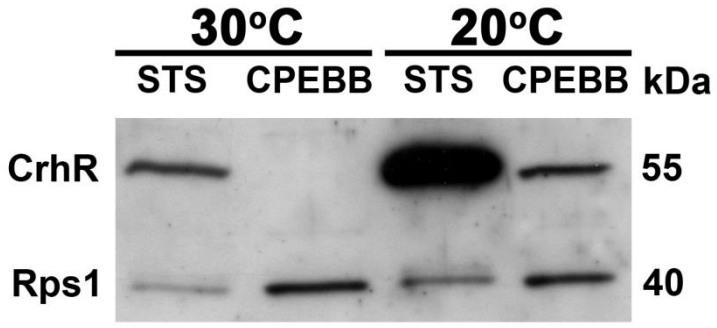

Figure 3.23: Initial analysis of CrhR cellular localization. Wild type cells were grown at 30°C to mid-log phase, half of the culture was cold shocked at 20°C for 3 hours. Cells were harvested and proteins were extracted using two different buffers: non-detergent, native protein isolation buffer (CPEBB) and triple detergent buffer (STS). Wild type CrhR (55 kDa) and Rps1 (40 kDa) proteins were identified by western analysis using anti-CrhR antibody (1:5000) and anti-*E. coli* Rps1 antibody (1:5000), respectively, and detected by ECL.

To further investigate the potential membrane association, a series of traditional treatments designed to differentially remove membrane-associated proteins were performed. The procedure involved six buffers, used to extract CrhR from crude membrane pellet left after mechanical lysis of wild type cells. Crude membrane pellets contained cellular compartments- mostly cell membranes that pelleted after soluble protein extraction. It was observed that in addition to STS buffer, 1M NaCl and 1% Brij 35 can extract a significant proportion of the CrhR present in the membranes fraction of cells growing at 30^{o}C (Figure 3.24). However, only NaCl can efficiently extract CrhR from the membrane fraction of cold shocked cells (Figure 3.25), indicating that the strength of CrhR interaction with the membranes changes in response to temperature shift. It also can be noted that CrhR protein is detected at different molecular weights depending on the buffer used for the extraction (Figures 3.24 and 3.25). This phenomenon could potentially be explained by different density and charge of the extraction buffers, which can slightly alter migration of the proteins in the particular samples. Overall, the experiments with various extraction buffers indicate that a significant portion of CrhR is membrane-associated in the wild type *Synechocystis* cells and the strength of this interaction is temperature-dependent.

3.5.2 Immunoelectron microscopy (IEM) of CrhR protein localization in wild type cells

Immunoelectron microscopy using anti-rabbit IgG coupled to 10 nm colloidal gold particles as a secondary antibody was performed on warm and cold

Figure 3.24: Cellular localization of CrhR protein at 30^{o}C. Cells were grown to the mid log phase at 30^{o}C, harvested and soluble proteins were extracted using mechanical lysis with CPEBB buffer and glass beads. Soluble protein was separated from the crude membrane fraction by centrifugation. The membrane fraction was treated with the indicated reagents for 30 min, followed by centrifugation. P and S represent the pellet and supernatant fractions after the second centrifugation step. Wild type CrhR protein (55 kDa) was identified by western analysis using anti-CrhR antibody (1:5000) and detected by ECL.

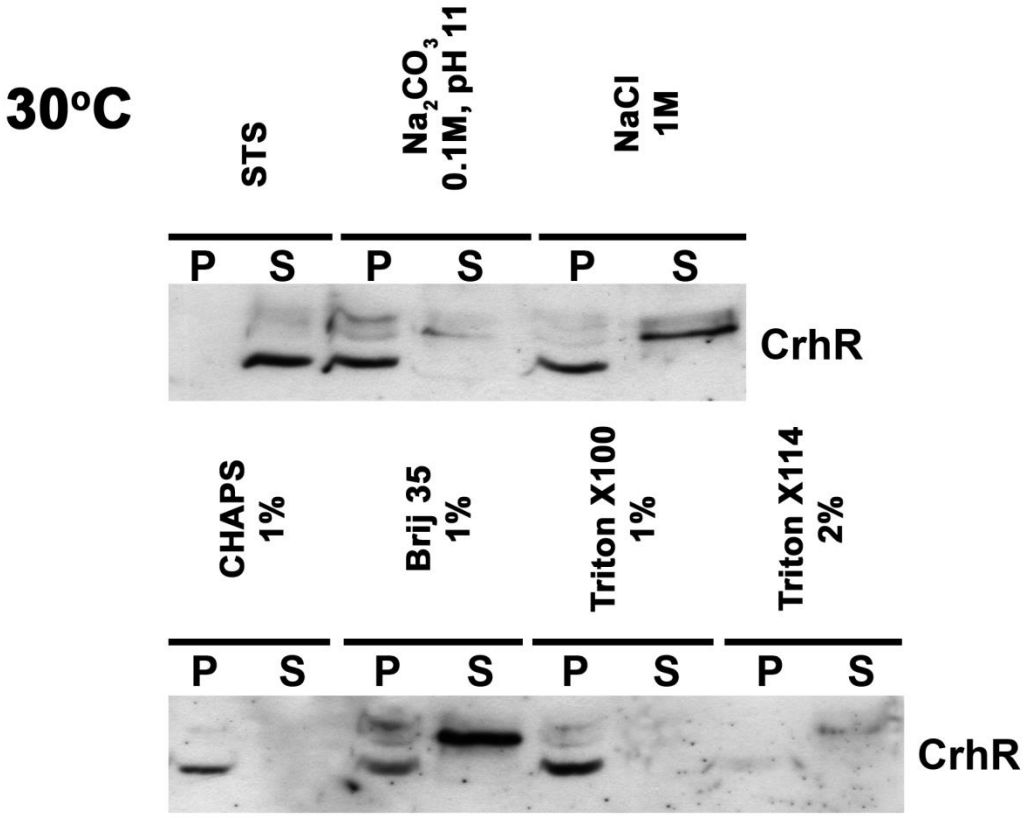
30°C
STS
Na2CO3 0.1M, pH 11
NaCl 1M
P S P S P S
CrhR
CHAPS 1%
Brij 35 1%
Triton X100 1%
Triton X114 2%
P S P S P S P S
CrhR

Figure 3.25: Cellular localization of CrhR protein at 20^{o}C. Cells were grown to the mid log phase at 30^{o}C and then cold shocked at 20^{o}C for 3 hours, harvested and soluble proteins were extracted using mechanical lysis with CPEBB buffer and glass beads. Soluble protein was separated from the crude membrane fraction by centrifugation. The membrane fraction was treated with indicated reagents for 30 min, followed by centrifugation. P and S represent the pellet and supernatant fractions after the second centrifugation step. Wild type CrhR protein (55 kDa) was identified by western analysis using anti-CrhR antibody (1:5000) and detected by ECL.

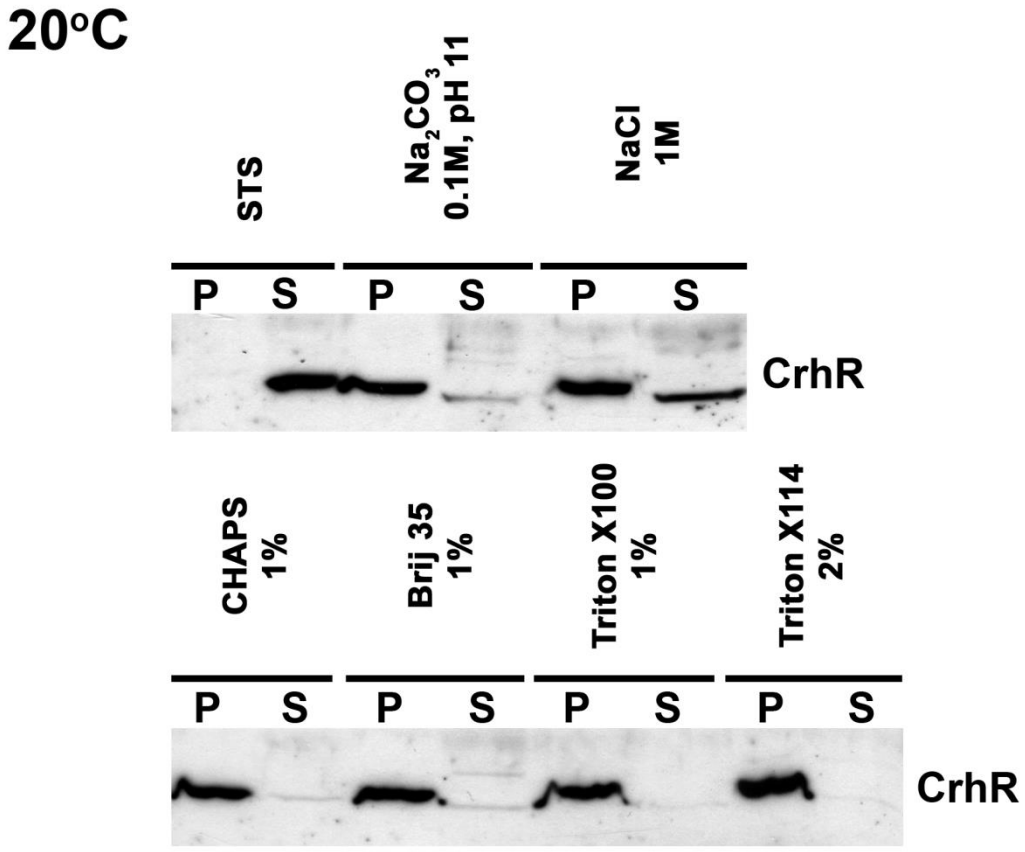
20°C
STS
Na2CO3 0.1M, pH 11
NaCl 1M
P S P S P S
CrhR
CHAPS 1%
Brij 35 1%
Triton X100 1%
Triton X114 2%
P S P S P S P S
CrhR

grown wild type *Synechocystis* cells in order to confirm membrane localization of the CrhR protein. As a control, the exact same procedure and cells were used, but primary anti-CrhR antibody was not added in order to account for non-specific binding of secondary antibody to cellular constituents.

Control cells demonstrate that secondary antibody is not binding non-specifically to cell sections, since approximately the same low number of gold particles is observed in the control (Figure 3.26 A,B) as well as in the background of all other images produced under experimental conditions (Figure 3.26 C,D; Figure 3.27). In addition, the number of gold particles found inside the control cells is significantly lower than the number of gold particles localized to the experimental cells (Table 3.1). Microscopy images of cells grown at 30^{o}C and 20^{o}C indicate that CrhR localizes to the thylakoid membrane region of the *Synechocystis* cells at both temperatures (Figure 3.26 C, D; Figure 3.27). As expected, significantly less CrhR is detected in the warm grown cells (Figure 3.26 C, D) compared to cold shocked cells (Figure 3.27) and most of it is localized to the thylakoid membrane region with limited detection in the cytoplasmic/nucleoid region (Table 3.1). This observation again supports the idea that CrhR is membrane associated at both growth temperatures. These results reconfirm that a low basal level of CrhR detected in the soluble fraction of proteins from cells grown at 30^{o}C is not the result of sequestration and storage of CrhR protein at some cellular compartment like inclusion bodies for the times when growth temperature shifts to cold.

Figure 3.26: Immunoelectronmicroscopy for cellular localization of CrhR protein. CrhR was detected in ultrathin sections of *Synechocystis* wild type cells grown at 30^{o}C using anti-CrhR polyclonal antibody at 1:100 dilution. Images A and B represent control sections that lacked primary anti-CrhR antibody. Images C and D represent sections exposed to the anti-CrhR antibody group with warm grown cells. Scale bars for each image are shown in the left bottom corner.

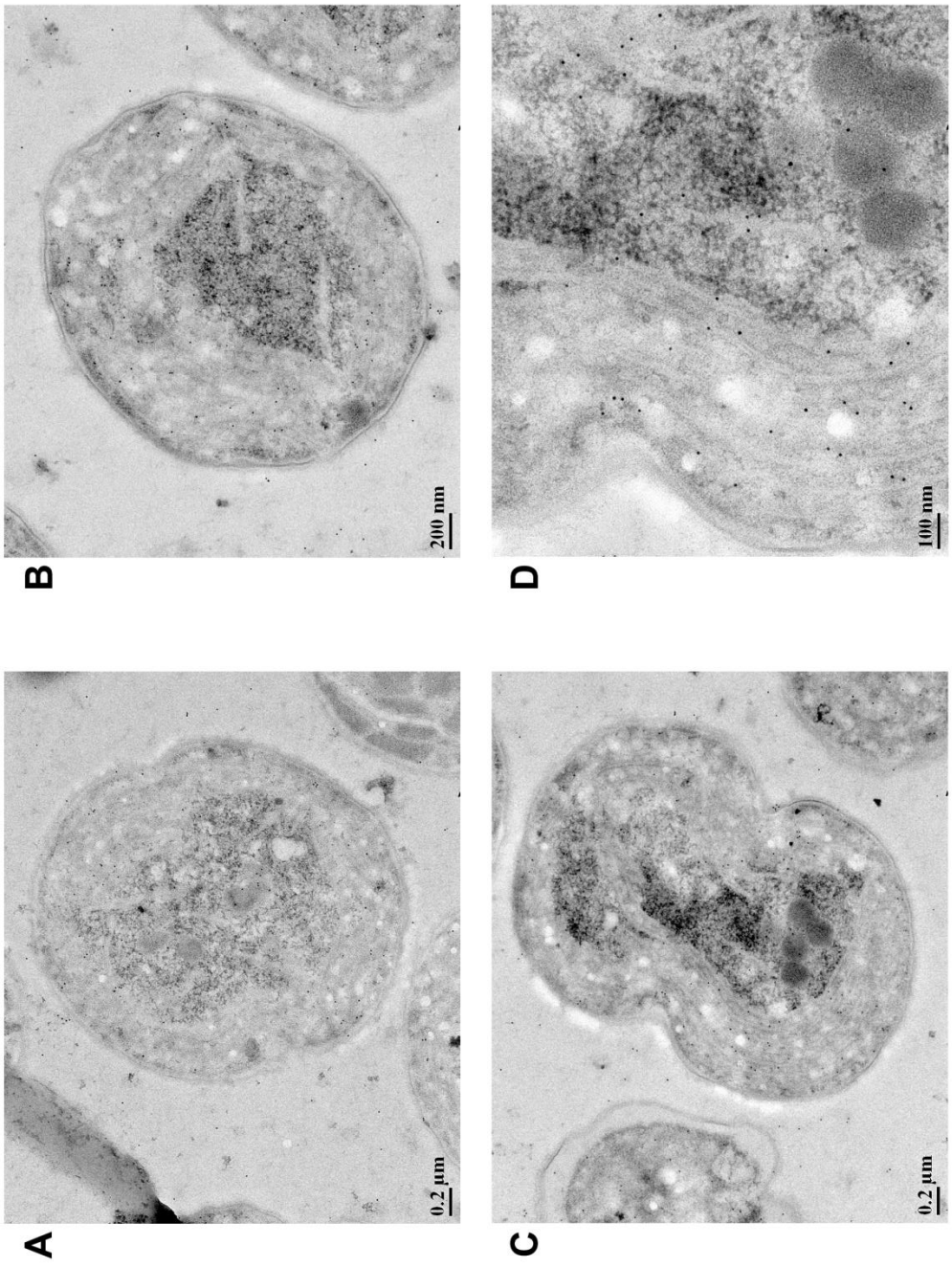
A
0.2 µm
B
200 nm
C
0.2 µm
D
100 nm

Figure 3.27: Immunoelectronmicroscopy for cellular localization of CrhR protein. CrhR was detected using anti-CrhR polyclonal antibody at 1:100 dilution in ultrathin sections of *Synechocystis* wild type cells grown at 30^{o}C and then cold shocked at 20^{o}C for 3 h. Scale bars for each image are shown in the left bottom corner.

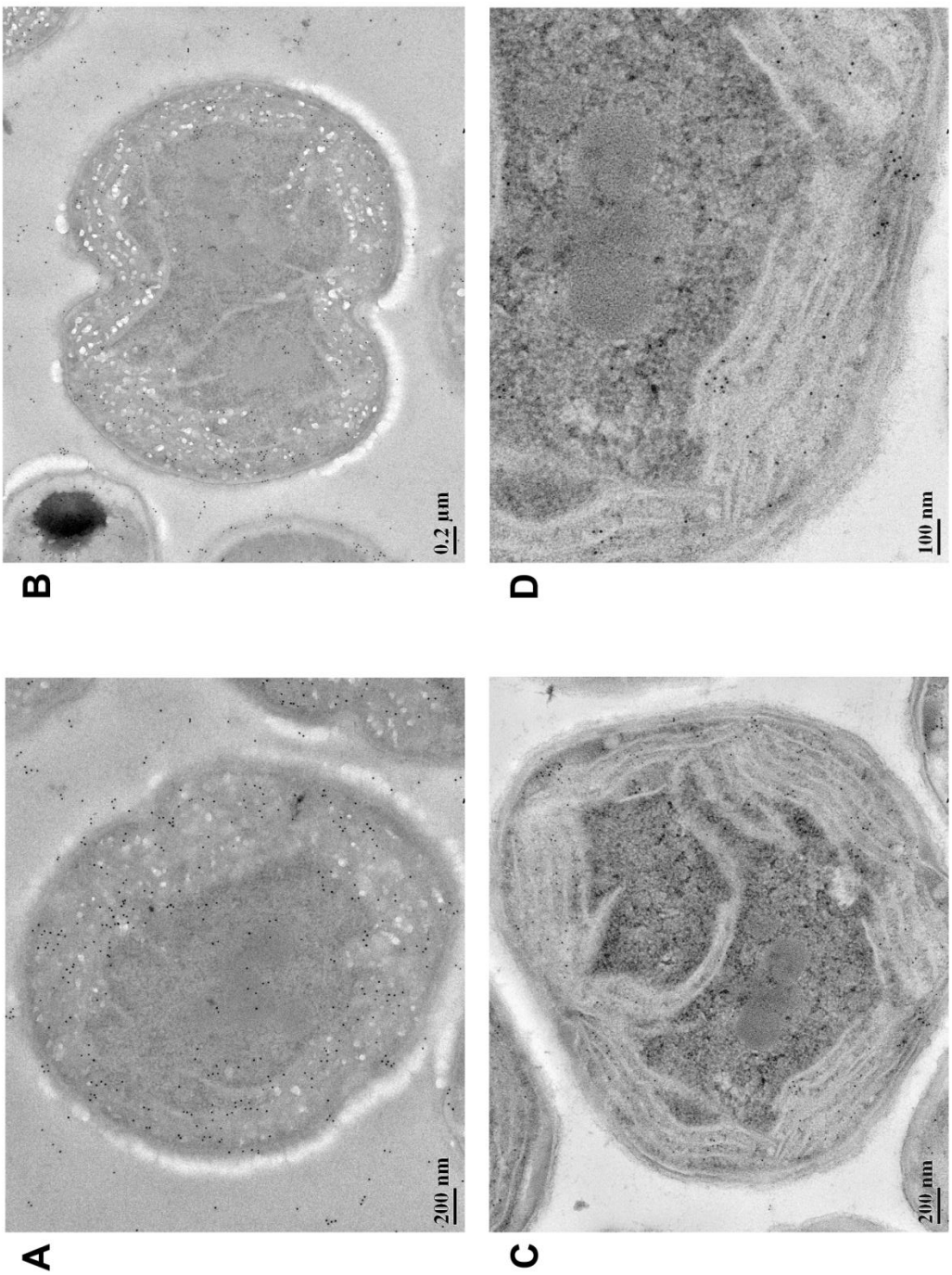
A
200 nm
B
0.2 µm
C
200 nm
D
100 nm

Table 3.1: Immunoelectron microscopy determination of CrhR cellular localization. Warm grown (30^{o}C) and cold shocked (20^{o}C for 2 hours) *Synechocystis* cells were viewed using immunoelectron microscopy. The numbers of gold particles were enumerated manually from the photographic images of ultrathin sections at various magnification (ranging from 45 000 to 60 000). In the control no primary antibody for CrhR protein was used. A total of 18 sections (6 per each temperature and control treatment) were utilized to count gold particles. Cytoplasm region defines intracellular space outside of thylakoid membranes region.

Growth temperature	Location	Total number of gold particles
30^{o}C	Thylakoid membranes region	278
30^{o}C	Cytoplasm region	110
20^{o}C	Thylakoid membranes region	888
20^{o}C	Cytoplasm region	265
gold control	Thylakoid membranes region	87
gold control	Cytoplasm region	71

3.6 Proteins interacting with CrhR

In an attempt to determine the physiological function of CrhR protein, proteins that interact with this helicase were identified by *in silico* prediction and co-immunoprecipitation analysis. *In silico* search using online Search Tool for the Retrieval of Interacting Genes/Proteins (STRING, www.string-db.org) was used for prediction of interacting proteins (Table 3.2, Figure 3.28). *In silico* prediction was followed by co-immunoprecipitation experiment using Δ*crhR* with pMon-HisR as experimental strains and Δ*crhR* as a control (Tables 3.3 and 3.4). Since results from the immunoelectron microscopy showed that CrhR is present in the cytoplasmic region as well as thylakoid membranes, both soluble (Table 3.3) and membrane fractions (Table 3.4) of the cell lysate were analyzed.

Proteins pulled down during co-immunoprecipitation were separated by 10% SDS-PAGE prior to identification by the mass spectrometry. CrhR co-immunoprecipitated proteins from the soluble fraction of the Δ*crhR* with pMon-HisR cells, when separated on SDS-PAGE, showed a number of polypeptides above 100 kDa and below 40 kDa whose abundance was different from the control strain (Figure 3.29, Eluate lane). Co-immunoprecipitated proteins from the membrane fraction of cell lysates from the same strains did not show a significant difference between experimental and control group visible by naked eye on the SDS-PAGE (Figure 3.30. Eluate lane). However, when lanes from both gels labeled “Eluate” (Figure 3.29 and 3.30) were analyzed by mass spectrometry, results showed a significant number of proteins from soluble and membrane

fraction, which are present in the experimental group Δ*crhR* with pMon-HisR, but not in the control Δ*crhR* (Tables 3.3 and 3.4).

Mass spectrometry identified a significant number of proteins from the co-immunoprecipitation experiment, which potentially interact with CrhR, with the majority being involved in metal-ion and nucleotide binding, and transport activity (Tables 3.3 and 3.4). The minority of the proteins precipitating with CrhR in both soluble and membrane fractions of the cell lysate belong to RNA, DNA and protein binding as well as signal transduction activity (Tables 3.3 and 3.4).

Proteins identified by co-immunoprecipitation differ from the proteins predicted by STRING online search tool (Figure 3.28, Table 3.2). From the list of proteins predicted to interact with CrhR only two proteins were confirmed by the co-immunoprecipitation experiment: Pnp (polynucleotide phosphorylase), which was also found in the soluble fraction of cell lysate (Table 3.2) and TypA (elongation factor EF-G) that is present in the membrane fraction (Table 3.4). Other proteins from STRING analysis (Table 3.2) were not confirmed with co-immunoprecipitation.

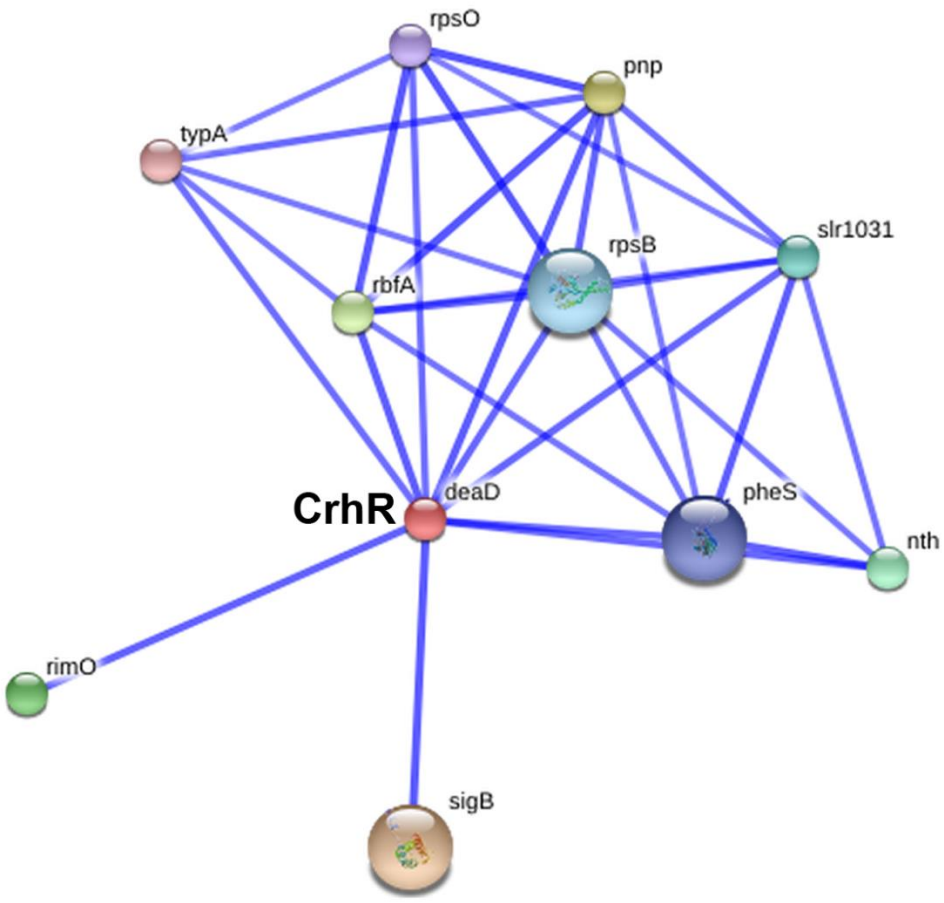

Figure 3.28: *Synechocystis* sp. PCC 6803 proteins interacting with CrhR as predicted by Search Tool for the Retrieval of Interacting Genes/Proteins (STRING, www.string-db.org, accessed on November 17, 2012). High confidence (0.700) was used as the criterion to predict interactions. Each line represents a possible interaction between the proteins. Stronger associations are represented by thicker lines. Bigger circles represent predicted interacting partners with known protein structure. Figure is directly adopted from www.string-db.org.

Table 3.2: Proteins predicted to interact with CrhR by Search Tool for the Retrieval of Interacting Genes/Proteins (STRING, www.string-db.org, accessed on November 17, 2012). High confidence (0.700) was used as the criterion to predict interactions. Protein names highlited with bold font represent interacting partners that were also confirmed by co-immunoprecipitation experiment. Protein that was also identified by mass spectrometry analysis of the proteins interacting with CrhR is in bold.

Protein	Definition of the protein
SigB	RNA polymerase sigma factor
Pnp	**polynucleotide phosphorylase/polyadenylase**
RbfA	ribosome-binding factor A
RimO	hypothetical protein
Nth	endonuclease III
slr1031	tyrosyl-tRNA synthetase
RpsB	30S ribosomal protein S2
PheS	phenylalanyl-tRNA synthetase subunit alpha
RpsO	30S ribosomal protein S15
TypA	**elongation factor EF-G**

Figure 3.29: Identification of soluble proteins interacting with CrhR. Anti-His antibody was crosslinked to protein A on Sepharose A beads. Total protein from the soluble fraction of cell lysates from cold shocked Δ*crhR* pMon-HisR and Δ*crhR* (control) strains were passed over the column. Cell lysate, collected wash and eluate fractions from the column and the supernatant from used boiled sepharose beads were separated by 10% SDS-PAGE and coomassie stained. Columns labelled "Eluate" were sent for mass spectrometry identification of the proteins.

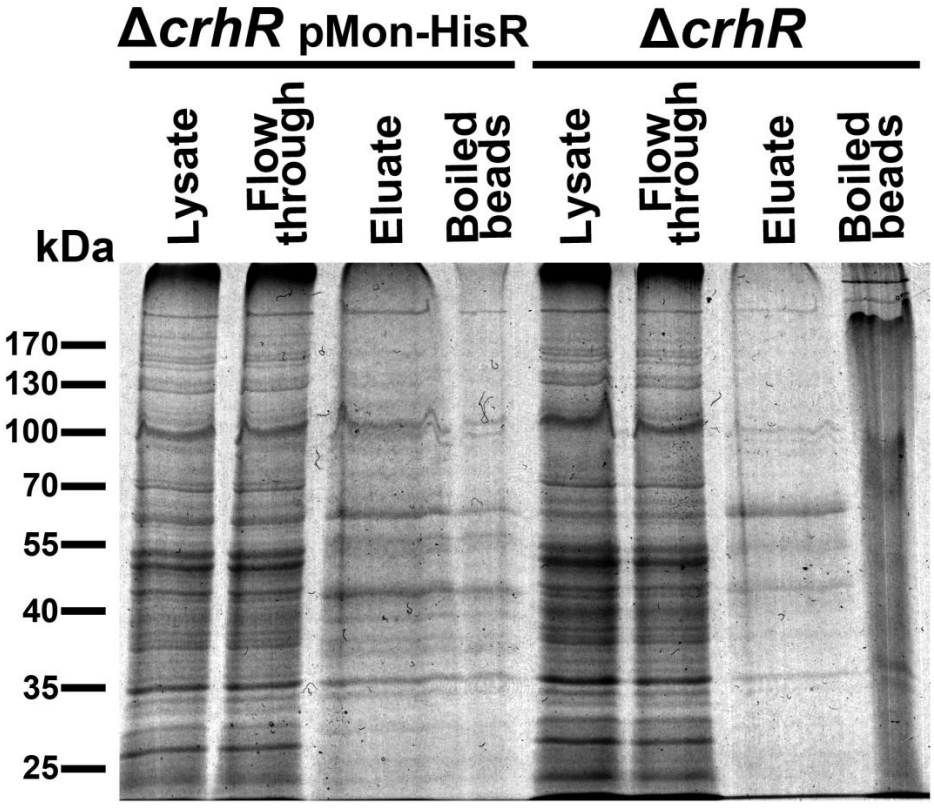
ΔcrhR pMon-HisR
ΔcrhR
Lysate
Flow through
Eluate
Boiled beads
Lysate
Flow through
Eluate
Boiled beads
kDa
170
130
100
70
55
40
35
25

Figure 3.30: Identification of membrane proteins interacting with CrhR. Anti-His antibody was crosslinked to protein A on Sepharose A beads. Total protein from the soluble fraction of cell lysates from cold shocked Δ*crhR* pMon-HisR and Δ*crhR* (control) strains were passed over the column. Cell lysate, collected wash and eluate fractions from the column and the supernatant from used boiled sepharose beads were separated by 10% SDS-PAGE and coomassie stained. Columns labelled "Eluate" were sent for mass spectrometry identification of the proteins.

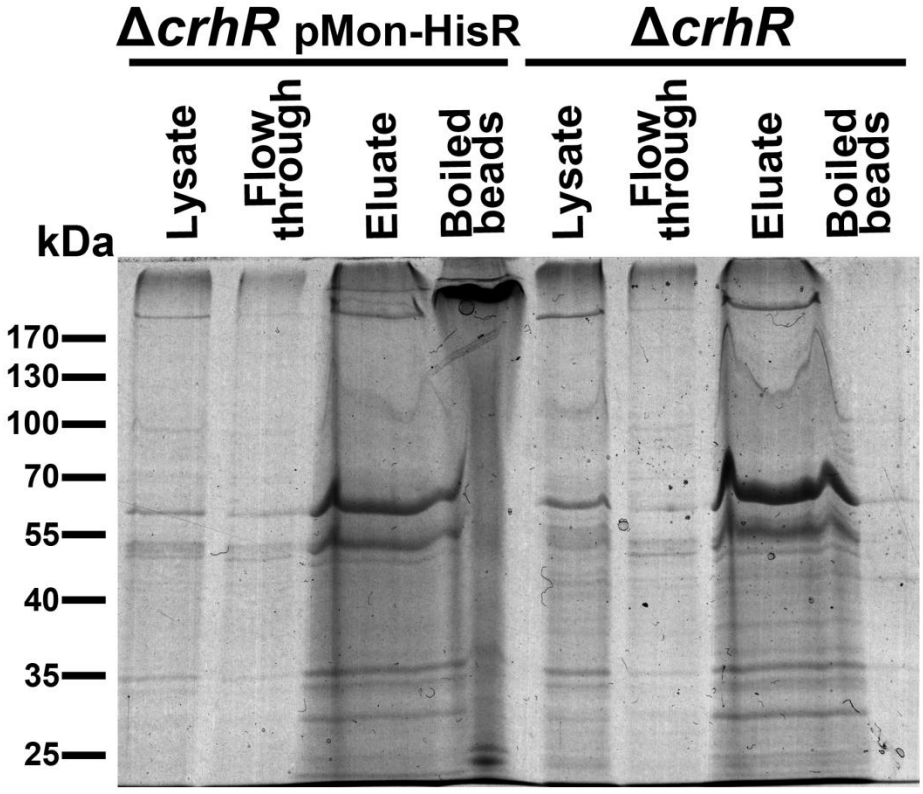
ΔcrhR pMon-HisR
ΔcrhR
Lysate
Flow through
Eluate
Boiled beads
Lysate
Flow through
Eluate
Boiled beads
kDa
170
130
100
70
55
40
35
25

Table 3.3: Mass spectrometry analysis of the soluble proteins interacting with His-R. Proteins found in both control Δ*crhR* and experimental Δ*crhR* pMon-HisR strains represent proteins that bind non-specifically to the column and therefore were omitted from the results. Protein that is also predicted to interact with CrhR by STRING (www.string-db.org) is in bold.

Protein	Description	Molecular Activity	Cellular Localization
CmpA	Bicarbonate transporter		
sll0443	Putative uncharacterized protein		
slr0909	Putative uncharacterized protein		
sll0446	Putative uncharacterized protein		
slr0731	Putative uncharacterized protein		
slr7024	Slr7024 protein		
slr0962	Putative uncharacterized protein		
slr1258	Putative uncharacterized protein		
slr0404	Putative uncharacterized protein		
slr0907	Putative uncharacterized protein		
slr1579	Putative uncharacterized protein		
slr1276	Putative uncharacterized protein		
sll0887	Putative uncharacterized protein		
slr0565	Putative uncharacterized protein		
sll1734	Putative uncharacterized protein		
slr0442	Putative uncharacterized protein		
slr1704	Putative uncharacterized protein		
sll0319	Putative uncharacterized protein		
sll0709	Restriction enzyme LlaI protein		
Ysf24	Fe-S assembly protein SufB		
slr1128	Putative uncharacterized protein		membrane
Phb	Prohibitin		membrane
sll0815	Putative uncharacterized protein		membrane
IsiA	Iron-stress chlorophyll-binding protein		membrane
EpsB	Exopolysaccharide export protein		membrane
Ycf4	Photosystem I assembly protein Ycf4		membrane
ApcA	Allophycocyanin a chain		membrane
sll1053	Putative uncharacterized protein		membrane
sll0141	Putative uncharacterized protein		membrane

Ndh	NADH dehydrogenase	catalytic activity	
sll1526	Putative uncharacterized protein	catalytic activity	
PdhB	Pyruvate dehydrogenase E1 beta subunit	catalytic activity	
ChlH	Mg-chelatase subunit	catalytic activity	
sll1178	Nodulation protein	catalytic activity	
MurQ	N-acetylmuramic acid 6-phosphate etherase	catalytic activity	
GlgA	Glycogen synthase	catalytic activity	
sll1558	Mannose-1-phosphate guanyltransferase	catalytic activity	
GlgP	Phosphorylase	catalytic activity	
AmiA	N-acetylmuramoyl-L-alanine amidase	catalytic activity	
MtnA	Methylthioribose-1-phosphate isomerase	catalytic activity	
slr0606	Putative uncharacterized protein	catalytic activity	
PrlC	Oligopeptidase A	catalytic activity	
TrpB	Tryptophan synthase beta chain	catalytic activity	
sll0602	Putative uncharacterized protein	catalytic activity	
sll1336	Putative uncharacterized protein	catalytic activity	cytoplasm
Tig	Trigger factor	catalytic activity	cytoplasm
AhcY	Adenosylhomocysteinase	catalytic activity	cytoplasm
GlnA	Glutamine synthetase	catalytic activity	cytoplasm
GidB	Ribosomal RNA small subunit methyltransferase G	catalytic activity	cytoplasm
Pds	Phytoene desaturase	catalytic activity	cytoplasm
HemL	Glutamate-1-semialdehyde 2,1-aminomutase	catalytic activity	cytoplasm
Shc	Squalene-hopene-cyclase	catalytic activity	extracellular
DnaN	DNA polymerase III subunit beta	catalytic activity; DNA binding	cytoplasm
HisD	Histidinol dehydrogenase	catalytic activity; DNA binding; metal ion binding; nucleotide binding	
RpoD	RNA polymerase sigma factor	catalytic activity; DNA binding; nucleotide binding	
MorR	MorR protein	catalytic activity; DNA binding; nucleotide binding	
TopA	DNA topoisomerase	catalytic activity; DNA binding; nucleotide binding	chromosome
UvrB	UvrABC system protein B	catalytic activity; DNA binding; nucleotide binding; protein binding	cytoplasm
slr1334	Putative uncharacterized protein	catalytic activity; metal ion binding	
ThiE	Thiamine-phosphate synthase	catalytic activity; metal ion	

		binding	
LeuC	3-isopropylmalate dehydratase large subunit	catalytic activity; metal ion binding	
ThiC	Phosphomethylpyrimidine synthase	catalytic activity; metal ion binding	
Ape2	Aminopeptidase	catalytic activity; metal ion binding	
TktA	Transketolase	catalytic activity; metal ion binding	
slr0591	Putative uncharacterized protein	catalytic activity; metal ion binding	
Als	Acetolactate synthase	catalytic activity; metal ion binding	
PykF	Pyruvate kinase	catalytic activity; metal ion binding	
AccD	Acetyl-coenzyme A carboxylase carboxyl transferase subunit beta	catalytic activity; metal ion binding	cytoplasm
HemH	Ferrochelatase	catalytic activity; metal ion binding	cytoplasm
FrpC	Iron-regulated protein	catalytic activity; metal ion binding	extracellular
NdhI	NAD(P)H-quinone oxidoreductase subunit I	catalytic activity; metal ion binding	membrane
PsbA	Photosystem Q(B) protein 2	catalytic activity; metal ion binding	membrane
PsbD	Photosystem II D2 protein	catalytic activity; metal ion binding	membrane
PetB	Cytochrome b6	catalytic activity; metal ion binding	membrane
NouB	NAD(P)H-quinone oxidoreductase subunit K	catalytic activity; metal ion binding	membrane
SucC	Succinate-CoA ligase	catalytic activity; metal ion binding; nucleotide binding	
ThrS	Threonine-tRNA ligase	catalytic activity; metal ion binding; nucleotide binding	cytoplasm
sll0672	Cation-transporting ATPase E1-E2 ATPase	catalytic activity; metal ion binding; nucleotide binding; transporter activity	membrane
sll1920	Cation-transporting ATPase E1-E2 ATPase	catalytic activity; metal ion binding; nucleotide binding; transporter activity	membrane
Pma1	Cation-transporting ATPase E1-E2 ATPase	catalytic activity; metal ion binding; nucleotide binding; transporter activity	membrane
slr6012	Slr6012 protein	catalytic activity; motor activity; nucleotide binding; protein binding	cytoplasm; cytoskeleton; membrane
DeaD (CrhR)	**ATP-dependent RNA helicase DeaD**	catalytic activity; nucleotide binding	
LepA	LepA gene product	catalytic activity; nucleotide	

		binding	
ChlP	Geranylgeranyl reductase	catalytic activity; nucleotide binding	
LivG	High-affinity branched-chain amino acid transport ATP-binding protein	catalytic activity; nucleotide binding	
PknA	Eukaryotic protein kinase	catalytic activity; nucleotide binding	
slr0049	Putative uncharacterized protein	catalytic activity; nucleotide binding	
HemA	Glutamyl-tRNA reductase	catalytic activity; nucleotide binding	
RfbB	dTDP-glucose 4-6-dehydratase	catalytic activity; nucleotide binding	
sll0489	ABC transporter	catalytic activity; nucleotide binding	
slr0864	ABC transporter	catalytic activity; nucleotide binding	
CrtQ	Zeta-carotene desaturase	catalytic activity; nucleotide binding	
sll0456	Putative uncharacterized protein	catalytic activity; nucleotide binding	
sll0576	Putative sugar-nucleotide epimerase/dehydratase	catalytic activity; nucleotide binding	
CarA	Carbamoyl-phosphate synthase small chain	catalytic activity; nucleotide binding	
slr1735	ABC transporter	catalytic activity; nucleotide binding	
sll1770	ABC1-like	catalytic activity; nucleotide binding	
sll0086	Putative uncharacterized protein	catalytic activity; nucleotide binding	
slr1794	Putative uncharacterized protein	catalytic activity; nucleotide binding	
sll0550	Flavoprotein	catalytic activity; nucleotide binding	
sll1927	ABC transporter	catalytic activity; nucleotide binding	
PilT	Twitching mobility protein	catalytic activity; nucleotide binding	
MurC	UDP-N-acetylmuramate-L-alanine ligase	catalytic activity; nucleotide binding	cytoplasm
GpsA	Glycerol-3-phosphate dehydrogenase [NAD(P)+]	catalytic activity; nucleotide binding	cytoplasm
GuaA	GMP synthase [glutamine-hydrolyzing]	catalytic activity; nucleotide binding	cytoplasm
TrpS	Tryptophanyl-tRNA synthetase	catalytic activity; nucleotide binding	cytoplasm
GlyQ	Glycine--tRNA ligase alpha subunit	catalytic activity; nucleotide binding	cytoplasm

slr1299	UDP-glucose dehydrogenase	catalytic activity; nucleotide binding	cytoplasm
ThrB	Homoserine kinase	catalytic activity; nucleotide binding	cytoplasm
SerS	Serine-tRNA ligase	catalytic activity; nucleotide binding	cytoplasm
AlaS	Alanyl-tRNA synthetase	catalytic activity; nucleotide binding	cytoplasm
SecA	Protein translocase subunit SecA	catalytic activity; nucleotide binding	cytoplasm; membrane
ClpC	ATP-dependent Clp protease ATP-binding subunit clpA homolog	catalytic activity; nucleotide binding	membrane
NdhH	NADH-quinone oxidoreductase subunit D	catalytic activity; nucleotide binding	membrane
ChlD	Mg chelatase subunit	catalytic activity; nucleotide binding; protein binding	
ArgC	N-acetyl-gamma-glutamyl-phosphate reductase	catalytic activity; nucleotide binding; protein binding	cytoplasm
ClpB	ClpB protein	catalytic activity; nucleotide binding; protein binding	cytoplasm
sll1334	Putative uncharacterized protein	catalytic activity; nucleotide binding; protein binding; receptor activity; signal transducer activity	membrane
sll1888	Sensory transduction histidine kinase Hik5	catalytic activity; nucleotide binding; protein binding; receptor activity; signal transducer activity	membrane
slr2019	ABC transporter	catalytic activity; nucleotide binding; protein binding; transporter activity	membrane
sll0043	CheA like protein Hik18	catalytic activity; nucleotide binding; receptor activity; signal transducer activity	cytoplasm
sll1871	Sensory transduction histidine kinase Hik6	catalytic activity; nucleotide binding; receptor activity; signal transducer activity	membrane
PrfC	Peptide chain release factor 3	catalytic activity; nucleotide binding; RNA binding	cytoplasm
Ffh	Signal recognition particle protein	catalytic activity; nucleotide binding; RNA binding	cytoplasm
HflX	GTPase HflX	catalytic activity; nucleotide binding; transporter activity	cytoplasm; membrane
NrtD	Nitrate transport protein subunit NrtD	catalytic activity; nucleotide binding; transporter activity	membrane
MalK	Cytoplasmic membrane protein for maltose uptake	catalytic activity; nucleotide binding; transporter activity	membrane
slr0615	ABC transporter	catalytic activity; nucleotide binding; transporter activity	membrane
slr1104	Putative uncharacterized protein	catalytic activity; protein binding	
slr1143	Putative uncharacterized protein	catalytic activity; protein binding	
sll0654	Alkaline phosphatase	catalytic activity; protein binding	

slr1102	Putative uncharacterized protein	catalytic activity; protein binding; signal transducer activity	
slr1983	Regulatory component of sensory transduction system Rre22	catalytic activity; receptor activity; signal transducer activity	membrane
slr1629	Pseudouridine synthase	catalytic activity; RNA binding	
slr0955	Putative uncharacterized protein	catalytic activity; RNA binding	
Zam	Protein conferring resistance to acetazolamide	catalytic activity; RNA binding	
Pnp	**Polyribonucleotide nucleotidyltransferase**	catalytic activity; RNA binding	cytoplasm
50S l2	50S ribosomal protein L2	catalytic activity; RNA binding; structural molecule activity	cytoplasm; ribosome
RbcR	Rubisco operon transcriptional regulator	DNA binding	
sll1638	Putative uncharacterized protein	metal ion binding	membrane
slr0938	Putative uncharacterized protein	nucleotide binding	
GspE	General secretion pathway protein E	nucleotide binding	
slr0929	Putative uncharacterized protein	nucleotide binding	
GroEL	60 kDa chaperonin (Fragment)	nucleotide binding	cytoplasm
DnaK	Chaperone protein DnaK 3	nucleotide binding; protein binding	
sll0147	Putative uncharacterized protein	nucleotide binding; structural molecule activity	cytoskeleton
sll0606	Putative uncharacterized protein	protein binding	
sll0103	Putative uncharacterized protein	protein binding	
slr7060	Slr7060 protein	protein binding	
sll0163	Beta transducin-like protein	protein binding	membrane
sll1252	Putative uncharacterized protein	RNA binding	
NusA	N utilization substance protein	RNA binding	
RpsJ	30S ribosomal protein S10	RNA binding; structural molecule activity	cytoplasm; ribosome
slr0209	Putative uncharacterized protein	signal transducer activity	
sll1757	Putative uncharacterized protein	structural molecule activity	
SrrA	Periplasmic sugar-binding protein of ABC transporter	transporter activity	
sll1699	Extracellular solute-binding protein	transporter activity	
slr0513	Periplasmic iron-binding protein	transporter activity	
slr1207	Putative uncharacterized protein	transporter activity	membrane
slr0042	Putative uncharacterized protein	transporter activity	membrane
SecD	Protein-export membrane protein SecD	transporter activity	membrane
sll0772	Putative uncharacterized protein	transporter activity	membrane
sll0142	Cation or drug efflux system protein	transporter activity	membrane
GlnHP	ABC-type transporter protein	transporter activity	membrane

GumB	GumB protein	transporter activity	membrane
slr0369	Cation or drug efflux system protein	transporter activity	membrane
sll0834	Low affinity sulfate transporter	transporter activity	membrane
slr2131	Cation or drug efflux system protein	transporter activity	membrane
Amt1	Ammonium/methylammonium permease	transporter activity	membrane

Table 3.4: Mass spectrometry analysis of the membrane fraction proteins interacting with His-R. Proteins found in both control Δ*crhR* and experimental Δ*crhR* pMon-HisR strains represent proteins that bind non-specifically to the column and therefore were omitted from the results. Protein that is also predicted to interact with CrhR by STRING (www.string-db.org) is in bold.

Protein	Description	Molecular Activity	Cellular Location
slr1704	Putative uncharacterized protein slr1704		
RbcS	Ribulose bisphosphate carboxylase small subunit		
sll1785	Putative uncharacterized protein sll1785		
sll1380	Putative uncharacterized protein sll1380		
Vipp 1	Plasma membrane protein essential for thylakoid formation		
slr0006	Putative uncharacterized protein slr0006		
slr1829	Putative uncharacterized protein slr1829		
slr1612	Putative uncharacterized protein slr1612		
slr1513	Putative uncharacterized protein slr1513		
slr0962	Putative uncharacterized protein slr0962		
sll1247	Putative uncharacterized protein sll1247		
slr275	Putative uncharacterized protein slr1275		
slr0637	Putative uncharacterized protein slr0637		
sll1390	Putative uncharacterized protein sll1390		
slr1702	Putative uncharacterized protein slr1702		
slr1819	Putative uncharacterized protein slr1819		
sll0623	Putative uncharacterized protein sll0623		
sll1532	Putative uncharacterized protein sll1532		
sll1663	Putative uncharacterized protein sll1663		
slr1852	Putative uncharacterized protein slr1852		
slr0575	Putative uncharacterized protein slr0575		
sll0413	Putative uncharacterized protein sll0413		
sll1004	Putative uncharacterized protein sll1004		
SpoIID	Sporulation protein SpoIID homolog		
NusG	Transcription antitermination protein nusG		
Hsp 17	16.6 kDa small heat shock protein, molecular chaperon		
DctP	C4-dicarboxylase binding protein		

SphX	SphX protein		
Frr PE	Ribosome-recycling factor		Cytoplasm
sll0752	Sll0752 protein		Membrane
sll0412	Putative uncharacterized protein sll0412		Membrane
slr1471	Inner membrane protein		Membrane
ApcC	Phycobilisome 7.8 kDa linker polypeptide, allophycocyanin-associated, core		Membrane
IsiA	Iron-stress chlorophyll-binding protein		Membrane
EpsB	Exopolysaccharide export protein		Membrane
sll1621	Membrane protein	antioxidant activity; catalytic activity	
slr1198	Rehydrin	antioxidant activity; catalytic activity	
PonA	Penicillin-binding protein 1A	catalytic activity	
slr1772	Putative uncharacterized protein slr1772	catalytic activity	
Ndh	NADH dehydrogenase	catalytic activity	
IlvE	Branched-chain amino acid aminotransferase	catalytic activity	
sll1178	Nodulation protein	catalytic activity	
sll1559	Soluble hydrogenase 42 kDa subunit	catalytic activity	
PdhB	Pyruvate dehydrogenase E1 beta subunit	catalytic activity	
PhbC	Poly(3-hydroxyalkanoate) synthase	catalytic activity	
GuaB	Inosine 5-monophosphate dehydrogenase	catalytic activity	
sll0480	LL-diaminopimelate aminotransferase	catalytic activity	
MtnA	Methylthioribose-1-phosphate isomerase	catalytic activity	
GlnN	Glutamate-ammonia ligase	catalytic activity	
ThrC	Threonine synthase	catalytic activity	
Sds	Solanesyl diphosphate synthase	catalytic activity	
RfbU	Mannosyltransferase B	catalytic activity	
sll0586	Putative uncharacterized protein sll0586	catalytic activity	
GltA	Citrate synthase	catalytic activity	Cytoplasm
GlnA	Glutamine synthetase	catalytic activity	Cytoplasm
AhcY	Adenosylhomocysteinase	catalytic activity	Cytoplasm
GylA	Serine hydroxymethyltransferase	catalytic activity	Cytoplasm
HemL	Glutamate-1-semialdehyde 2,1-aminomutase	catalytic activity	Cytoplasm
AccB	Biotin carboxyl carrier protein of acetyl-CoA carboxylase	catalytic activity	Cytoplasm
ChlM	Mg-protoporphyrin IX methyl transferase	catalytic activity	Cytoplasm
HlyD	Hemolysin secretion protein	catalytic activity	cytoplasm; cytoskeleton; membrane; mitochondrion
PlsX	Phosphate acyltransferase	catalytic activity	cytoplasm; membrane

NuoH	NAD(P)H-quinone oxidoreductase subunit 1	catalytic activity	Membrane
GyrA	DNA gyrase A subunit	catalytic activity; DNA binding; nucleotide binding	chromosome; nucleus
TktA	Transketolase	catalytic activity; metal ion binding	
Sir	Ferredoxin-sulfite reductase	catalytic activity; metal ion binding	
IlvD	Dihydroxy-acid dehydratase	catalytic activity; metal ion binding	
Dxs	1-deoxy-D-xylulose-5-phosphate synthase	catalytic activity; metal ion binding	
TalB	Transaldolase	catalytic activity; metal ion binding	Cytoplasm
AccD	Acetyl-coenzyme A carboxylase carboxyl transferase subunit beta	catalytic activity; metal ion binding	Cytoplasm
NdhI	NAD(P)H-quinone oxidoreductase subunit I	catalytic activity; metal ion binding	Membrane
PsaC	Photosystem I iron-sulfur center	catalytic activity; metal ion binding	Membrane
NuoB	NAD(P)H-quinone oxidoreductase subunit K	catalytic activity; metal ion binding	Membrane
GshB	Glutathione synthetase	catalytic activity; metal ion binding; nucleotide binding	
slr1616	Carbamoyl phosphate synthase-like-protein	catalytic activity; metal ion binding; nucleotide binding	
FtsH	ATP-dependent zinc metalloprotease FtsH 3	catalytic activity; metal ion binding; nucleotide binding	Membrane
IlvG	Acetolactate synthase	catalytic activity; metal ion binding; structural molecule activity	cytoplasm; ribosome
Dead (CrhR)	**ATP-dependent RNA helicase DeaD**	catalytic activity; nucleotide binding	
LepA	LepA gene product	catalytic activity; nucleotide binding	
slr0374	Cell division cycle protein	catalytic activity; nucleotide binding	
sll0471	Putative uncharacterized protein sll0471	catalytic activity; nucleotide binding	
SqdB	Sulfolipid biosynthesis protein SqdB	catalytic activity; nucleotide binding	
slr0049	Putative uncharacterized protein slr0049	catalytic activity; nucleotide binding	
FabG	3-oxoacyl-[acyl-carrier protein] reductase	catalytic activity; nucleotide binding	
PknA	Eukaryotic protein kinase	catalytic activity; nucleotide binding	

sll0576	Putative sugar-nucleotide epimerase/dehydratase	catalytic activity; nucleotide binding	
sll0759	ABC transporter	catalytic activity; nucleotide binding	
CitH	Malate dehydrogenase	catalytic activity; nucleotide binding	
HemA	Glutamyl-tRNA reductase	catalytic activity; nucleotide binding	
slr1617	Putative uncharacterized protein slr1617	catalytic activity; nucleotide binding	
sll0209	Putative uncharacterized protein sll0209	catalytic activity; nucleotide binding	
EnvM	Enoyl-[acyl-carrier-protein] reductase [NADH]	catalytic activity; nucleotide binding	
UrtE	Urea transport system ATP-binding protein	catalytic activity; nucleotide binding	
ChlI	Mg chelatase subunit	catalytic activity; nucleotide binding	
Dfp	Bifunctional phosphopantothenoylcysteine decarboxylase/phosphopantothenate synthase	catalytic activity; nucleotide binding	
sll0489	ABC transporter	catalytic activity; nucleotide binding	
CobO	Cob(I)yrinic acid a,c-diamide adenosyltransferase	catalytic activity; nucleotide binding	
sll0086	Putative uncharacterized protein sll0086	catalytic activity; nucleotide binding	
GspE	General secretion pathway protein E	catalytic activity; nucleotide binding	
FtsZ	Cell division protein ftsZ	catalytic activity; nucleotide binding	Cytoplasm
ClpP3	ATP-dependent Clp protease proteolytic subunit 3	catalytic activity; nucleotide binding	Cytoplasm
ClpP	ATP-dependent Clp protease proteolytic subunit 1	catalytic activity; nucleotide binding	Cytoplasm
ClpP2	ATP-dependent Clp protease proteolytic subunit 2	catalytic activity; nucleotide binding	Cytoplasm
ProC	Pyrroline-5-carboxylate reductase	catalytic activity; nucleotide binding	Cytoplasm
AccA	Acetyl-coenzyme A carboxylase carboxyl transferase subunit alpha	catalytic activity; nucleotide binding	Cytoplasm
GuaA	GMP synthase [glutamine-hydrolyzing	catalytic activity; nucleotide binding	Cytoplasm
PetH	Ferredoxin-NADP oxidoreductase	catalytic activity; nucleotide binding	Membrane
ClpB	ClpB protein	catalytic activity; nucleotide binding; protein binding	Cytoplasm
slr1414	Sensory transduction histidine kinase Hik11	catalytic activity; nucleotide binding; receptor activity; signal	Membrane

		transducer activity	
TypA	**Elongation factor EF-G**	catalytic activity; nucleotide binding; RNA binding	
MalK	Cytoplasmic membrane protein for maltose uptake	catalytic activity; nucleotide binding; transporter activity	Membrane
sll0654	Alkaline phosphatase	catalytic activity; protein binding	
Prc	Carboxyl-terminal protease	catalytic activity; protein binding	
HhoA	Protease	catalytic activity; protein binding	
slr0955	Putative uncharacterized protein slr0955	catalytic activity; RNA binding	
Zam	Protein conferring resistance to acetazolamide	catalytic activity; RNA binding	
slr0073	Sensory transduction histidine kinase Hik36/PilL	catalytic activity; signal transducer activity	
SbpA	Sulfate binding protein SbpA	catalytic activity; transporter activity	
NtcA	Global nitrogen regulator	DNA binding	
rpoD	RNA polymerase sigma factor	DNA binding	
RpoD1	RNA polymerase sigma factor (Fragment)	DNA binding	
DnaJ	Chaperone protein DnaJ	metal ion binding; nucleotide binding; protein binding	Cytoplasm
FhuA	Ferrichrome-iron receptor	metal ion binding; receptor activity; transporter activity	Membrane
YchF	Putative uncharacterized protein ychF	nucleotide binding	
slr0929	Putative uncharacterized protein slr0929	nucleotide binding	
GroES	10 kDa chaperonin	nucleotide binding	Cytoplasm
GroEL	60 kDa chaperonin 2	nucleotide binding; protein binding	Cytoplasm
HtpG	Heat shock protein	nucleotide binding; protein binding	Cytoplasm
KtrA	Na-activated K transporter subunit KtrA	nucleotide binding; transporter activity	
sll0103	Putative uncharacterized protein sll0103	protein binding	
slr1196	Putative uncharacterized protein slr1196	protein binding	
sll0606	Putative uncharacterized protein sll0606	protein binding	
sll0163	Beta transducin-like protein	protein binding	Membrane
IutA	Ferric aerobactin receptor	receptor activity; transporter activity	Membrane
sll1252	Putative uncharacterized protein sll1252	RNA binding	

NusA	N utilization substance protein	RNA binding	
InfC	Translation initiation factor IF-3	RNA binding	Cytoplasm
50 S RP	50S ribosomal protein L3	RNA binding; structural molecule activity	cytoplasm; ribosome
30S RP	30S ribosomal protein S4	RNA binding; structural molecule activity	cytoplasm; ribosome
Rps1	30S ribosomal protein S1	RNA binding; structural molecule activity	cytoplasm; ribosome
30S RP	30S ribosomal protein S5	RNA binding; structural molecule activity	cytoplasm; ribosome
30S RP	30S ribosomal protein S17	RNA binding; structural molecule activity	cytoplasm; ribosome
30S RP	30S ribosomal protein S11	RNA binding; structural molecule activity	cytoplasm; ribosome
30S RP	30S ribosomal protein S7	RNA binding; structural molecule activity	cytoplasm; ribosome
50S RP	50S ribosomal protein L24	RNA binding; structural molecule activity	cytoplasm; ribosome
sll0038	PatA subfamily protein PixG/PisG/TaxP1/Rer1/Rre36	signal transducer activity	
slr0513	Periplasmic iron-binding protein	transporter activity	
slr1740	Extracellular solute-binding protein	transporter activity	
SrrA	Periplasmic sugar-binding protein of ABC transporter	transporter activity	
PstS	Periplasmic phosphate binding protein	transporter activity	Membrane
sll0142	Cation or drug efflux system protein	transporter activity	Membrane

IV. DISCUSSION

Temperature fluctuations, being one of the major environmental stresses, have a range of effects on the growth and survival of bacteria. In order to counteract those negative effects bacteria have evolved mechanisms that allow them to rapidly adapt and survive in the new environment. The cold-shock response is one such mechanism, which involves a number of processes ranging from alteration of membrane fluidity to changes in global protein expression, occurring during growth temperature downshift (Yamanaka *et al.,* 1998; Thieringer *et al.,* 1998; Golovlev, 2003; Phadtare, 2004).

Similar to the heat shock response, cold stress induces expression of a number of proteins that aid adaptation of cellular processes to the new condition. Proteins involved in response to environmental stresses are produced in induced quantities to immediately help the cell, whose growth is impaired by the negative effects of temperature change (Brandi *et al.,* 1999; Lopez and Makhatadze, 2000; El-Sharoud and Graumann, 2007). This is a very energetically costly process for bacteria and involves rapid usage of cell resources and temporary decrease or even cessation of production of other proteins. Once this critical point is past and the cell has been successfully adapted to the decreased growth temperature or the new environmental condition becomes favorable, production of stress proteins has to stop and the adaptation proteins have to be eliminated from the cells. A number of mechanisms that function at the transcription, translation and post-translational levels participate in the prevention of further production and elimination of already induced stress proteins (Goldstein *et al.*, 1990; Shenhar *et al.*, 2009). One

such post-translational mechanism is proteolysis, during which stress proteins are degraded when they are no longer needed (Shenhar *et al.*, 2009; Meyer and Baker, 2011; Gur *et al.*, 2011).

Tight control of stress proteins at transcriptional, translational and post-translational levels is an important process, since these proteins play a major role in adaptation to various stress conditions including temperature downshift. As already mentioned, cold stress causes a range of negative effects at different cellular levels including a major decrease in translation due to the reduction of ribosome function. Decrease of protein translation during cold stress is thought to be primarily caused by stabilization of mRNA secondary structures, which results in accumulation of 70S ribosomes stalled at the translation initiation step (Friedman *et al.*, 1971; Farewell and Neidhardt, 1998; Kaberdin and Blaesi, 2006; Kaczanowska and Ryden-Aulin, 2007). There are a number of proteins including translation initiation and ribosome factors that also assist the translation process during cold stress (Jones *et al.*, 1987; Jones *et al.*, 1996). These proteins also include a large family of RNA chaperones such as the cold shock proteins or Csp's, which have been well studied in *E. coli* and *B. subtilis*.

Some RNA helicases are also specifically produced during environmental stresses in a number of prokaryotic systems and therefore considered to be directly involved in resolving secondary structures in mRNA to enhance protein translation during cold shock. Major examples of such RNA helicases include CsdA (DeaD) initially discovered in *E. coli* (Toone *et al.*, 1991; Kalman *et al.*, 1991; Jones *et al.*, 1996; Charollais *et al.*, 2004; Peil *et al.*, 2008; Jagessar and

Jain, 2010; Rawling and Baserga, 2012), but its homologues have now been discovered in a number of bacterial species including *Bacillus* species, *Listeria monocytogenes*, *Yersinia pseudotuberculosis*, *Clostridium perfringens* and others (Lim *et al.*, 2000; Briolat and Reysset, 2002; Chan *et al.*, 2007; Markkula *et al.*, 2012a; Markkula *et al.*, 2012b) and two cyanobacterial helicases, CrhC in *Anabaena* sp. PCC 7120 and CrhR in *Synechocystis* sp. PCC 6803 (Chamot and Owttrim, 2000; Rosana *et al.*, 2012a). CrhR is also induced during other stress conditions causing reduction of the photosynthetic electron transport chain (Chamot *et al.*, 1999; Kujat and Owttrim, 2000; Chamot and Owttrim, 2000; Yu and Owttrim, 2000; El-Fahmawi and Owttrim, 2003; Prakash *et al.*, 2010; Rowland *et al.*, 2011; Sireesha *et al.*, 2012; Rosana *et al.*, 2012a).

Cyanobacterial DEAD-box RNA helicase, CrhR, in *Synechocystis* sp. PCC 6803, was examined in this thesis with the main focus on autoregulation of its protein levels by a proteolytic mechanism that is functional at 30^{o}C, but not at 20^{o}C.

Analysis of CrhR helicase in the Owttrim lab has primarily focused on its induction by cold and other abiotic stresses (Kujat and Owttrim, 2000; Rosana *et al.*, 2012b). The fate of induced levels of CrhR protein, when cells are returned to warm temperatures after cold shock, was not previously studied. A mechanism involved in rapid reduction of protein levels of CrhR at 30^{o}C is discussed in this study. Various experiments support the hypothesis that CrhR is proteolytically degraded in response to a temperature upshift to 30^{o}C. This proteolytic mechanism is CrhR-dependent as $crhR_{TR}$ mutant exhibit elevated levels of

truncated non-functional $CrhR_{TR}$ protein regardless of the temperature. Several approaches were used to characterize degradation of the CrhR protein and identify proteins involved in this process. Due to the observations from these experiments a model for temperature regulation of CrhR expression is proposed.

4.1. Effect of *crhR* mutation and overexpression of CrhR protein on the growth and survival of *Synechocystis* cells.

In order to assess the importance of CrhR RNA helicase in *Synechocystis* cells, growth of wild type at 30^{o}C (warm) and 20^{o}C (cold) was compared to *crhR* mutants. It was observed that $crhR_{TR}$ mutant grows essentially as well as wild type at 30^{o}C (Figure 3.1) but it exhibits a significantly reduced growth rate at 20^{o}C (Figure 3.2). Survival of wild type cells and $crhR_{TR}$ mutant at two temperatures follows a similar trend (Figure 3.2). All of the cells from both strains survive at 30^{o}C, and only wild type cells survive at 20^{o}C. Survival of $crhR_{TR}$ mutant cells drops immediately after transfer to 20^{o}C and 80% of mutant cells die in the first 4 days. There is no data about $crhR_{TR}$ mutant growth and survival for more than 7 days at 20^{o}C, therefore it is unclear whether those 20% surviving $crhR_{TR}$ cells are capable of cold adaptation to the point that they start to grow and multiply again. This observation would imply that in the absence of CrhR other RNA helicases or RNA chaperones become active to substitute for CrhR loss. However, it may also be possible that those 20% surviving mutant cells are in a dormant state until growth temperature becomes favourable again.

The *crhR*$_{TR}$ mutant differs from wild type as it expresses a truncated CrhR$_{TR}$ protein and accumulates abnormal levels of this mutant protein regardless of the temperature (Figure 3.5). Truncated CrhR$_{TR}$ protein is not capable of annealing and unwinding RNA (Dr. Danuta Chamot, personal communication). It is possible that the mutant phenotype observed with *crhR*$_{TR}$, which includes impared growth, reduced viability, cell size and DNA content at 20^{o}C (Rosana *et al*., 2012) is not solely attributable to the absence of wild type CrhR helicase but can also be a result of abnormally high levels of partially functional CrhR$_{TR}$, that leads to dominant negative mutant phenotype. Microarray data demonstrates that *crhR* mutation affects the accumulation of ~100 mRNAs and abundance of ~100 sRNAs in *Synechocystis* (Jens Georg, unpublished data). It is possible that even though CrhR$_{TR}$ is not capable of unwinding and annealing RNAs, it may still bind and sequester target mRNAs and sRNAs. This may lead to significant reduction in translation of essential proteins and disrupted regulation of vital cellular processes, leading to reduced growth and survival of the *crhR*$_{TR}$ mutant. A similar negative effect of mutant protein binding to its targets was observed with eukaryotic RNA helicase-like PRP2 protein (Plumpton *et al.*, 1994). In *Saccharomyces cerevisiae* PRP2 protein is essential for pre-mRNA splicing and its mutants have severely impaired growth. Dominant negative mutant expresses non-functional PRP2-dn1 protein with a single amino acid change within the conserved SAT motif, which is required for RNA unwinding in the prototype eIF-4A helicase. It was demonstrated that mutant PRP2-dn1 helicase is capable of binding to its target splicing complex. However, since the mutant helicase is non-

functional, it stalls pre-mRNA splicing and causes accumulation of splicing complexes, causing death of the cells (Plumpton *et al.*, 1994). The same scenario can be applied to dominant mutant phenotype observed in *crhR*$_{TR}$ mutant.

There is also another possible explanation for observed mutant phenotype in *crhR*$_{TR}$. Not enough information is known about other proteins in *Synechocystis* that can at least partially substitute for the function of CrhR, primarily because cellular function of CrhR remains unknown. If such proteins exist, they may not be expressed in the presence of truncated CrhR$_{TR}$ in the mutant and therefore will not be able to rescue *crhR*$_{TR}$ mutant phenotype. Therefore, *crhR*$_{TR}$ is a poor strain choice to study the effect of *crhR* mutation on the *Synechocystis* cell growth, due to its dominant negative mutant phenotype.

To get more information about the sole effect of *crhR* mutation on the cell growth, a Δ*crhR* mutant was constructed (Figure 3.3 and 3.4). This mutant has a complete deletion of *crhR* ORF and does not produce CrhR protein at any temperature (Figure 3.5). As opposed to the *crhR*$_{TR}$ mutant, that has potential dominant negative phenotype due to the abnormal levels of non-functional CrhR$_{TR}$, the Δ*crhR* mutant gives more reliable information about the effect of *crhR* ORF complete deletion on the growth of cells at different temperatures. As the growth curve (Figure 3.6) demonstrates, the Δ*crhR* mutant is capable of growing exponentially at 30^{o}C similar to the wild type (Figure 3.2) in contrast to the *crhR*$_{TR}$ mutant, whose growth plateaus after 4 days. In addition, it is observed that Δ*crhR* does not grow at 20^{o}C similar to *crhR*$_{TR}$. These growth patterns support the hypothesis that the dominant negative mutant phenotype of *crhR*$_{TR}$

may only be partially attributed to $CrhR_{TR}$ presence. These results also confirm that CrhR has an important yet unknown function at 20^{o}C, as previously concluded from the results obtained during *crhR$_{TR}$* analysis (Rosana *et al.*, 2012a). Rosana *et al*. (2012a) proposed the involvement of CrhR in photosynthetic carbon fixation in *Synechocystis* cells at 20^{o}C, as *crhR$_{TR}$* death at 20^{o}C was primarily caused by lack of carbon fixation. It is obvious that CrhR as an RNA helicase may not be directly involved in carbon fixation, but it may aid the expression of proteins required for this process. I suggest observing the effect of *crhR* mutation on carbon fixation in the Δ*crhR$_{TR}$* mutant to confirm CrhR involvement in regulation of this cellular process.

In order to observe the effect of potential overexpression of CrhR on *Synechocystis* cells, pMon-HisR was constructed, in which expression of His-tagged CrhR (His-R) is regulated by the pNir promoter. His-R encoded in pMon-HisR plasmid is produced constitutively in *Synechocystis* cells when grown on nitrate media. It is interesting that the presence of this construct negatively impacts the growth of the wild type and Δ*crhR* at 30^{o}C and has little to no effect on the growth of *crhR$_{TR}$* (Figure 3.6). However, the effect of His-R presence was very different at 20^{o}C (Figure 3.6). His-R completely rescued Δ*crhR* mutant growth in the cold, partially rescued the *crhR$_{TR}$* mutant and again had a negative effect on the wild type cells. It is evident from the wild type results that higher than natural levels of CrhR have a negative impact on the growth of cells regardless of the temperature. These results show that the presence of low basal levels of CrhR in the wild type at 30^{o}C and high levels at 20^{o}C have to be tightly

controlled and maintained at specific level set for each temperature. The observed negative impact of His-R expression in the wild type can be explained by partially or completely non-functional His-R, which may sequester CrhR targets or interacting partners leading to impaired growth and development of His-R expressing cells. However, since presence of His-R completely rescued Δ*crhR* mutant, the possibility of His-R being non-functional can be rejected.

These growth pattern data again support the hypothesis that mutant $crhR_{TR}$ phenotype is mainly attributable to the presence of abnormal amounts of non-functional $CrhR_{TR}$ rather than to the absence of wild type CrhR helicase, since the presence of His-R was not able to rescue this mutant. $CrhR_{TR}$ production in the mutant uses cellular resources to produce non-functional protein at induced quantities. In addition, $CrhR_{TR}$ potentially binds irreversibly CrhR targets, so that functional His-CrhR does not have access to them. Thus, with constant negative effects of $CrhR_{TR}$ it is impossible to rescue $crhR_{TR}$ mutant phenotype with additional expression of functional His-R helicase. Even though $crhR_{TR}$ has many disadvantages when used for growth experiments, this mutant may be very useful to pull down CrhR target RNAs if $CrhR_{TR}$ binds them irreversibly.

Apart from observing the effect of His-R on rescuing growth in the mutant, it was also interesting to know whether the presence of His-R would restore temperature regulation of $CrhR_{TR.}$ It was observed in Figure 3.7 that $CrhR_{TR}$ levels in the $crhR_{TR}$ mutant changes with the presence of pMon-HisR plasmid. In $crhR_{TR}$ mutant with pMon-HisR, levels of truncated $CrhR_{TR}$ were reduced at 30^{o}C. This resembles the wild type pattern of CrhR protein, which is

basal at 30^{o}C and is induced at 20^{o}C (Figure 3.7). Even though the pattern of protein accumulation becomes similar to the wild type, the growth of the *crhR$_{TR}$* mutant expressing His-R remains low at both temperatures (Figures 3.6) as discussed above. What was surprising to observe is that the accumulation of His-R was changing in response to temperature in the wild type and *crhR$_{TR}$* mutant transformed with pMon-HisR, even though His-R should be constitutively expressed in *Synechocystis* cells. In addition CrhR$_{TR}$ levels in the same strain look similar to wild type due to the presence of functional His-R protein. These results suggest that there is a post-translational mechanism controlling CrhR levels, which is responsible for reduction of constitutively produced His-R at 30^{o}C. This mechanism is potentially autoregulated, as it was restored with functional His-R presence in the *crhR$_{TR}$* mutant. Therefore, this post-translational mechanism controlling levels of His-R and CrhR in the cells was further investigated by monitoring CrhR abundance at 20^{o}C and 30^{o}C in a series of *in vivo* and *in vitro* experiments.

4.2 Proteolytic autoregulation of CrhR protein at 30^{o}C

In vivo and *in vitro* experiments were conducted to monitor the accumulation of CrhR wild type and mutant protein levels in *Synechocystis* cells grown at various temperatures.

In vivo experiments demonstrated that CrhR protein level linearly decreases in the first 3 h upon the transfer of wild type culture from cold to warm (Figure 3.8 and 3.9). However, the level of CrhR$_{TR}$ does not decrease in the

crhR$_{TR}$ mutant in the same type of experiment. Rps1 protein served as a loading control and remained constant regardless of the temperature in both wild type and mutant cells (Figure 3.8).

Decrease of protein levels at 30^{o}C can be attributed to two reasons: decrease in transcript levels and/or proteolytic degradation of protein. CrhR transcript was shown to decrease in the wild type to basal levels after 4 hours of cold incubation (Rosana *et al.*, 2012), however CrhR protein remains elevated up to 24 hours even in the absence of transcript (Figure 3.8). This indicates CrhR is a stable protein since it can remain in the cell without *de novo* protein synthesis for up to 24 hours at 20^{o}C. Therefore, to rapidly decrease levels of such a stable protein upon the transfer of wild type cells to 30^{o}C there should be another mechanism apart from transcriptional regulation. The rapid linear decrease of CrhR that we observe in the warm is mostly indicative of proteolysis, thus making low transcript levels a subsequent regulation component that keeps CrhR levels basal after proteolytic degradation at 30^{o}C.

The hypothesis that proteolytic degradation of CrhR is occurring at 30^{o}C was also tested using *in vitro* experiments (Figures 3.10 and 3.11). *In vitro*, wild type CrhR from cold shocked cells was degraded only in the presence of cell lysate from wild type warm grown cells (Figure 3.10). This indicates that the active proteolytic machinery capable of degrading CrhR is present only at 30^{o}C.

When the *crhR*$_{TR}$ cell lysate was used for *in vitro* experiments, CrhR$_{TR}$ protein remained constant with and without addition of protein lysate from warm or cold grown mutant cells (Figure 3.11), which coincides with the results of the

in vivo experiment (Figure 3.8). There are two possibilities that can explain the observed phenomenon. The first one is the absence of the C-terminal extension in truncated $CrhR_{TR}$ that may harbour a recognition sequence required for proteolytic degradation. Since non-functional $CrhR_{TR}$ lacks almost half of the protein it may not be able to participate in the events that may change the protein conformation and thus accessibility of recognition sequence (Gottesman, 2003). Such events include: binding of substrates, interacting with protein partners, dimerization or oligomerization, as it was shown for wild type CrhR (Skeik, 2012). Changes in accessibility or presence of a recognition sequence were previously shown to affect regulation of protein levels by proteolysis (Gottesman, 2003). The first described recognition signal is the one at the N-terminus of eukaryotic and prokaryotic proteins, this is also referred to as the N-end rule (Varshavsky, 1992). In *E. coli* degradation signal is presented by big hydrophobic residues (Y, F, W) and leucine (L) at the N-terminus of proteins targeted for degradation (Tobias *et al.*, 1991; Shrader *et al.*, 1993). The N-end rule is not applicable to CrhR, since it lacks the required amino acids at the N-terminus of the protein. Moreover, the N-end rule is not used by all of the proteases, as some require a specific amino acid signal at the C terminus such as SsrA tag (AANDENYALAA) (Plumpton *et al.*, 1994; Levchenko *et al.*, 1997; Gottesman, 2003). N-end rule tag and SsrA are just examples: there are lots of other proteolysis tags that appear to be targets-, proteases- and even species-specific and continue to be discovered with every new proteolytic target identification. Known proteolysis recognition sequences encountered during the literature review

for this thesis were not found in the CrhR protein sequence. However, it does not mean that CrhR may not be degraded by already known degradation mechanisms due to the reasons described above.

As an example of requirement for specific recognition sequence for proteolysis, the MuA protein, will be described. MuA has a specific sequence at the C-terminus (RRKKAI), which is recognized by Clp protease. If this recognition sequence is mutated or is bound by MuB and therefore is hidden from the protease, MuA is stabilized (Levchenko *et al.*, 1997; Jones *et al.*, 1998). This could also be true for association of increased $CrhR_{TR}$ stability with the absence of its C-terminus.

The second explanation of the observed *in vitro* and *in vivo* degradation results for $crhR_{TR}$ involves the absence of active degradation machinery when wild type functional CrhR is not present in the cell, suggesting CrhR autoregulation. Examples of proteins autoregulating their own degradation are rare in the literature. The only example known today is in *Bacillus subtilis*, which involves CstR regulation of *clpC* transcription by functioning as a transcriptional repressor (Kruger *et al.*, 2001). Since ClpC is involved in subsequent degradation of CstR, this mechanism is autoregulated (Kruger *et al.*, 2001).

Examples mentioned above show that there are two possibilities that can explain the absence of degradation of $CrhR_{TR}$ in the mutant cells: absence of the signal required for recognition by the protease and the involvement of functional CrhR in the regulation of its own degradation. These two possibilities were explored using two *in vitro* experiments.

In vitro experiment with exogenous His-R showed that His-R is degraded only in the presence of total protein from wild type cells grown at 30^{o}C (Figure 3.12 A). This confirms that only wild type cells grown at warm temperature have active degradation machinery. Mixtures of cell lysates from warm or cold grown *crhR$_{TR}$* mutant with His-R did not demonstrate degradation of either endogenous CrhR$_{TR}$ protein or exogenous His-R (Figure 3.12 C and D). Therefore CrhR$_{TR}$ protein does not lack the recognition signal for the protease, but instead results suggest that functional degradation machinery is not present in the absence of functional CrhR. However, *E. coli* His-R is an exogenous protein produced in another type of bacteria and therefore may not be properly assembled or post-translationally modified. If the degradation machinery in the *crhR$_{TR}$* mutant is weak and cannot recognize His-R for the mentioned reasons, it may not be degraded by proteases in the mutant *crhR$_{TR}$* cell lysate. Thus, the conclusions from the first experiment need more support.

To provide more experimental support to the hypothesis that the mutant does not have functional degradation machinery another *in vitro* experiment was conducted. This time, cell lysates from wild type cells were mixed with mutant lysates in two different combinations (Figure 3.13). In each combination, lysate from warm grown cells served as a potential source of degradation machinery and cold lysate provided CrhR or CrhR$_{TR}$ as a substrate for degradation. Results showed that truncated CrhR$_{TR}$ can be degradaded by functional degradation machinery only from wild type grown at 30^{o}C (Figure 3.13 A), again supporting the hypothesis that there is no recognition sequence in the C-terminus of CrhR

that is required for degradation. Conversely, if mutant warm grown cells are used as a source of degradation machinery, CrhR from wild type cold cells is not degraded, which supports the results of the previous experiment. Therefore, CrhR is involved in the formation of the active degradation machinery that regulates its levels at 30^{o}C, this involvement is most likely indirect.

It is very important to understand that the degradation machinery does not involve only proteases: in this thesis this term is used for accessory proteins as well, which may be involved in the CrhR degradation process. A similar system involving Clp proteases in cyanobacterium *Synechococcus elongatus* PCC 7942 (Stanne *et al.*, 2007) will be used as an example to show the complexity and number of functional parts involved in this process. In *Synechococcus* there are several proteins that assemble into two functional protease cores, ClpP1 and ClpP2 or ClpP3 and ClpR. Each of these protease complexes has a particular chaperone partner: ClpC in the case of ClpP3/R proteolytic core and ClpX for the ClpP1/P2 core. These chaperone partners help to unfold and solubilize protease targets and prevent the formation of insoluble aggregates, that may damage the cell (Lindner *et al.*, 2008; Gur *et al.*, 2011). There are also two adaptor proteins ClpS1 and ClpS2 that interact with ClpC chaperone protein, likely increasing the number of substrates for Clp proteases in *Synechococcus* (Stanne *et al.*, 2007). This example shows how complex the degradation machinery can be. CrhR RNA helicase may be involved in the stability of mRNA or unwinding secondary structures on the mRNA of one or several proteins from the degradation machinery, thus participation in autoregulation of proteolysis. Therefore,

"degradation machinery" term will continue to be used, keeping in mind that it can be any of the participating proteins.

To learn more about the functionality of the degradation machinery and to determine how constitutive expression of His-R will affect CrhR and $CrhR_{TR}$ regulation, wild type and two mutants *crhR*$_{TR}$ and Δ*crhR* were transformed with pMon-HisR plasmid. Unexpectedly, it was observed that His-R levels appear to be downregulated in the first hours of incubation at 30^{o}C in all of the strains. The reduction in His-R levels was therefore unexpected because nitrate reductase promoter pNir regulating the expression of His-R is constitutive in *Synechocystis* cells continuously grown in the presence of nitrate (Enrique Frias and Flores, 2010). In order to rule out the possibility that these results occur because of a temperature effect on pNir promoter activity, *E. coli* transformed with the same pMon-HisR construct was used to confirm that pNir promoter does not respond to temperature fluctuations (Figure 3.15). Levels of His-R in the *E. coli* remained constant regardless of the temperature confirming that pNir is not temperature regulated. This means that downregulated levels of His-R in *Synechocystis* cells in the first hours of 30^{o}C incubation are not a result of temperature regulation of the pNir promoter and suggest proteolytic degradation (Figure 3.14).

It is extremely insightful to note that in wild type cells, levels of His-R and CrhR are linearly reduced in the first 3 h of warm incubation. At longer exposures to warm temperature, proteolysis halts and basal levels of native CrhR are further kept low by basal transcript, observed at 30^{o}C (Rosana *et al.*, 2012).

Thus, observed increase in level of His-R at long incubation 30^{o}C is due to the constitutive expression and halted proteolysis.

In growth experiments the presence of His-R in *crhR$_{TR}$* and Δ*crhR* rescues the mutant phenotype in terms of ability to grow at 20^{o}C (Figure 3.6). It was interesting to see if the presence of His-R in these mutants could also rescue regulation of CrhR$_{TR}$ levels by proteolytic degradation at 30^{o}C (Figure 3.14 Δ*crhR* and *crhR$_{TR}$*). No degradation of CrhR$_{TR}$ is observed in *crhR$_{TR}$* mutant (Figure 3.14 *crhR$_{TR}$*), however CrhR$_{TR}$ protein levels are so elevated that they may obscure any effect of partially or fully rescued proteolysis of the mutant CrhR$_{TR}$. The observed results once again confirm that formation of functional degradation machinery is regulated by its own substrate – CrhR. As briefly mentioned above, proteolytic regulation of CrhR is similar to CtsR in *B. subtilis.*This complex autoregulation process involves several proteins as part of degradation machinery. In *Bacillus* heat-induced ClpC, part of ClpC/P protease, is transcriptionally repressed by CstR at normal growth temperature (Kruger *et al*., 2001). Dimerization of CstR, which converts it to a functional repressor, is thought to be mediated by McsA. Stabilization of CstR by McsA and binding to its target DNA makes it inaccessible for degradation by basal levels of ClpC/P protease. During heat stress, a putative kinase McsB is induced, which outcompetes McsA protein interaction with CstR and abolishes CstR DNA binding activity by modification, presumably phosphorylation. Inactive CtsR detaches from DNA allowing induced expression of ClpC protease subunit. ClpC and ClpP proteins assemble into an

active protease that degrades CtsR, thus temporarily shutting the system down (Kruger *et al*., 2001).

Using CtsR as an example, it was decided to investigate CrhR proteolysis further by testing whether *de novo* protein synthesis is required for the production of active degradation machinery at 30^{o}C. For this purpose two translation inhibitors, chloramphenicol (Cm) and kanamycin (Km), were added to the cold-shocked wild type cells prior to the transfer to 30^{o}C (Figure 3.16). It is observed that with addition of the kanamycin, which inhibits initiation of translation, degradation of CrhR still proceeds similar to the control (Figure 3.16 +Km). However addition of Cm, which specifically inhibits translation elongation, leads to the prevention of CrhR degradation as evidenced by CrhR levels remaining constant even in the warm (Figure 3.16 +Cm). One explanation of these observations is that translation is already initiated and ribosomes are bound to the mRNA of proteins involved in the formation of the degradation machinery at 20^{o}C. However ribosomes are stalled on those mRNAs and elongation proceeds only when the cells are transferred to 30^{o}C. This mechanism would be able to immediately produce degradation machinery specifically at 30^{o}C to rapidly degrade CrhR.

The observed results of experiments with translational inhibitors are also similar to regulation of D1 protein expression in *Synechocystis* cells (Tyystjarvi *et al.*, 2001). The D1 protein is stable in the dark, but undergoes rapid turnover in the light. It was shown that translation of D1 mRNA initiates in the dark, but elongation does not proceed in the dark. The arrest in elongation of the D1 protein

is released only in the light. This release is proposed to be caused by targeting D1 peptide to the thylakoid membrane (Tyystjarvi *et al.,* 2001).

It is also important to mention that CrhR levels also depend on the redox status of the photosynthetic electron transport chain and therefore should also be reduced in response to a light-dark transition (Kujat and Owttrim, 2000). To test the effect of a light-dark transition on the degradation machinery another *in vivo* experiment was conducted, during which one of the culture flasks was wrapped in aluminum foil to imitate darkness. The results show that CrhR degradation is delayed in the dark (Figure 3.17). Since CrhR is regulated by the redox status of the photosynthetic electron transport chain (Kujat and Owttrim, 2000), one would predict that CrhR would be downregulated in the dark due to the activation of the degradation machinery. However, the observed effect on the activity of degradation machinery was opposite, its proteolytic activity is delayed in the dark. This may be attributed to the slower signal transduction for the CrhR degradation in the dark. There is no other explanation yet from the physiological point of view for this phenomenon but there is an environmental explanation that can be proposed. In nature darkness is also frequently associated with a drop in temperature, for instance during cloudy weather or at the end of the day before the cool night. Therefore, if dark is a signal for the cell that the growth temperature is going to decrease soon, the cell would prefer to maintain CrhR levels for some time in case of cold stress. This may explain the necessity for the observed delay of CrhR degradation in the dark.

4.3 Protease(s) involved in the degradation of CrhR at 30^{o}C

As already discussed a number of proteins can be involved in the degradation process of CrhR protein at 30^{o}C, the process of their identification can be very laborious and is not possible for the scope of this thesis. However, one approach would be to use protease mutants. Construction of complete deletion mutants is a time consuming process in *Synechocystis* due to the presence of several genome copies in each cell (Kaneko *et al.*, 2001). Thus, other methods were used to find participating protease(s).

It was previously demonstrated using microarray analysis that the abundance of transcripts encoding two proteases, FtsH and ClpC, changed in the *crhR*$_{TR}$ mutant (Jens Georg, unpublished data), suggesting that they may be involved in proteolysis of CrhR. In an attempt to test this hypothesis, FtsH and ClpC antibodies were used to identify the levels of these proteins in the wild type and mutant cells at 20^{o}C and 30^{o}C. Results showed that FtsH is induced at 20^{o}C in the wild type and Δ*crhR* mutant, but the opposite is observed in the *crhR*$_{TR}$ mutant (Figure 3.18). It is hard to interpret the FtsH results, because the *Synechocystis* genome encodes four *ftsH* genes, *ftsH1, ftsH2, ftsH3* and *ftsH4* (*sll1463, slr0228, slr1604* and *slr1390* respectively), encoding four proteins of approximately the same size (74 kDa). Thus, the major peptide detected during western analysis is representative of all or some FtsH proteins combined together. The results potentially suggest that FtsH proteins may not be involved in CrhR degradation as they have low levels of protein at 30^{o}C in the wild type. The data also suggest that the changes in FtsH levels observed in *crhR*$_{TR}$ are not related to the absence of

functional CrhR helicase, since the same effect is not observed in both *crhR* mutants. Even though FtsH proteases are involved in many regulatory degradation processes including degradation of protein D1 in *Synechocystis* (Lindahl *et al.*, 2000), CrhR does not appear to be one of its targets. This conclusion was also supported by an *in vivo* experiment with *ftsH2* and *ftsH4* mutants (Figure 3.20). In both of these mutants, CrhR was still degraded at 30^{o}C. This result suggests that proteases FtsH2 and FtsH4 are not involved in CrhR regulation. However, there are another two proteases from FtsH family, FtsH1 and FtsH3, that were not tested due to the lack of mutants. Their involvement in CrhR regulation cannot be rejected until the mutants in these genes are also tested.

We were not able to obtain *clp* protease mutants, and therefore we only measured the level of ClpC chaperone protein in wild type and *crhR* mutants to test if Clp protease may be involved in CrhR degradation. It was observed that ClpC protein levels increase after 6 hours in the cold and also in the warm grown wild type cells. In both mutants, the level of this protein is constant regardless of the temperature (Figure 3.19). ClpC is not part of the protease core, it is a chaperone partner of the ClpP3/R protease core (Stanne *et al.*, 2007), therefore it is correlated but may not be fully representative of protease levels. It is also important to note that Clp proteases involved in the general stress response, in which unfolded proteins have to be eliminated from the cell (Porankiewicz and Clarke, 1997). Some proteases from the Clp family were shown to be induced by high salt, heat, extreme cold and UV-B irradiation (Porankiewicz and Clarke, 1997; Porankiewicz *et al.*, 1998; Schelin *et al.*, 2002), stresses facilitating protein

unfolding and other damaging effects. Thus, it is not surprizing to see induction of ClpC in response to prolonged cold incubation and during heat shock at 30^{o}C in wild type cells. However, since ClpC levels are constant in both mutants it is concluded that CrhR may be involved in the regulation of ClpC expression. This supports the microarray data that shows change of ClpC expression in *crhR$_{TR}$* mutant (Jens Georg, unpublished data). Therefore from the data in the Figure 3.19, it is impossible to conclude that CrhR is a target for proteolytic degradation by Clp proteases at 30^{o}C without further testing of Clp protease mutants for the presence of proteolytic regulation of CrhR at 30^{o}C.

These attempts to identify proteases involved in CrhR degradation were not successful and further experiments involving protease(s) mutants are required. Testing mutants in various proteases remains the most straightforward approach for identification of proteases if the target is known. The main caveat of this approach is that multiple proteases may target one substrate (Gottesman, 2003). An example of such case is Lambda Xis protein that is degraded by both Lon and FtsH proteases, with either being sufficient (Weisberg and Gottesman, 1971; Leffers and Gottesman, 1998). Thus, to extend this research topic and find CrhR regulating protease(s), *Synechocystis* mutants in various proteases are needed.

4.4 Post-translational modification of CrhR protein

During western analysis of CrhR abundance in several *in vitro* experiments it was noticed that wild type CrhR peptide from cells grown at 20^{o}C detected at a slightly higher molecular weight than the same protein from the

mixture of protein lysates from cells grown at 30^{o}C and 20^{o}C (Figure 3.21). This slight change of molecular weight may be an indicator of removal of a post-translational modification from CrhR at 30^{o}C. As mentioned above, it is proposed that CstR repressor is phosphorylated by McsB kinase, which leads to its disassembly from the target DNA and degradation by Clp protease (Kruger *et al.*, 2001). However, it is unclear whether phosphorylation or DNA detachment is triggering degradation. In the case of CrhR, removal of a post-translational modification at 30^{o}C may be the trigger for proteolytic degradation. Attempts to separate modified and unmodified CrhR peptide on the SDS-PAGE gel of different acrylamide concentrations and gel sizes were not successful. Keeping in mind that there are a number of possible modifications, it was decided to test if CrhR is post-translationally modified by phosphorylation, one of the most common modifications that are used in bacteria to alter proteins' functionality as well as a tag for initiation of various processes including degradation. Two phosphatases were used in standard and tripled concentration to modify CrhR (Figure 3.22). This experiment lacks positive control to check whether phosphatases used are functional, thus it should be repeated to confirm observed results. Nevertheless, results from Figure 3.22 demonstrated that post-translational modification noticed on CrhR protein is not phosphorylation. It may be other kinds of post-translational modification including attachment of biochemical functional groups, for instance acetate, various lipids or carbohydrates. It is also possible that with the change of temperature, CrhR itself is cleaved to expose a degradation signal. This was demonstrated for the LexA protein, during DNA-

damage response in *E. coli* (Neher *et al.*, 2003). It was shown that intact LexA is stable, but its auto-cleavage fragments are degraded rapidly. During DNA-damage RecA protein stimulates LexA autocatalytic cleavage, which leads to exposure of sequence motifs that flank auto-cleavage sites similar in sequence to the ssrA tag. ClpXP protease recognizes flanking motifs and degrades LexA (Neher *et al.*, 2003).

Identification of post-translational modifications remains a challenging problem in proteomics. However, there are mass spectrometry method, that precisely identify post-translational modifications. One such method is selectively excluded mass screening analysis (SEMSA) of unfolded peptides during liquid chromatography-electrospray-ionization-quadrupole-time-of-flight tandem mass spectrometry (LC-ESI-q-TOF MS/MS) through replicated runs of a purified protein on two-dimensional gel (Seo *et al.*, 2008). Identification of CrhR post-translational modification by SEMSA or other procedures may be used.

4.5 Cellular localization of CrhR protein

It is hard to propose possible proteases involved in CrhR regulation without knowledge of CrhR cellular localization. Thus as an additional project cellular localization of CrhR protein was determined using two methods. Initially, cellular localization of CrhR was identified using extraction of proteins from wild type cold and warm grown cells using various buffers (Figures 3.23, 3.24 and 3.25). The results indicated that CrhR is located in the crude membrane fraction obtained after clarification of lysed *Synechocystis* cells, as only detergent and high

salt containing buffers were able to extract CrhR from the crude membrane pellet. In addition to the detergent and high salt, Brij 35 was able to extract CrhR from crude membrane pellet of warm grown cells (Figure 3.24). Detergents such as SDS and high salt are capable of removing internal membrane proteins, however non-ionic detergent Brij 35 is not capable of extracting internal proteins and only works on the peripherally bound proteins. These results suggest that CrhR differently associates with the membranes depending on the growth temperature, being more tightly associated with the membrane at 20^{o}C. This may be important for CrhR regulation, if by changing its localization at 30^{o}C it becomes accessible to the proteases in the cytoplasm/nucleoid region of the cell.

The *in vitro* membrane association experiments do not identify with which of the three membranes in *Synechocystis* CrhR interacts. Membrane localization of CrhR protein was also confirmed by immunoelectron microscopy (Figures 3.26 and 3.27). Results showed that the majority of CrhR protein is localized between the thylakoid membranes at both 30^{o}C and 20^{o}C, with limited CrhR detected in outer and cytoplasm membranes or in the cytoplasm/nucleoid region. Unfortunately, this approach was not suitable for confirmation of membrane association of CrhR protein depending on the growth temperature. Localization of CrhR in the cell membranes partially coincide with the results for CrhC cold induced RNA helicase that is found in *Anabaena* sp. PCC 7120 (El-Fahmawi and Owttrim, 2003). CrhC was found in the plasma membrane of *Anabaena* cells with no evidence of a soluble-cytoplasmic form. In contrast, CrhR was found in both the cytoplasm and membranes with the majority localized to the thylakoid

membranes (Table 3.1). The immunoelectron microscopy also suggests that the basal level of CrhR detected in cells grown at 30^{o}C is not the result of protein sequestration into membranes.

4.6 Interacting partners of CrhR protein

In attempt to identify proteins that interact with CrhR and thus determine its physiological role, online prediction by STRING with subsequent confirmation of partners by co-immunoprecipitation was used. Co-immunoprecipitation experiment could also reveal the proteins involved in CrhR degradation. Even though interaction of target and protease should be a very transient process and may not be possible to detect, other proteins of degradation machinery such as adaptors, for example, may interact with CrhR for a longer period of time. If that is the case, detection of such adaptors may lead to identification of proteolytic machinery. Proteins from soluble and membrane fractions of cell lysate were used for co-immunoprecipitation with His-CrhR from wild type *Synechocystis* cells transformed with pMon-HisR construct (Figures 3.28 and 3.29), since CrhR appears to be localized mostly to the thylakoid regions with some protein present in the soluble cytoplasm/nucleoid region.

STRING identified 10 proteins that possibly interact with CrhR according to the published results of other research (Table 3.2). All of the predicted proteins are involved in either transcription or translation, which is expected according to the known functions of other RNA helicases such as transcriptional regulation (Westermarck *et al.*, 2002), RNA turover (Khemici and Carpousis, 2004;

Purusharth *et al.*, 2005) or ribosome biogenesis (Jones *et al.*, 1996; Charollais *et al.*, 2003).

In contrast, co-immunoprecipitation identified a number of interacting proteins, which were grouped according to their molecular activity and cellular location (Table 3.3 and 3.4). However, the number of interacting proteins was surprisingly large, casting doubts on the reliability of the pull-down method. Clp proteases are among identified interacting partners, but due to the issue with data reliability it cannot be stated that Clp proteases interact with CrhR. Co-immunoprecipitation was a poor choice of method to identify proteases involved in CrhR degradation, as this interaction may be very transient and would not be detected by this method. Instead, as already mentioned, testing various protease mutants should be used to identify CrhR degrading proteases, which seems to be the only reliable method for this type of research (Gottesman, 2003). Co-immunoprecipitation can still be used to pull-down interacting partners to infer cellular functions of CrhR helicase, but the use of other affinity tags should be used.

4.7 Model for CrhR protein autoregulation by proteolysis in response to abiotic stress

The results presented in this thesis demonstrate and characterize autoregulation of CrhR protein abundance mediated by proteolytic degradation in response to temperature change. In summary, the CrhR degradation machinery appears to be present and active only at 30^{o}C in wild type cells. Degradation of

$CrhR_{TR}$ does not occur in *crhR*$_{TR}$ mutant regardless of the temperature, which demonstrates the involvement of CrhR in the formation of its degradation machinery. Translation of proteolytic machinery is initiated at 20^{o}C, but stalled until the cells are shifted to the warm. At 30^{o}C the degradation machinery appears to be functional only in the first few hours, subsequently the basal level of CrhR is controlled by low transcript levels. Evidence is provided that CrhR helicase is also post-translationally modified, which may be required for its physiological function and/or recognition by the degradation machinery at 30^{o}C.

crhR mutants demonstrate major problems with cell growth as well as physiological and morphological deficiencies (Rosana *et al.*, 2012a) and various studies show that CrhR is involved in regulation of various mRNAs and sRNAs (Jens Georg, unpublished data; (Rowland *et al.*, 2011). Our data showed that a number of proteins participating in different cellular process were co-immunoprecipitating and thus may interact with CrhR. Therefore the indirect involvement of CrhR in the regulation of its own degradation by stabilization of one or several mRNAs encoding degradation machinery proteins seems to be one function out of many that CrhR has in the *Synechocystis* cells.

The regulation of CrhR protein abundance reported in this thesis is similar to the recently discovered proteolytic regulation of RNase R protein in *E. coli* (Chen and Deutscher, 2010). RNase R exoribonuclease levels dramatically increase under a variety of environmental stresses including cold shock (Cairrao *et al.*, 2003; Chen and Deutscher, 2005). It was previously suggested that the elevated levels of RNase R protein during the decrease of temperature from 37^{o}C

to 10^{o}C is a consequence of a quantitatively elevated amount of *rnr* transcription (Cairrao *et al.,* 2003). However, it was unclear how elevated levels of transcript at 10^{o}C can be the sole factor increasing RNase R protein levels, if lower level of protein translation was observed at cold temperature (Chen and Deutscher, 2010). A series of experiments by the Chen group (2010) indicated that RNAse R is an extremely unstable protein at 37^{o}C, which is stabilized during cold shock and other stress conditions due to the absence of active proteolytic degradation. Lon protease was found to be involved in RNase R degradation at 37^{o}C. However, at the present moment no data are available about the details of this proteolytic regulatory mechanism, such as target recognition requirements or possible involvement of adaptor proteins. Understanding of this process may also contribute into understanding of CrhR proteolytic regulation since RNAse R and CrhR exhibit similar protein accumulation patterns and thus may be involved in a similar cellular processes.

CspC protein in *E. coli* is another example of a protein regulated by proteolysis at elevated temperatures. Similar to CrhR, CspC is a cold inducible RNA chaperone, which is degraded by proteolysis upon the shift of *E. coli* cells from 37^{o}C to 42^{o}C (Shenhar *et al.,* 2009). This RNA chaperone is proposed to be involved in the tight regulation of the transient heat shock response, as it regulates stability of the mRNA of heat shock genes. The heat shock response involves temperature-dependent induction of the heat shock regulon, which includes mainly genes coding for proteins such as chaperons and proteases. Immediately following the induction, transcription and protein levels of heat shock genes

decrease until their level reaches a steady state typical for the new temperature. This temperature regulated change in protein levels is required, since amount of heat shock protein has to be correlated with the amount of unfolded substrates, their targets (Tomoyasu *et al.*, 1998). Since CspC stabilizes mRNA of heat shock transcripts, degradation of CspC immediately after the temperature increase ensures fast and accurate shutdown of the heat shock response (Shenhar *et al.*, 2009). This regulatory process is physiologically important, as evident from findings that constantly elevated levels of heat shock proteins as a result of overexpression of CspC at the elevated temperatures leads to the inhibition of *E. coli* growth (Shenhar *et al.*, 2009).

Systems involving regulation of CrhR and CspC have definite similarities, such as induction during cold stress and regulation by rapid degradation during warm incubation or heat stress. Both of these proteins are involved in stabilization of mRNAs. Therefore, there is a possibility that CrhR is similar to CspC in the regulation of heat shock. CrhR may bind and prevent translation of mRNAs encoding heat shock proteins during cold. Once CrhR is degraded at 30^{o}C, the released mRNAs are available for translation, a mechanism that would rapidly produce proteins required for growth at the elevated temperature.

However, elevated temperature, at which CrhR is proteolytically degraded, 30^{o}C, is not considered a heat shock for *Synechocystis*, since it grows exponentially at this temperature, without even transient inhibition of growth upon the transfer. It was also shown by the growth experiments that *crhR* mutants do not have reduced growth at 30^{o}C. Therefore, CrhR may have very different

function than CspC. CrhR could possibly stabilize mRNAs of cold shock genes at 20^{o}C and thus prevent formation of cold shock proteins at warm temperature since CrhR is degraded at 30^{o}C. Pull-down of RNAs associated with CrhR at 20^{o}C and 30^{o}C is required to acquire more information about CrhR mRNA targets to draw definite conclusions about the involvement of CrhR helicase in the regulation of either cold shock or heat shock response.

Using the results of this thesis and knowledge of proteolytic regulation of previously described proteins, a working model of CrhR regulation by proteolytic degradation was proposed (Figure 4.1) Figure 4.1 shows the general model proposed, Figure 4.2, is a snapshot of events associated with the absence or production of degradation machinery at two different temperatures in the wild type cells.

In wild type cells, CrhR is induced at 20^{o}C, the protein is post-translationally modified at 20^{o}C by a protein that will be called an activator. The presence of the modification on the CrhR protein makes it functionally active RNA helicase or allows it to dimerize to form functional CrhR dimer (Skeik, 2012). mRNA for the degradation machinery (DM mRNA) is transcribed at reduced temperatures. One of the functions that CrhR has at 20^{o}C is assisting initiation of translation of these DM mRNAs. For instance, it may help during initiation of translation by unwinding secondary structures on the DM mRNA to allow proper ribosome binding (Figure 4.2). Ribosomes bind to DM mRNA and initiate translation, but they are stalled until the cells are transferred to the warm. Once the growth temperature changes to 30^{o}C, formation of new protein and

degradation of unnecessary proteins starts as a part of the adaptation to the new conditions. There is a protein formed at warm temperatures that allows removal of the post-translational modification of CrhR, a deactivator protein (Figure 4.1). Deactivator removes the post-translational modification making CrhR non-functional at 30^{o}C since more than a normal amount of CrhR in the warm appeared to negatively affect cell growth. Non-functional CrhR detaches from DM mRNA allowing its translation at 30^{o}C and the functional degradation machinery is formed (Figure 4.2). The absence of the post-translational modification of the CrhR protein at 30^{o}C allows its recognition and proteolytic degradation (Figure 4.1). There is a certain amount of DM mRNA present when cells are transferred from cold to warm and therefore a defined amount of degradation proteins are formed. Once the degradation machinery proteins have reduced CrhR protein to basal levels no further degradation machinery is produced at 30^{o}C. The basal level of CrhR is further maintained by basal transcription.

In the *crhR$_{TR}$* mutant the situation is very different. Truncated protein CrhR$_{TR}$ cannot be post-translationally modified by the activator at 20^{o}C. This is caused by inability of activator to recognize the amino-acid sequence to be modified, because of the C-terminus truncation or improper folding of this protein. Thus CrhR$_{TR}$ cannot bind to DM mRNA to facilitate its translation initiation. When the mutant is transferred to 30^{o}C, there is no formation of the degradation machinery and thus no proteolysis of CrhR$_{TR}$. That is why CrhR$_{TR}$ protein remains at high levels at both temperatures.

The proposed model attempts to explain the complicated mechanism of CrhR autoregulation by proteolysis, as suggested by the results provided in this thesis. According to the scientific literature this is the second example of autoregulated proteolysis and the first example among the known RNA helicases. Further studies should focus on the identification of the exact protease(s) and accessory proteins involved in this proteolytic regulation mechanism. In addition, experiments should be conducted to identify RNA targets of CrhR helicase. The knowledge of CrhR targets will not only contribute into the research presented in this thesis by confirming CrhR involvement in translation of DM mRNAs, but will provide insights into the unknown cellular function of unique proteolytically autoregulated cyanobacterial RNA helicase CrhR.

Figure 4.1: Working model of CrhR proteolytic autoregulation in response to temperature change. In the wild type cells, CrhR protein (bright orange four diamonds) is post-translationally modified by activator protein (purple star) at 30^{o}C making it a functional protein. CrhR helicase binds to the degradation machinery mRNAs (DM mRNA) to resolve unfavourable secondary RNA structures. Ribosomes initiate translation, but not elongation of DM mRNA at 20^{o}C. Upon cell transfer to 30^{o}C, deactivator protein (red star) removes the post-translational modification from CrhR making it inactive. CrhR dissociates from DM mRNA. Proteins for DM are produced and functional DM is formed (yellow packmen), which proteolytically degrades non-functional CrhR at 30^{o}C. In the *crhR$_{TR}$* mutant, CrhR$_{TR}$ (dark orange rectangle) cannot be activated by post-translational modification. CrhR$_{TR}$ does not unwind post-secondary structures on DM mRNA and thus its translation is not initiated at 20^{o}C. Functional DM cannot be formed at 30^{o}C in the mutant and therefore high levels of CrhR$_{TR}$ remain in the cell.

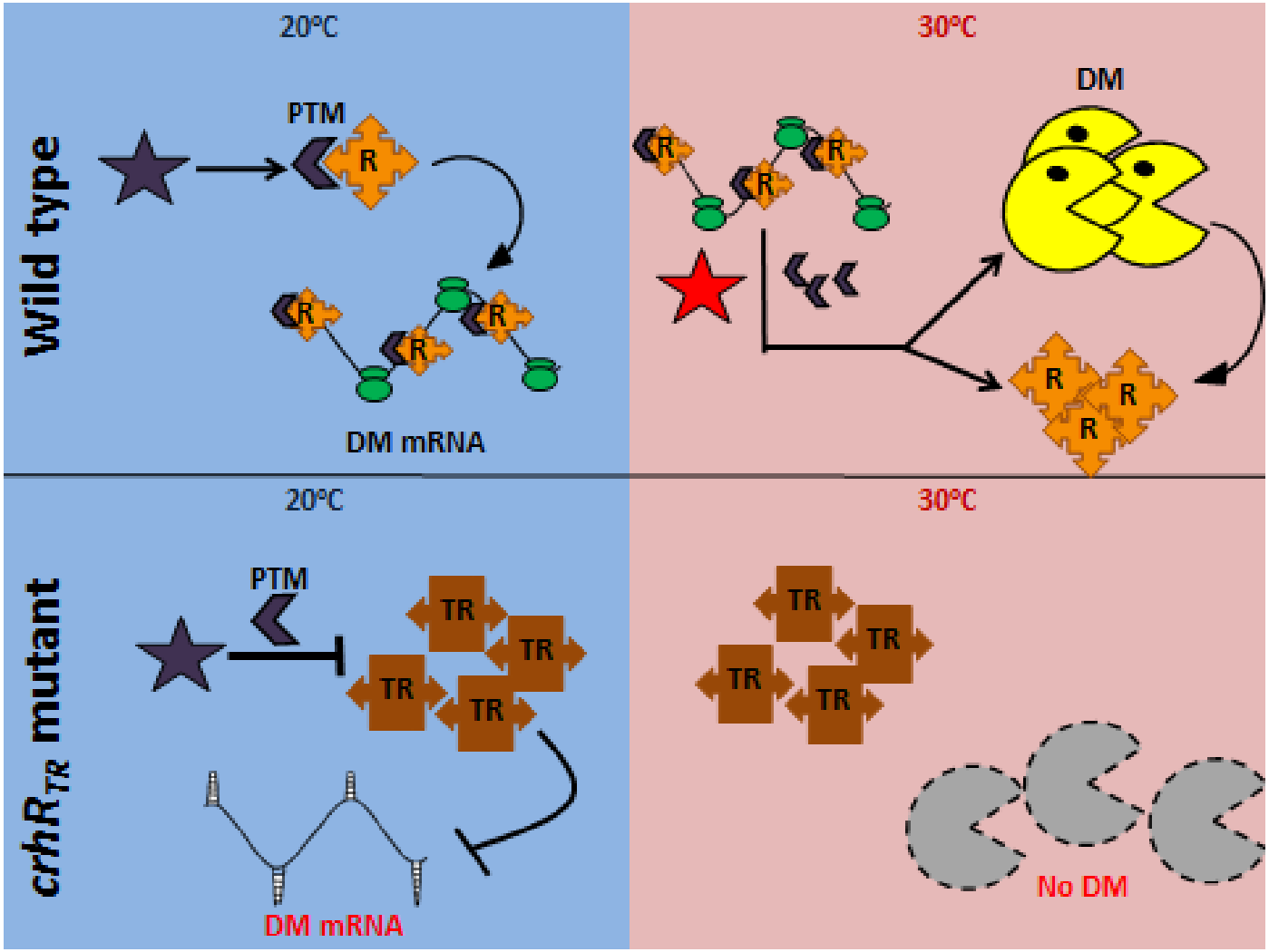
20°C
30°C
Wild type
PTM
R
DM
DM mRNA
20°C
30°C
crhR_TR mutant
PTM
TR
DM mRNA
No DM

Figure 4.2: CrhR participation in the formation of its degradation machinery in wild type *Synechocystis*. In the cold, secondary structures are formed on the degradation machinery proteins mRNA (DM mRNA) that prevent binding of ribosomes. Functional CrhR (dark orange diamonds) unwinds those structures and allows initiation of translation by the ribosomes. Upon transfer of the culture to 30^{o}C, CrhR becomes non-functional due to removal of the post-translational modification and detaches from the DM mRNA. This allows translation of one or several proteins involved in the formation or activation of the degradation machinery (yellow packmen), which regulates CrhR protein levels at 30^{o}C.

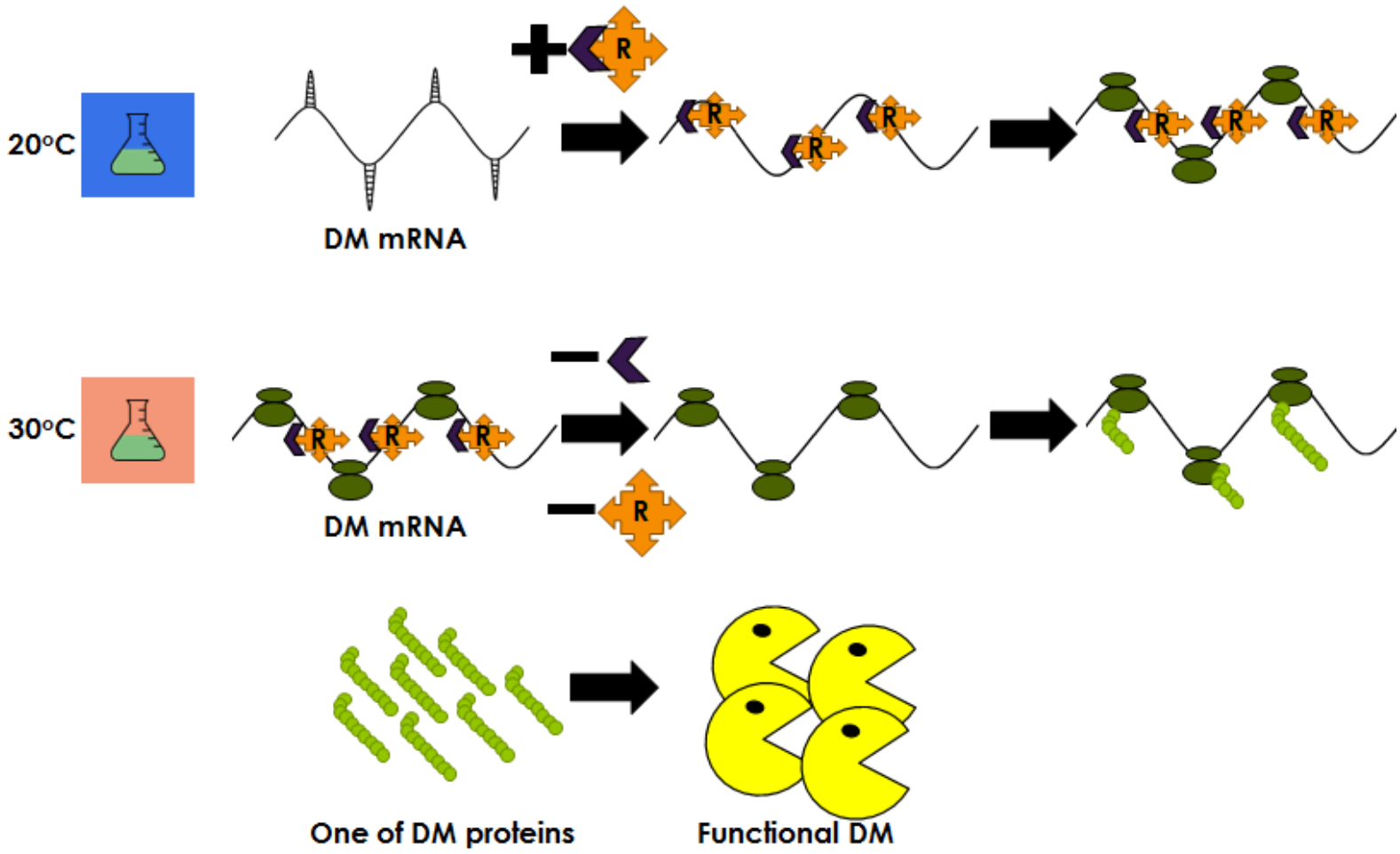
20°C
R
R
R
R
R
R
DM mRNA
30°C
R
R
R
R
DM mRNA
One of DM proteins
Functional DM

V. REFERENCES

Aguilar P. S., Lopez P., De Mendoza D. (1999). Transcriptional control of the low-temperature-inducible *des* gene, encoding the delta 5 desaturase of *Bacillus subtilis*. *J Bacteriol* 181, 7028-7033.

Alexeyev M. F., Shokolenko I. N., Croughan T. P. (1995). Improved antibiotic-resistance gene cassettes and omega elements for escherichia coli vector construction and *in vitro* deletion/insertion mutagenesis. *Gene* 160, 63-67.

Allen M. M. (1968). Simple conditions for growth of unicellular blue-green algae on plates. *J Phycol* 4, 1-12.

Allen M. M. & Stanier R. Y. (1968). Selective isolation of blue-green algae from water and soil. *J Gen Microbiol* 51, 203-2011.

Awano N., Xu C., Ke H., Inoue K., Inouye M., Phadtare S. (2007). Complementation analysis of the cold-sensitive phenotype of the *Escherichia coli csdA* deletion strain. *J Bacteriol* 189, 5808-5815.

Bae W. H., Xia B., Inouye M., Severinov K. (2000). Escherichia coli CspA-family RNA chaperones are transcription antiterminators. *Proc Natl Acad Sci U S A* 97, 7784-7789.

Beckering C. L., Steil L., Weber M. H. W., Volker U., Marahiel M. A. (2002). Genomewide transcriptional analysis of the cold shock response in *Bacillus subtilis. J Bacteriol* 184, 6395-6402.

Berthelot K., Muldoon M., Rajkowitsch L., Hughes J., McCarthy J. E. G. (2004). Dynamics and processivity of 40S ribosome scanning on mRNA in yeast. *Mol Microbiol* 51, 987-1001.

Bischof J. C. & He X. M. (2005). Thermal stability of proteins. Cell Injury: Mechanisms, Responses, and Repair. Annals of the New York Academy of Sciences 1066, 12-33.

Bizebard T., Ferlenghi I., Iost I., Dreyfus M. (2004). Studies on three *E. coli* DEAD-box helicases point to an unwinding mechanism different from that of model DNA helicases. *Biochem (N Y)* 43, 7857-7866.

Blot N., Mella-Flores D., Six C., le Corguillé G., Boutte C., Peyrat A., Monnier A., Ratin M., Gourvil P., Campbell D. A., Garczarek L. (2011). Light history influences the response of the marine cyanobacterium *Synechococcus* sp. WH7803 to oxidative stress. *Plant Physiol* 156, 1934-1954.

Brandi A., Pon C. L., Gualerzi C. O. (1994). Interaction of the main cold shock protein CspA of *Escherichia coli* with the promoter region of hns. *Biochimie* 76, 1090-1098.

Brandi A., Spurio R., Gualerzi C., Pon C. (1999). Massive presence of the *Escherichia coli* 'major cold-shock protein' CspA under non-stress conditions. *EMBO J* 18, 1653-1659.

Brandi A., Pietroni P., Gualerzi C. O., Pon C. L. (1996). Post-transcriptional regulation of CspA expression in *Escherichia coli*. *Mol Microbiol* 19, 231-240.

Briolat V. & Reysset G. (2002). Identification of the clostridium perfringens genes involved in the adaptive response to oxidative stress. *J Bacteriol* 184, 2333-2343.

Cairrao F., Cruz A., Mori H., Arraiano C. M. (2003). Cold shock induction of RNase R and its role in the maturation of the quality control mediator SsrA/tmRNA. *Mol Microbiol* 50, 1349-1360.

Carpousis A. J. (2002). The *Escherichia coli* RNA degradosome: Structure, function and relationship to other ribonucleolytic multienyzme complexes. *Biochem Soc Trans* 30, 150-155.

Caruthers J. M. & McKay D. B. (2002). Helicase structure and mechanism. *Curr Opin Struct Biol* 12, 123-133.

Castenholz R. (1988). Culturing methods for cyanobacteria. *Meth Enzymol* 167, 68-93.

Chamot D. & Owttrim G. W. (2000). Regulation of cold shock-induced RNA helicase gene expression in the cyanobacterium *Anabaena* sp. strain PCC 7120. *J Bacteriol* 182, 1251-1256.

Chamot D., Colvin K. R., Kujat-Choy S. L., Owttrim G. W. (2005). RNA structural rearrangement via unwinding and annealing by the cyanobacterial RNA helicase, CrhR. *J Biol Chem* 280, 2036-2044.

Chamot D., Magee W. C., Yu E., Owttrim G. W. (1999). A cold shock-induced cyanobacterial RNA helicase. *J Bacteriol* 181, 1728-1732.

Chan Y. C., Raengpradub S., Boor K. J., Wiedmann M. (2007). Microarray-based characterization of the *Listeria monocytogenes* cold regulon in log- and stationary-phase cells. *Appl Environ Microbiol* 73, 6484-6498.

Charollais J., Dreyfus M., Iost I. (2004). CsdA, a cold-shock RNA helicase from *Escherichia coli*, is involved in the biogenesis of 50S ribosomal subunit. *Nucleic Acids Res* 32, 2751-2759.

Charollais J., Pflieger D., Vinh J., Dreyfus M., Iost I. (2003). The DEAD-box RNA helicase SrmB is involved in the assembly of 50S ribosomal subunits in *Escherichia coli*. *Mol Microbiol* 48, 1253-1265.

Chen C. L. & Deutscher M. P. (2005). Elevation of RNase R in response to multiple stress conditions. *J Biol Chem* 280, 34393-34396.

Chen C. & Deutscher M. P. (2010). RNase R is a highly unstable protein regulated by growth phase and stress. *Rna-a Publication of the Rna Society* 16, 667-672.

Coburn G. A., Miao X., Briant D. J., Mackie G. A. (1999). Reconstitution of a minimal RNA degradosome demonstrates functional coordination between a 3 ' exonuclease and a DEAD-box RNA helicase. *Genes Dev* 13, 2594-2603.

Cordin O., Banroques J., Tanner N. K., Linder P. (2006). The DEAD-box protein family of RNA helicases. *Gene* 367, 17-37.

Das S., Roymondal U., Chottopadhyay B., Sahoo S. (2012). Gene expression profile of the cynobacterium *Synechocystis* genome. *Gene* 497, 344-352.

de la Cruz J., Kressler D., Linder P. (1999). Unwinding RNA in saccharomyces cerevisiae: DEAD-box proteins and related families. *Trends Biochem Sci* 24, 192-198.

Dersch P., Kneip S., Bremer E. (1994). The nucleoid-associated DNA-binding protein H-NS is required for the efficient adaptation of *Escherichia coli* K-12 to a cold environment. *Molecular and General Genetics* 245, 255-259.

Dias C. L., Ala-Nissila T., Wong-ekkabut J., Vattulainen I., Grant M., Karttunen M. (2010). The hydrophobic effect and its role in cold denaturation. *Cryobiology* 60, 91-99.

Ducruet J., Peeva V., Havaux M. (2007). Chlorophyll thermofluorescence and thermoluminescence as complementary tools for the study of temperature stress in plants. *Photosynth Res* 94, 159-171.

El-Fahmawi B. & Owttrim G. W. (2003). Polar-biased localization of the cold stress-induced RNA helicase, CrhC, in the cyanobacterium *Anabaena* sp strain PCC 7120. *Mol Microbiol* 50, 1439-1448.

Elhai J. & Wolk C. P. (1988). A versatile class of positive-selection vectors based on the nonviability of palindrome-containing plasmids that allows cloning into long polylinkers. *Gene* 68, 119-138.

ElhaI J., Vepritskiy A., MuroPastor A. M., Flores E., Wolk C. P. (1997). Reduction of conjugal transfer efficiency by three restriction activities of *Anabaena* sp. strain PCC 7120. *J Bacteriol* 179, 1998-2005.

El-Sharoud W. M. & Graumann P. L. (2007). Cold shock proteins aid coupling of transcription and translation in bacteria. *Sci Prog* 90, 15-27.

Endoh H., Maruyama K., Masuhiro Y., Kobayashi Y., Goto M., Tai H., Yanagisawa J., Metzger D., Hashimoto S., Kato S. (1999). Purification and identification of p68 RNA helicase acting as a transcriptional coactivator specific for the activation function 1 of human estrogen receptor alpha. *Mol Cell Biol* 19, 5363-5372.

Enrique Frias J. & Flores E. (2010). Negative regulation of expression of the nitrate assimilation *nirA* operon in the heterocyst-forming cyanobacterium *Anabaena* sp strain PCC 7120. *J Bacteriol* 192, 2769-2778.

Ermolenko D. N. & Makhatadze G. I. (2002). Bacterial cold-shock proteins. *Cell Mol Life Sci* 59, 1902-1913.

Estruch F. & Cole C. N. (2003). An early function during transcription for the yeast mRNA export factor Dbp5p/Rat8p suggested by its genetic and physical interactions with transcription factor IIH components. *Mol Biol Cell* 14, 1664-1676.

Etchegaray J. P. & Inouye M. (1999). CspA, CspB, and CspG, major cold shock proteins of *Escherichia coli*, are induced at low temperature under conditions that completely block protein synthesis. *J Bacteriol* 181, 1827-1830.

Fairman M. E., Maroney P. A., Wang W., Bowers H. A., Gollnick P., Nilsen T. W., Jankowsky E. (2004). Protein displacement by DExH/D "RNA helicases" without duplex unwinding. *Science* 304, 730-734.

Fairman-Williams M. E., Guenther U., Jankowsky E. (2010). SF1 and SF2 helicases: Family matters. *Curr Opin Struct Biol* 20, 313-324.

Falsone S. F., Weichel M., Crameri R., Breitenbach M., Kungl A. J. (2002). Unfolding and double-stranded DNA binding of the cold shock protein homologue Clah8 from *Cladosporium herbarum*. *J Biol Chem* 277, 16512-16516.

Fang L., Hou Y., Inouye M. (1998). Role of the cold-box region in the 5 ' untranslated region of the *cspA* mRNA in its transient expression at low temperature in *Escherichia coli*. *J Bacteriol* 180, 90-95.

Fang L., Jiang W. N., Bae W. H., Inouye M. (1997). Promoter-independent cold-shock induction of *cspA* and its derepression at 37^{o}C by mRNA stabilization. *Mol Microbiol* 23, 355-364.

Farewell A. & Neidhardt F. C. (1998). Effect of temperature on *in vivo* protein synthetic capacity in *Escherichia coli*. *J Bacteriol* 180, 4704-4710.

Feng W. Q., Tejero R., Zimmerman D. E., Inouye M., Montelione G. T. (1998). Solution NMR structure and backbone dynamics of the major cold-shock protein (CspA) from *Escherichia coli*: Evidence for conformational dynamics in the single-stranded RNA-binding site. *Biochem (N Y)* 37, 10881-10896.

Feng Y., Huang H. J., Liao J., Cohen S. N. (2001). *Escherichia coli* poly(A)-binding proteins that interact with components of degradosomes or impede RNA decay mediated by polynucleotide phosphorylase and RNase E. *J Biol Chem* 276, 31651-31656.

Friedman H., Lu P., Rich A. (1971). Temperature control of initiation of protein synthesis in *Escherichi coli*. *J Mol Biol* 61, 105-112.

Friedrich K., Gualerzi C. O., Lammi M., Losso M. A., Pon C. L. (1988). Proteins from the prokaryotic nucleoid - interaction of nucleic-acids with the 15 kda *Escherichia coli* histone-like protein H-NS. *FEBS Lett* 229, 197-202.

Fuller-Pace F. V. & Ali S. (2008). The DEAD box RNA helicases p68 (Ddx5) and p72 (Ddx17): Novel transcriptional co-regulators. *Biochem Soc Trans* 36, 609-612.

Giangrossi M., Gualerzi C. O., Pon C. L. (2001). Mutagenesis of the downstream region of the *Escherichia coli hns* promoter. *Biochimie* 83, 251-259.

Gierga G., Voss B., Hess W. R. (2012). Non-coding RNAs in marine *Synechococcus* and their regulation under environmentally relevant stress conditions. *ISME J* 6, 1544-1557.

Giovannoni S. J., Turner S., Olsen G. J., Barns S., Lane D. J., Pace N. R. (1988). Evolutionary relationships among cyanobacteria and green chloroplasts. *J Bacteriol* 170, 3584-3592.

Giuliodori A. M., Di Pietro F., Marzi S., Masquida B., Wagner R., Romby P., Gualerzi C. O., Pon C. L. (2010). The *cspA* mRNA is a thermosensor that modulates translation of the cold-shock protein CspA. *Mol Cell* 37, 21-33.

Goldenberg D., Azar I., Oppenheim A. B. (1996). Differential mRNA stability of the *cspA* gene in the cold-shock response of *Escherichia coli*. *Mol Microbiol* 19, 241-248.

Goldstein J., Pollitt N., Inouye M. (1990). Major cold shock protein of *Escherichia coli*. *Proc Natl Acad Sci U S A* 87, 283-287.

Golovlev E. (2003). Bacterial cold shock response at the level of DNA transcription, translation, and chromosome dynamics. *Microbiology* 72, 1-7.

Gottesman S. (2003). Proteolysis in bacterial regulatory circuits. *Annu Rev Cell Dev Biol* 19, 565-587.

Graumann P. & Marahiel M. A. (1996). Some like it cold: Response of microorganisms to cold shock. *Arch Microbiol* 166, 293-300.

Graumann P., Wendrich T. M., Weber M. H. W., Schroder K., Marahiel M. A. (1997). A family of cold shock proteins in *Bacillus subtilis* is essential for cellular growth and for efficient protein synthesis at optimal and low temperatures. *Mol Microbiol* 25, 741-756.

Graumann P. & Marahiel M. (1998). A superfamily of proteins that contain the cold-shock domain. *Trends Biochem Sci* 23, 286-290.

Grigorieva G. & Shestakov S. (1982). Transformation in the cyanobacterium *Synechocystis* sp 6803. *FEMS Microbiol Lett* 13, 367-370.

Gualerzi C., Giuliodori A., Pon C. (2003). Transcriptional and post-transcriptional control of cold-shock genes. *J Mol Biol* 331, 527-539.

Gur E., Biran D., Ron E. Z. (2011). Regulated proteolysis in Gram negative bacteria - how and when? *Nature Reviews Microbiology* 9, 839-848.

Halls C., Mohr S., Del Campo M., Yang Q., Jankowsky E., Lambowitz A. M. (2007). Involvement of DEAD-box proteins in group I and group II intron splicing. biochemical characterization of Mss116p, ATP hydrolysis-dependent and -independent mechanisms, and general RNA chaperone activity. *J Mol Biol* 365, 835-855.

Harlow D. & Lane D., editors. (1988). Antibodies: A Laboratory Manual. New York, USA: Cold Spring Harbor Laboratory Press.

Horn G., Hofweber R., Kremer W., Kalbitzer H. R. (2007). Structure and function of bacterial cold shock proteins. *Cell Mol Life Sci* 64, 1457-1470.

Iost I. & Dreyfus M. (2006). DEAD-box RNA helicases in *Escherichia coli*. *Nucleic Acids Res* 34, 4189-4197.

Iost I. & Dreyfus M. (1994). Messenger RNAs can be stabilized by dead-box proteins. *Nature* 372, 193-196.

Jagessar K. L. & Jain C. (2010). Functional and molecular analysis of *Escherichia coli* strains lacking multiple DEAD-box helicases. *Rna-a Publication of the Rna Society* 16, 1386-1392.

Jankowsky E. (2011). RNA helicases at work: Binding and rearranging. *Trends Biochem Sci* 36, 19-29.

Jankowsky E. & Fairman M. E. (2007). RNA helicases - one fold for many functions. *Curr Opin Struct Biol* 17, 316-324.

Jarmoskaite I. & Russell R. (2011). DEAD-box proteins as RNA helicases and chaperones. *Wiley Interdisciplinary Reviews-Rna* 2, 135-152.

Jiang W. N., Hou Y., Inouye M. (1997). CspA, the major cold-shock protein of *Escherichia coli*, is an RNA chaperone. *J Biol Chem* 272, 196-202.

Jiang W. N., Fang L., Inouye M. (1996). The role of the 5'-end untranslated region of the mRNA for CspA, the major cold-shock protein of *Escherichia coli*, in cold-shock adaptation. *J Bacteriol* 178, 4919-4925.

Jiang W. N., Jones P., Inouye M. (1993). Chloramphenicol induces the transcription of the major cold shock gene of *Escherichia coli*, CspA. *J Bacteriol* 175, 5824-5828.

Jiang X., Zhang H., Yang J., Liu M., Feng H., Liu X., Cao Y., Feng D., Xian M. (2012). Induction of gene expression in bacteria at optimal growth temperatures. *Appl Microbiol Biotechnol* , 1-9.

Jones J. M., Welty D. J., Nakai H. (1998). Versatile action of *Escherichia coli* ClpXP as protease or molecular chaperone for bacteriophage mu transposition. *J Biol Chem* 273, 459-465.

Jones P. G., Vanbogelen R. A., Neidhardt F. C. (1987). Induction of proteins in response to low-temperature in *Escherichia coli*. *J Bacteriol* 169, 2092-2095.

Jones P. G., Cashel M., Glaser G., Neidhardt F. C. (1992). Function of a relaxed-like state following temperature downshifts in *Escherichia coli*. *J Bacteriol* 174, 3903-3914.

Jones P. G., Mitta M., Kim Y., Jiang W. N., Inouye M. (1996). Cold shock induces a major ribosomal-associated protein that unwinds double-stranded RNA in *escherichia coli*. *Proc Natl Acad Sci U S A* 93, 76-80.

Kaberdin V. R. & Blaesi U. (2006). Translation initiation and the fate of bacterial mRNAs. *FEMS Microbiol Rev* 30, 967-979.

Kaczanowska M. & Ryden-Aulin M. (2007). Ribosome biogenesis and the translation process in *Escherichia coli*. *Microbiology and Molecular Biology Reviews* 71, 477-483.

Kalman M., Murphy H., Cashel M. (1991). Rhlb, a new *Escherichia coli* K-12 gene with an rna helicase-like protein-sequence motif, one of at least 5 such possible genes in a prokaryote. *New Biol* 3, 886-895.

Kandror O. & Goldberg A. L. (1997). Trigger factor is induced upon cold shock and enhances viability of *Escherichia coli* at low temperatures. *Proc Natl Acad Sci U S A* 94, 4978-4981.

Kaneko T., Sato S., Kotani H., Tanaka A., Asamizu E., Nakamura Y., Miyajima N., Hirosawa M., Sugiura M.& other authors. (1996). Sequence analysis of the genome of the unicellular cyanobacterium *Synechocystis* sp. strain PCC6803. II. sequence determination of the entire genome and assignment of potential protein-coding regions. *DNA Research : An International Journal for Rapid Publication of Reports on Genes and Genomes* 3, 109-36.

Kaneko T., Nakamura Y., Sasamoto S., Wolk C. P., Tabata S. (2001). Genome sequence analysis of cyanobacteria, *Anabaena* sp. PCC7120, *Synechococcus elongatus, Gloeobacter violaceus* PCC7421. *Plant and Cell Physiol* 42, 176-176.

Karow A. R. & Klostermeier D. (2010). A structural model for the DEAD box helicase YxiN in solution: Localization of the RNA binding domain. *J Mol Biol* 402, 629-637.

Khemici V. & Carpousis A. J. (2004). The RNA degradosome and poly(A) polymerase of *Escherichia coli* are required *in vivo* for the degradation of small mRNA decay intermediates containing REP-stabilizers. *Mol Microbiol* 51, 777-790.

Klein W., Weber M. H. W., Marahiel M. A. (1999). Cold shock response of *Bacillus subtilis*: Isoleucine-dependent switch in the fatty acid branching pattern for membrane adaptation to low temperatures. *J Bacteriol* 181, 5341-5349.

Kressler D., Linder P., de la Cruz J. (1999). Protein trans-acting factors involved in ribosome biogenesis in *Saccharomyces cerevisiae*. *Mol Cell Biol* 19, 7897-7912.

Krispin O. & Allmansberger R. (1995). Changes in DNA supertwist as a response of *Bacillus subtilis* towards different kinds of stress. *FEMS Microbiol Lett* 134, 129-135.

Kruger E., Zuhlke D., Witt E., Ludwig H., Hecker M. (2001). Clp-mediated proteolysis in Gram positive bacteria is autoregulated by the stability of a repressor. *EMBO J* 20, 852-863.

Kuhn B., Abdelmonem M., Krell H., Hoffmannberling H. (1979). Evidence for 2 mechanisms for DNA unwinding catalyzed by DNA helicases. *J Biol Chem* 254, 1343-1350.

Kujat S. L. & Owttrim G. W. (2000). Redox-regulated RNA helicase expression. *Plant Physiol* 124, 703-713.

Lee S., Xie A., Jiang W., Etchegaray J., Jones P., Inouye M. (1994). Family of the major cold-shock protein, Cspa (Cs7.4), of *Escherichia coli*, whose members show a high sequence similarity with the eukaryotic Y-box binding-proteins. *Mol Microbiol* 11, 833-839.

Leffers G. G. & Gottesman S. (1998). Lambda xis degradation *in vivo* by Lon and FtsH. *J Bacteriol* 180, 1573-1577.

Lehnik-Habrink M., Rempeters L., Kovács A. T., Wrede C., Baierlein C., Krebber H., Kuipers O. P., Stülke J. (2013). Dead-box RNA helicases in *Bacillus subtilis* have multiple functions and act independently from each other. *J Bacteriol* 195, 534-544.

Levchenko I., Yamauchi M., Baker T. A. (1997). ClpX and MuB interact with overlapping regions of mu transposase: Implications for control of the transposition pathway. *Genes Dev* 11, 1561-1572.

Lim J., Thomas T., Cavicchioli R. (2000). Low temperature regulated DEAD-box RNA helicase from the antarctic archaeon, *Methanococcoides burtonii*. *J Mol Biol* 297, 553-567.

Lindahl M., Spetea C., Hundal T., Oppenheim A. B., Adam Z., Andersson B. (2000). The thylakoid FtsH protease plays a role in the light-induced turnover of the photosystem II D1 protein. *Plant Cell* 12, 419-431.

Linder P. (2003). Yeast RNA helicases of the DEAD-box family involved in translation initiation. *Biology of the Cell* 95, 157-167.

Linder P. & Jankowsky E. (2011). From unwinding to clamping, the DEAD box RNA helicase family. *Nat Rev Mol Cell Biol* 12, 505-516.

Linder P., Lasko P. F., Ashburner M., Leroy P., Nielsen P. J., Nishi K., Schnier J., Slonimski P. P. (1989). Birth of the D-E-A-D box. *Nature* 337, 121-122.

Linder P. (2006). Dead-box proteins: A family affair - active and passive players in RNP-remodeling. *Nucleic Acids Res* 34, 4168-4180.

Lindner A. B., Madden R., Dernarez A., Stewart E. J., Taddei F. (2008). Asymmetric segregation of protein aggregates is associated with cellular aging and rejuvenation. *Proc Natl Acad Sci U S A* 105, 3076-3081.

Lopez M. M. & Makhatadze G. I. (2000). Major cold shock proteins, CspA from *Escherichia coli* and CspB from *Bacillus subtilis*, interact differently with single-stranded DNA templates. *Biochim Et Biophysica Acta-Protein Structure and Molecular Enzymology* 1479, 196-202.

Lopez M. M., Yutani K., Makhatadze G. I. (1999). Interactions of the major cold shock protein of *Bacillus subtilis* CspB with single-stranded DNA templates of different base composition. *J Biol Chem* 274, 33601-33608.

Luking A., Stahl U., Schmidt U. (1998). The protein family of RNA helicases. *Crit Rev Biochem Mol Biol* 33, 259-296.

Markkula A., Mattila M., Lindstrom M., Korkeala H. (2012a). Genes encoding putative DEAD-box RNA helicases in *Listeria monocytogenes* EGD-e are needed for growth and motility at 3^{o}C. *Environ Microbiol* 14, 2223-2232.

Markkula A., Lindstrom M., Johansson P., Bjorkroth J., Korkeala H. (2012b). Roles of four putative DEAD-box RNA helicase genes in growth of *Listeria monocytogenes* EGD-e under heat, pH, osmotic, ethanol, and oxidative stress conditions. *Appl Environ Microbiol* 78, 6875-6882.

Meyer A. S. & Baker T. A. (2011). Proteolysis in the *Escherichia coli* heat shock response: A player at many levels. *Curr Opin Microbiol* 14, 194-199.

Mitta M., Fang L., Inouye M. (1997). Deletion analysis of *cspA* of *Escherichia coli*: Requirement of the AT-rich UP element for *cspA* transcription and the downstream box in the coding region for its cold shock induction. *Mol Microbiol* 26, 321-335.

Mizushima T., Kataoka K., Ogata Y., Inoue R., Sekimizu K. (1997). Increase in negative supercoiling of plasmid DNA in *Escherichia coli* exposed to cold shock. *Mol Microbiol* 23, 381-386.

Montero-Lomeli M., Morais B. L. B., Figueiredo D. L., Neto D. C. S., Martins J. R. P., Masuda C. A. (2002). The initiation factor eIF4A is involved in the

response to lithium stress in *Saccharomyces cerevisiae*. *J Biol Chem* 277, 21542-21548.

Mukhopadhyay A., He Z. L., Alm E. J., Arkin A. P., Baidoo E. E., Borglin S. C., Chen W. Q., Hazen T. C., He Q.& other authors. (2006). Salt stress in *Desulfovibrio vulgaris hildenborough*: An integrated genomics approach. *J Bacteriol* 188, 4068-4078.

Murata N. & Wada H. (1995). Acyl-lipid desaturases and their importance in the tolerance and acclimatization to cold of cyanobacteria (Originally published in Biochem. J. (1995) 308, 1-8) Edited by A. E. Pegg.

Mustardy L., Los D., Gombos Z., Murata N. (1996). Immunocytochemical localization of acyl-lipid desaturases in cyanobacterial cells: Evidence that both thylakoid membranes and cytoplasmic membranes are sites of lipid desaturation. *Proc Natl Acad Sci U S A* 93, 10524-10527.

Nakashima K., Kanamaru K., Mizuno T., Horikoshi K. (1996). A novel member of the *cspA* family of genes that is induced by cold shock in *Escherichia coli*. *J Bacteriol* 178, 2994-2997.

Neher S. B., Flynn J. M., Sauer R. T., Baker T. A. (2003). Latent ClpX-recognition signals ensure LexA destruction after DNA damage. *Genes Dev* 17, 1084-1089.

Newkirk K., Feng W. Q., Jiang W. N., Tejero R., Emerson S. D., Inouye M., Montelione G. T. (1994). Solution NMR structure of the major cold shock protein (CspA) from *Escherichia coli* - identification of a binding epitope for DNA. *Proc Natl Acad Sci U S A* 91, 5114-5118.

Ng W., Zentella R., Wang Y., Taylor J., Pakrasi H. (2000). *phrA*, the major photoreactivating factor in the cyanobacterium *Synechocystis* sp strain PCC 6803 codes for a cyclobutane-pyrimidine-dimer-specific DNA photolyase. *Arch Microbiol* 173, 412-417.

Okajima K., Sato S., Ochiai Y., Katayama M., Tabata S., Ikeuchi M. (2006). Specific interaction between the blue light receptor PixD (BLUF) and PatA type response regulator PixE in cyanobacterium *Synechocystis* sp PCC 6803. *Plant Cell Physiol* 47, 158-158.

Pakrasi H. B. (1995). Genetic analysis of the form and function of photosystem I and photosystem II. *Annu Rev Genet* 29, 755-776.

Peil L., Virumaee K., Remme J. (2008). Ribosome assembly in *Escherichia coli* strains lacking the RNA helicase DeaD/CsdA or DbpA. *Febs Journal* 275, 3772-3782.

Phadtare S. & Inouye M. (2008). Cold-shock proteins. Edited by R. Margesin, F. Schinner, J. Marx & C. Gerday.

Phadtare S. & Severinov K. (2005). Extended-10 motif is critical for activity of the *cspA* promoter but does not contribute to low-temperature transcription. *J Bacteriol* 187, 6584-6589.

Phadtare S. & Inouye M. (2001). Role of CspC and CspE in regulation of expression of RpoS and UspA, the stress response proteins in *Escherichia coli*. *J Bacteriol* 183, 1205-1214.

Phadtare S. & Inouye M. (1999). Sequence-selective interactions with RNA by CspB, CspC and CspE, members of the CspA family of *Escherichia coli*. *Mol Microbiol* 33, 1004-1014.

Phadtare S., Inouye M., Severinov K. (2002a). The nucleic acid melting activity of *Escherichia coli* CspE is critical for transcription antitermination and cold acclimation of cells. *J Biol Chem* 277, 7239-7245.

Phadtare S., Tyagi S., Inouye M., Severinov K. (2002b). Three amino acids in *Escherichia coli* CspE surface-exposed aromatic patch are critical for nucleic acid melting activity leading to transcription antitermination and cold acclimation of cells. *J Biol Chem* 277, 46706-46711.

Phadtare S. (2004). Recent developments in bacterial cold-shock response. *Curr Issues Mol Biol* 6, 125-136.

Phadtare S. & Severinov K. (2010). RNA remodeling and gene regulation by cold shock proteins. *Rna Biology* 7, 788-795.

Plumpton M., McGarvey M., Beggs J. D. (1994). A dominant negative mutation in the conserved RNA helicase motif 'SAT' causes splicing factor PRP2 to stall in spliceosomes. *EMBO J* 13, 879-887.

Pon C. L., Calogero R. A., Gualerzi C. O. (1988). Identification, cloning, nucleotide-sequence and chromosomal map location of hns, the structural gene for *Escherichia coli* DNA-binding protein H-NS. *Molecular & General Genetics* 212, 199-202.

Porankiewicz J. & Clarke A. K. (1997). Induction of the heat shock protein ClpB affects cold acclimation in the cyanobacterium *Synechococcus* sp. strain PCC 7942. *J Bacteriol* 179, 5111-5117.

Porankiewicz J., Schelin J., Clarke A. K. (1998). The ATP-dependent clp protease is essential for acclimation to UV-B and low temperature in the cyanobacterium *Synechococcus. Mol Microbiol* 29, 275-283.

Prakash J. S. S., Krishna P. S., Sirisha K., Kanesaki Y., Suzuki I., Shivaji S., Murata N. (2010). An RNA helicase, CrhR, regulates the low-temperature-inducible expression of heat-shock genes groES, groEL1 and groEL2 in *Synechocystis* sp PCC 6803. *Microbiology-Sgm* 156, 442-451.

Prud'homme-Genereux A., Beran R. K., Iost I., Ramey C. S., Mackie G. A., Simons R. W. (2004). Physical and functional interactions among RNase E, polynucleotide phosphorylase and the cold-shock protein, CsdA: Evidence for a 'cold shock degradosome'. *Mol Microbiol* 54, 1409-1421.

Purusharth R. I., Klein F., Sulthana S., Jager S., Jagannadham M. V., Evguenieva-Hackenberg E., Ray M. K., Klug G. (2005). Exoribonuclease R interacts with endoribonuclease e and an RNA helicase in the psychrotrophic bacterium *Pseudomonas syringae*. *J Biol Chem* 280, 14572-14578.

Py B., Higgins C. F., Krisch H. M., Carpousis A. J. (1996). A DEAD-box RNA helicase in the *Escherichia coli* RNA degradosome. *Nature* 381, 169-172.

Rawling D. C. & Baserga S. J. (2012). *In vivo* approaches to dissecting the function of RNA helicases in eukaryotic ribosome assembly. *Rna Helicases* 511, 289-321.

Rocak S. & Linder P. (2004). Dead-box proteins: The driving forces behind RNA metabolism. *Nature Reviews Molecular Cell Biology* 5, 232-241.

Rogers G. W., Lima W. F., Merrick W. C. (2001). Further characterization of the helicase activity of eIF4A - substrate specificity. *J Biol Chem* 276, 12598-12608.

Rogers G. W., Richter N. J., Merrick W. C. (1999). Biochemical and kinetic characterization of the RNA helicase activity of eukaryotic initiation factor 4A. *J Biol Chem* 274, 12236-12244.

Rosana A. R. R., Ventakesh M., Chamot D., Patterson-Fortin L. M., Tarassova O., Espie G. S., Owttrim G. W. (2012a). Inactivation of a low temperature-induced RNA helicase in *Synechocystis* sp. PCC 6803: Physiological and morphological consequences. *Plant Cell Physiol* 53, 646-658.

Rosana A. R. R., Chamot D., Owttrim G. W. (2012b). Autoregulation of RNA helicase expression in response to temperature stress in *Synechocystis* sp PCC 6803. *Plos One* 7, e48683.

Rossler O. G., Straka A., Stahl H. (2001). Rearrangement of structured RNA via branch migration structures catalysed by the highly related DEAD-box proteins p68 and p72. *Nucleic Acids Res* 29, 2088-2096.

Rowland J. G., Simon W. J., Prakash J. S. S., Slabas A. R. (2011). Proteomics reveals a role for the RNA helicase crhR in the modulation of multiple metabolic pathways during cold acclimation of *Synechocystis* sp PCC6803. *Journal of Proteome Research* 10, 3674-3689.

Sakamoto T. & Bryant D. A. (1997). Temperature-regulated mRNA accumulation and stabilization for fatty acid desaturase genes in the cyanobacterium *Synechococcus* sp. strain PCC 7002. *Mol Microbiol* 23, 1281-1292.

Sanan-Mishra N., Pham X. H., Sopory S. K., Tuteja N. (2005). Pea DNA helicase 45 overexpression in tobacco confers high salinity tolerance without affecting yield. *Proc Natl Acad Sci USA* 102, 509-514.

Sato N. (1995). A family of cold-regulated RNA-binding protein genes in the cyanobacterium *Anabaena variabilis* M3. *Nucleic Acids Res* 23, 2161-2167.

Sato S., Ikeuchi M., Nakamoto H. (2008). Expression and function of a groEL paralog in the thermophilic cyanobacterium *Thermosynechococcus elongatus* under heat and cold stress. *FEBS Lett* 582, 3389-3395.

Schade B., Jansen G., Whiteway M., Entian K. D., Thomas D. Y. (2004). Cold adaptation in budding yeast. *Mol Biol Cell* 15, 5492-5502.

Schelin J., Lindmark F., Clarke A. K. (2002). The clpP multigene family for the ATP-dependent clp protease in the cyanobacterium *Synechococcus*. *Microbiology* 148, 2255-2265.

Schindelin H., Marahiel M. A., Heinemann U. (1993). Universal nucleic acid-binding domain revealed by crystal-structure of the *Bacillus subtilis* major cold-shock protein. *Nature* 364, 164-168.

Schindelin H., Jiang W. N., Inouye M., Heinemann U. (1994). Crystal-structure of cspa, the major cold shock protein of *Escherichia coli*. *Proc Natl Acad Sci U S A* 91, 5119-5123.

Schnuchel A., Wiltscheck R., Czisch M., Herrler M., Willimsky G., Graumann P., Marahiel M. A., Holak T. A. (1993). Structure in solution of the major cold-shock protein from *Bacillus subtilis*. *Nature* 364, 169-171.

Seo J., Jeong J., Kirn Y. M., Hwang N., Paek E., Lee K. (2008). Strategy for comprehensive identification of post-translational modifications in cellular proteins, including. low abundant modifications: Application to glyceraidehyde-3-phosphate dehydrogenase. *Journal of Proteome Research* 7, 587-602.

Shenhar Y., Rasouly A., Biran D., Ron E. Z. (2009). Adaptation of *Escherichia coli* to elevated temperatures involves a change in stability of heat shock gene transcripts. *Environ Microbiol* 11, 2989-2997.

Shrader T. E., Tobias J. W., Varshavsky A. (1993). The N-end rule in *Escherichia coli* - cloning and analysis of the leucyl, phenylalanyl-transfer rna-protein transferase gene aat. *J Bacteriol* 175, 4364-4374.

Silverman E., Edwalds-Gilbert G., Lin R. J. (2003). DExD/H-box proteins and their partners: Helping RNA helicases unwind. *Gene* 312, 1-16.

Singleton M. R., Dillingham M. S., Wigley D. B. (2007). Structure and mechanism of helicases and nucleic acid translocases. *Annu Rev Biochem* 76, 23-50.

Sireesha K., Radharani B., Krishna P. S., Sreedhar N., Subramanyam R., Mohanty P., Prakash J. S. S. (2012). RNA helicase, CrhR is indispensable for the energy redistribution and the regulation of photosystem stoichiometry at low temperature in *Synechocystis* sp PCC6803. *Biochim Et Biophysica Acta-Bioenergetics* 1817, 1525-1536.

Skeik R. (2012) Dimerization of DEAD-box RNA helicase, CrhR. University of Alberta.

Sprengart M. L., Fuchs E., Porter A. G. (1996). The downstream box: An efficient and independent translation initiation signal in *Escherichia coli*. *EMBO J* 15, 665-674.

Stanne T. M., Pojidaeva E., Andersson F. I., Clarke A. K. (2007). Distinctive types of ATP-dependent clp proteases in cyanobacteria. *J Biol Chem* 282, 14394-14402.

Straus D., Walter W., Gross C. A. (1990). Dnak, Dnaj, and Grpe heat-shock proteins negatively regulate heat-shock gene expression by controlling the synthesis and stability of sigma-32. *Genes Dev* 4, 2202-2209.

Straus D. B., Walter W. A., Gross C. A. (1989). The activity of sigma-32 is reduced under conditions of excess heat-shock protein production in *Escherichia coli*. *Genes Dev* 3, 2003-2010.

Susin M. F., Baldini R. L., Gueiros-Filho F., Gomes S. L. (2006). GroES/GroEL and DnaK/DnaJ have distinct roles in stress responses and during cell cycle progression in *Caulobacter crescentus*. *J Bacteriol* 188, 8044-8053.

Suzuki I., Los D. A., Kanesaki Y., Mikami K., Murata N. (2000). The pathway for perception and transduction of low-temperature signals in *Synechocystis*. *EMBO J* 19, 1327-1334.

Thieringer H., Jones P., Inouye M. (1998). Cold shock and adaptation. *Bioessays* 20, 49-57.

Tijerina P., Bhaskaran H., Russell R. (2006). Nonspecific binding to structured RNA and preferential unwinding of an exposed helix by the CYT-19 protein, a DEAD-box RNA chaperone. *Proc Natl Acad Sci U S A* 103, 16698-16703.

Tobias J. W., Shrader T. E., Rocap G., Varshavsky A. (1991). The N-end rule in bacteria. *Science* 254, 1374-1377.

Tomoyasu T., Ogura T., Tatsuta T., Bukau B. (1998). Levels of DnaK and DnaJ provide tight control of heat shock gene expression and protein repair in *Escherichia coli*. *Mol Microbiol* 30, 567-581.

Tomoyasu T., Gamer J., Bukau B., Kanemori M., Mori H., Rutman A. J., Oppenheim A. B., Yura T., Yamanaka K.& other authors. (1995). *Escherichia coli*FtsH is a membrane-bound, atp-dependent protease which degrades the heat-shock transcription factor sigma 32. *EMBO J* 14, 2551-2560.

Toone W. M., Rudd K. E., Friesen J. D. (1991). Dead, a new *Escherichia coli* gene encoding a presumed atp-dependent rna helicase, can suppress a mutation in rpsb, the gene encoding ribosomal protein-S2. *J Bacteriol* 173, 3291-3302.

Tyystjarvi T., Herranen M., Aro E. (2001). Regulation of translation elongation in cyanobacteria: Membrane targeting of the ribosome nascent-chain complexes controls the synthesis of D1 protein. *Mol Microbiol* 40, 476-484.

Uhlmann-Schiffler H., Jalal C., Stahl H. (2006). Ddx42p - a human DEAD box protein with RNA chaperone activities. *Nucleic Acids Res* 34, 10-22.

Vanbogelen R. A. & Neidhardt F. C. (1990). Ribosomes as sensors of heat and cold shock in *Escherichia coli*. *Proc Natl Acad Sci U S A* 87, 5589-5593.

Varshavsky A. (1992). The N-end rule. *Cell* 69, 725-735.

Vijayan V., Jain I. H., O'Shea E. K. (2011). A high resolution map of a cyanobacterial transcriptome. *Genome Biol* 12.

Vinnemeier J. & Hagemann M. (1999). Identification of salt-regulated genes in the genome of the cyanobacterium *Synechocystis* sp. strain PCC 6803 by subtractive RNA hybridization. *Arch Microbiol* 172, 377-386.

Wang J. & Syvanen M. (1992). Dna twist as a transcriptional sensor for environmental changes. *Mol Microbiol* 6, 1861-1866.

Wang N., Yamanaka K., Inouye M. (1999). CspI, the ninth member of the CspA family of *Escherichia coli*, is induced upon cold shock. *J Bacteriol* 181, 1603-1609.

Watanabe M., Yanagisawa J., Kitagawa H., Takeyama K., Ogawa S., Arao Y., Suzawa M., Kobayashi Y., Yano T.& other authors. (2001). A subfamily of RNA-binding DEAD-box proteins acts as an estrogen receptor alpha coactivator through the N-terminal activation domain (AF-1) with an RNA coactivator, SRA. *EMBO J* 20, 1341-1352.

Weber M. H. W., Klein W., Muller L., Niess U. M., Marahiel M. A. (2001). Role of the *Bacillus subtilis* fatty acid desaturase in membrane adaptation during cold shock. *Mol Microbiol* 39, 1321-1329.

Weirich C. S., Erzberger J. P., Berger J. M., Weis K. (2004). The N-terminal domain of Nup159 forms a beta-propeller that functions in mRNA export by tethering the helicase Dbp5 to the nuclear pore. *Mol Cell* 16, 749-760.

Weisberg R. A. & Gottesman M. E. (1971). The Stability of Int and His Functions. Bacteriophage Lambda. Cold Spring Harbor, NY. 489-500.

Westermarck J., Weiss C., Saffrich R., Kast J., Musti A. M., Wessely M., Ansorge W., Seraphin B., Wilm M., Valdez B. C., Bohmann D. (2002). The DEXD/H-box RNA helicase RHII/gu is a co-factor for activated transcription. *EMBO J* 21, 451-460.

Willimsky G., Bang H., Fischer G., Marahiel M. A. (1992). Characterization of *cspb*, a *Bacillus subtilis* inducible cold shock gene affecting cell viability at low-temperatures. *J Bacteriol* 174, 6326-6335.

Wilson B. J., Bates G. J., Nicol S. M., Gregory D. J., Perkins N. D., Fuller-Pace F. V. (2004). The p68 and p72 DEAD box RNA helicases interact with HDACI and repress transcription in a promoter-specific manner. *Bmc Molecular Biology* 5, 11.

Wilson K. E., Ivanov A. G., Öquist G., Grodzinski B., Sarhan F., Huner N. P. A. (2006). Energy balance, organellar redox status, and acclimation to environmental stress. *Can J Bot* 84, 1355-1370.

Xia B., Ke H. P., Inouye M. (2001). Acquirement of cold sensitivity by quadruple deletion of the *cspA* family and its suppression by PNPase S1 domain in *Escherichia coli*. *Mol Microbiol* 40, 179-188.

Yamanaka K. (1999). Cold shock response in *Escherichia coli*. *J Mol Microbiol Biotechnol* 1, 193-202.

Yamanaka K. & Inouye M. (1997). Growth-phase-dependent expression of *csp*D, encoding a member of the CspA family in *Escherichia coli*. *J Bacteriol* 179, 5126-5130.

Yamanaka K., Fang L., Inouye M. (1998). The CspA family in *Escherichia coli*: Multiple gene duplication for stress adaptation. *Mol Microbiol* 27, 247-255.

Yamanaka K., Mitani T., Ogura T., Niki H., Hiraga S. (1994). Cloning, sequencing, and characterization of multicopy suppressors of a mukb mutation in *Escherichia coli*. *Mol Microbiol* 13, 301-312.

Yang Q. S. & Jankowsky E. (2005). ATP- and ADP-dependent modulation of RNA unwinding and strand annealing activities by the DEAD-box protein DED1. *Biochemistry (N Y)* 44, 13591-13601.

Yang Q. & Jankowsky E. (2006). The DEAD-box protein Ded1 unwinds RNA duplexes by a mode distinct from translocating helicases. *Nature Structural & Molecular Biology* 13, 981-986.

Yang Q., Del Campo M., Larnbowitz A. M., Jankowsky E. (2007). DEAD-box proteins unwind duplexes by local strand separation. *Mol Cell* 28, 253-263.

Yu E. & Owttrim G. W. (2000). Characterization of the cold stress-induced cyanobacterial DEAD-box protein CrhC as an RNA helicase. *Nucleic Acids Res* 28, 3926-3934.

Zang X., Liu B., Liu S., Arunakumara K. K. I. U., Zhang X. (2007). Optimum conditions for transformation of *Synechocystis* sp PCC 6803. *Journal of Microbiology* 45, 241-245.

Zhao J., Jin S. B., Bjokroth B., Wieslander L., Daneholt B. (2002). The mRNA export factor Dbp5 is associated with balbiani ring mRNP from gene to cytoplasm. *EMBO J* 21, 1177-1187.